

INFORMATION TO USERS

This manuscript has been reproduced from the microfilm master. UMI films the text directly from the original or copy submitted. Thus, some thesis and dissertation copies are in typewriter face, while others may be from any type of computer printer.

The quality of this reproduction is dependent upon the quality of the copy submitted. Broken or indistinct print, colored or poor quality illustrations and photographs, print bleedthrough, substandard margins, and improper alignment can adversely affect reproduction.

In the unlikely event that the author did not send UMI a complete manuscript and there are missing pages, these will be noted. Also, if unauthorized copyright material had to be removed, a note will indicate the deletion.

Oversize materials (e.g., maps, drawings, charts) are reproduced by sectioning the original, beginning at the upper left-hand corner and continuing from left to right in equal sections with small overlaps. Each original is also photographed in one exposure and is included in reduced form at the back of the book.

Photographs included in the original manuscript have been reproduced xerographically in this copy. Higher quality 6" x 9" black and white photographic prints are available for any photographs or illustrations appearing in this copy for an additional charge. Contact UMI directly to order.

UMI

**A Bell & Howell Information Company
300 North Zeeb Road, Ann Arbor MI 48106-1346 USA
313/761-4700 800/521-0600**



UNIVERSITY OF OKLAHOMA
GRADUATE COLLEGE

**LEAK-OFF AND CLEANUP BEHAVIOR OF FRACTURING
FLUIDS IN THE PRESENCE OF MOBILE HYDROCARBONS**

A Dissertation

SUBMITTED TO THE GRADUATE FACULTY

in partial fulfillment of the requirements for the

degree of

Doctor of Philosophy

By

BALKRISHNA GADIYAR

Norman, Oklahoma

1997

UMI Number: 9810312

**UMI Microform 9810312
Copyright 1997, by UMI Company. All rights reserved.**

**This microform edition is protected against unauthorized
copying under Title 17, United States Code.**

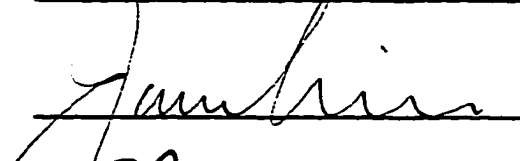
UMI
300 North Zeeb Road
Ann Arbor, MI 48103

**LEAK-OFF AND CLEANUP BEHAVIOR OF FRACTURING
FLUIDS IN THE PRESENCE OF MOBILE HYDROCARBONS**

**A DISSERTATION APPROVED FOR THE
SCHOOL OF PETROLEUM AND GEOLOGICAL ENGINEERING**

By











**© Copyright by Balkrishna R. Gadiyar 1997
All Rights Reserved.**

ACKNOWLEDGEMENTS

I would like to take this opportunity to express my sincere gratitude and thanks to the following:

Dr. Anuj Gupta, for his excellent guidance and advise throughout my graduate research. I really enjoyed working with him. He has always shared his rich experience with me as a result I learned a lot. His optimism, moral support, and friendly nature made my efforts much easier.

Dr. Faruk Civan, for serving as a co-chairman on my dissertation committee and for always being open to discussion.

Dr. Subhash Shah, for serving on my dissertation committee. He has always been open to discussion and has given me valuable assistance.

Dr. Roy Knapp and Dr. Thomas Dewers, for serving on my dissertation committee.

School of Petroleum and Geological Engineering and Dr. Anuj Gupta, for providing me financial support throughout my graduate work.

Mike Shaw and Craig Bodenhamer, for their help in building and maintaining the experimental apparatus.

Fracturing Fluid Characterization Facility (FFCF), for providing the necessary chemicals, and for giving permission to conduct experiments at the facility.

Milt Bishop, Joe Flenniken, Ruth Brown, Paul Gracey, and other personnel at FFCF for their help, support, and friendship.

Uday Shivaswamy, Wenwu Xia, and Mahadev Ammachathram, for helping me in collecting data for my experiments, and for their friendship.

Naval Goel, for lending his technical expertise in using the Bohlin rheometer, and for his friendship.

A very special thanks goes to Uday Shivaswamy, Rajeev Chhabra, Vishal Bansal, Vishal Singal, Umesh Chitnis, Rajat and Tripti Bhatnagar, Parag Karmarkar, Umesh Choori, Manesh, Grazina, Anu and Priya Halasyam, Bhanu, and Bharath Rao who have been very close pals and for morally supporting me.

To all my friends, especially to Kit Jongkittinarukorn, Wei Wang, Sezai Ucan, Mike Hankinson, Steve Kelly, David Larkin, Brian Tate, Rohit Panse, Arvind Salecha,

Vibhas, Shailesh Ekbote, and Shilpa Pandey, and so many others for their friendship and support.

To my family, without whose love, encouragement, and support I would not have been here today.

Last but not the least, to god, for all the blessings.

Dedicated to my parents

TABLE OF CONTENTS

ACKNOWLEDGEMENTS	iv
LIST OF TABLES	ix
LIST OF FIGURES	x
ABSTRACT	xv
Chapter 1 Introduction and Background	1
1.1 Introduction.....	1
1.2 Review of Previous Work.....	8
1.3 Objectives.....	10
Chapter 2 Experimental Setup and Procedures	12
2.1 Experimental Setup.....	12
2.1.1 Dynamic Leak-off Core Holder.....	12
2.1.2 Fracturing Fluid Circulation System.....	15
2.1.3 Proportioning Pump.....	17
2.1.4 Pressure Transducer Manifold.....	17
2.1.5 Data Acquisition.....	17
2.1.6 Back Pressure Regulator (BPR).....	17
2.1.7 Gas flow-meter and Balance.....	18
2.2 General Experimental Procedures.....	18
2.2.1 Core Sample Preparation.....	18
2.2.2 Initial Permeability.....	18
Chapter 3 Model Development	20
3.1 Model Formulation.....	20
3.1.1 Transport of Fluid Phases.....	20
3.1.1.1 Initial Condition.....	23
3.1.1.2 Boundary Conditions.....	23
3.1.2 Polymer Concentration in the Filtrate.....	24
3.1.3 Filter Cake Model.....	25
3.2 Numerical Solution.....	26
Chapter 4 Dynamic Leak-off in Gas Reservoirs	28
4.1 Introduction.....	28
4.2 Experimental Procedures.....	28
4.2.1 Core Samples.....	28
4.2.2 Initial Permeability.....	29
4.2.3 Fracturing Fluids.....	29
4.2.4 Leak-off in the Presence of Mobile Gas Saturation.....	30
4.2.4 Single-Phase Leak-off.....	30
4.3 Discussion of Experimental Results.....	32
4.3.1 Comparison of Single-Phase and Two-Phase Leak-off.....	32
4.3.2 Effectiveness of Fluid Loss Additive During Two-Phase Leak-off.....	37

4.4 Discussion of Model Results	40
Chapter 5 Dynamic Leak-off in Oil Reservoirs	48
5.1 Introduction.....	48
5.2 Experimental Procedures	49
5.3 Results and Discussion.....	50
5.3.1 Impact of Mobile Oil Saturation on the Leak-off of Linear Fluids	50
5.3.1.1 Comparison Between Single-Phase and Two-Phase Leak-off.....	53
5.3.1.2 Effect of Sectional Permeability on Two-Phase Leak-off	58
5.3.1.3 Effectiveness of Fluid Loss Additives During Two-Phase Leak-off	58
5.3.1.4 Simulation Results.....	63
5.3.1.5 Post-treatment Leak-off Behavior	63
5.3.2 Impact of Mobile Oil Saturation on the Leak-off of Crosslinked Fluids.....	71
5.3.2.1 Leak-off of Crosslinked Guar	72
5.3.2.2 Leak-off of Crosslinked HPG	74
5.3.2.3 Effect of FLA on Leak-off.....	77
5.3.2.4 Leak-off of Linear Fluids.....	81
5.3.2.5 Effect of crude oil on the Leak-off of Crosslinked HPG.....	81
5.3.2.6 Effect of pressure drop on leak-off.....	86
5.3.2.7 Effect of First Section Permeability on C_w	86
5.3.2.8 Simulation Results.....	86
Chapter 6 Return Permeability Testing for Oil Reservoirs	98
6.1 Introduction.....	98
6.2 Experimental Procedures	99
6.3 Results and Discussion.....	103
6.3.1 Recovery of Return Permeability After Leak-off With Crosslinked Guar .	103
6.3.2 Recovery of Return Permeability After Leak-off With Crosslinked HPG .	107
6.3.3 Return Permeability After Leak-off of Linear Gel in Oil Cores.....	110
6.3.4 Effect of Fluid Loss Additives and Shut-in Time.....	112
6.3.5 Effect of Crude Oil on Regain Permeability	116
Chapter 7 Development of a Dimensionless Correlation.....	120
7-1 Introduction	120
7-2 Model Formulation.....	122
7.3 Results and Discussion.....	124
Chapter 8 Conclusions and Recommendations	133
8.1 Conclusions Drawn from Leak-off Studies	133
8.2 Conclusions Drawn from Return Permeability Study	134
8.3 Conclusions Drawn from Dimensionless Model Study.....	134
8.4 Future Work.....	135
NOMENCLATURE.....	136
LITERATURE CITED	138
APPENDIX A.....	141
Calculation of Cake Permeability	141

LIST OF TABLES

Table 4.1: Summary of core properties	29
Table 4.2: Initial sectional brine permeabilities	29
Table 4.3: Operating conditions	30
Table 4.4: Summary of C_w and V_{sp} for linear fluids in the presence of gas	34
Table 4.5: Input parameters for simulations	40
Table 5.1: Core and fluid properties and operating conditions	52
Table 5.2: Initial sectional permeability to brine	52
Table 5.3: Apparent viscosity of the effluent filtrate	52
Table 5.4: Summary of C_w and V_{sp} for linear fluids in the presence of oil	53
Table 5.5: Estimated filter cake permeabilities	55
Table 5.6: Initial sectional and overall brine and oil permeability	71
Table 5.7: Summary of operating conditions	72
Table 5.8: Summary of C_w and V_{sp} for crosslinked fluids in the presence of oil	72
Table 6.1: Sectional and overall brine and oil permeability	102
Table 6.2: Fluids and FLA used and summary of total leak-off volume	102
Table 7.1: Summary of optimized parameters	126

LIST OF FIGURES

Fig. 1-1: Schematic of Fracture Propagation and Development of Zones.....	3
Fig. 1-2: Typical Cumulative Leak-off Plot.....	5
Fig. 1-3: Effect of C_w on Fracture Half Length.....	7
Fig. 2-1: Schematic of Experimental Setup for Gas Reservoirs.....	13
Fig. 2-2: Schematic of Experimental Setup for Oil Reservoirs.....	14
Fig. 2-3 Cross Section of the Core Holder.....	16
Fig. 3-1: Schematic of Model Flow System.....	22
Fig. 3-2: Flow Chart of the Model.....	27
Fig. 4-1: Measured Relative Permeability Curves for Gas and Brine.....	31
Fig. 4-2: Comparison of Leakoff Behavior of 60 lb/Mgal HPG With Fluid Loss Additive in Single Phase and Two Phase.....	33
Fig. 4-3: Pressure Drop Profile During Single Phase Leakoff.....	35
Fig. 4-4: Pressure Drop Profile During Leakoff in the Presence of Gas Saturation.....	36
Fig. 4-5: Comparison of Fluid Loss for a 60 lb/Mgal HPG With and Without Fluid Loss Additive in the Presence of Gas Saturation.....	38
Fig. 4-6: Comparison of Leakoff Velocity for Fracturing Fluid With and Without Additive.....	39
Fig. 4-7: Comparison of Experimental and Simulation Results (Single Phase).....	42
Fig. 4-8: Comparison of Experimental and Simulated Pressure Drop Profile During Single Phase Leakoff.....	43
Fig. 4-9: Comparison of Experimental and Simulation Results During Two Phase Leakoff.....	44
Fig. 4-10: Comparison of Experimental and Simulated Pressure Drop Profile During Leakoff in the Presence of Gas.....	45
Fig. 4-11: Comparison of Simulation and Experimental Results During Two Phase Leakoff in the Absence of Additive.....	46

Fig. 4-12: Comparison of Experimental and Simulated Pressure Drop Profiles During Leakoff in the Presence of Gas (without Additive)	47
Fig. 5-1: Measured Pore Throat Size Distribution of Berea Sandstone Core Sample ..	51
Fig. 5-2: Comparison of Single and Two Phase Dynamic Leakoff Behavior of 40 lb/Mgal HPG with Silica Flour	54
Fig. 5-3: Pressure Drop Profile During Single Phase Leakoff (Test 5-1).....	56
Fig. 5-4: Pressure Drop Profile During Two Phase Leakoff (Test 5-4).....	57
Fig. 5-5: Effect of First Section Permeability on Two Phase Leakoff.....	59
Fig. 5-6: Functional Dependency of 40 lb/Mgal Linear HPG Leakoff on Fracture Face Permeability.....	60
Fig. 5-7: Effect of Fluid Loss Additive on Leakoff During Single and Two Phase Dynamic Leakoff.....	62
Fig. 5-8: Sectional Pressure Gradient During Two Phase Leakoff (Test 5-4).....	64
Fig. 5-9: Comparison of Experimental and Simulated Leakoff in Presence of Mobile Oil Saturation (Test 5-2)	65
Fig. 5-10: Comparison of Experimental and Simulated Leakoff in Presence of Mobile Oil Saturation (Test 5-3).....	66
Fig. 5-11: Comparison of Experimental and Simulated Leakoff in Presence of Mobile Oil Saturation (Test 5-4).....	67
Fig. 5-12: Effect of Shut-in on the Leakoff Behavior of 35 lb/Mgal HPG with 25 lb/Mgal Silica Flour (Test 5-5).....	69
Fig. 5-13: Effect of Shut-in on the Leakoff Behavior of 40 lb/Mgal HPG with 50 lb/Mgal Silica Flour	70
Fig. 5-14: Comparison Between Leakoff of crosslinked 35 lb/Mgal Guar in Brine and Oil Cores	73
Fig. 5-15: Pressure Gradient Profile in the 0-2" Section of Brine and Oil Cores During the Leakoff of Crosslinked Guar	75
Fig. 5-16: Comparison Between Leakoff of Crosslinked 35 lb/Mgal HPG in Brine and Oil Cores	76

Fig. 5-17: Effect of Fluid Loss Additive (FLA) on the Leakoff of Crosslinked 35 lb/Mgal HPG in Oil Cores.....	78
Fig. 5-18: Sectional Pressure Gradient During Leakoff of 35 lb/Mgal Crosslinked HPG + FLA in Oil Core.....	79
Fig. 5-19: Sectional Pressure Gradient During Leakoff of 35 lb/Mgal Crosslinked HPG in Oil Core.....	80
Fig. 5-20: Comparison Between Linear and Crosslinked 35 lb/Mgal Guar and HPG Leakoff in Oil Cores	82
Fig. 5-21: Sectional Pressure Gradient During Leakoff of 35 lb/Mgal Linear HPG in Oil Core	83
Fig. 5-22: Sectional Pressure Gradient During Leakoff of 35 lb/Mgal Linear Guar in Oil Core	84
Fig. 5-23: Comparison Between Leakoff of Crosslinked 35 lb/Mgal HPG in Mineral and Crude Oil Core.....	85
Fig. 5-24: Effect of Pressure Drop on the Leakoff of 35 lb/Mgal Crosslinked HPG in Crude Oil Saturated Core Samples.....	87
Fig. 5-25: Effect of Fracture Face Permeability on C_w of 35 lb/Mgal Crosslinked HPG in Mineral Oil Saturated Core Samples.....	88
Fig. 5-26: Comparison of Model Predicted and Experimentally Measured Leak-off (Test 6-1)	90
Fig. 5-27: Comparison of Predicted and Observed Pressure Gradient (Test 6-1)	91
Fig. 5-28: Comparison of Model Predicted and Experimentally Measured Leak-off (Test 6-4)	92
Fig. 5-29: Comparison of Predicted and Observed Pressure Gradient (Test 6-4)	93
Fig. 5-30: Comparison of Model Predicted and Experimentally Measured Leak-off (Test 6-7)	94
Fig. 5-31: Comparison of Model Predicted and Experimentally Measured Leak-off (Test 6-8)	95
Fig. 5-32: Comparison of Predicted and Observed Pressure Gradient (Test 6-7)	96

Fig. 5-33: Comparison of Model Predicted and Experimentally Measured Leak-off (Test 6-9)	97
Fig. 6-1: Schematic of Flow Directions and Permeability Measurement Locations	101
Fig. 6-2: Effect of 35 lb/Mgal Crosslinked Guar Leakoff on the Regain Permeability of Brine Core (Test 6-1)	104
Fig. 6-3: Effect of 35 lb/Mgal Crosslinked Guar Leakoff on the Regain Permeability of Oil Core (Test 6-2)	105
Fig. 6-4: Effect of 35 lb/Mgal Crosslinked HPG Leakoff on the Regain Permeability of Brine Core (Test 6-3)	108
Fig. 6-5: Effect of 35 lb/Mgal Crosslinked HPG Leakoff on the Regain Permeability of Oil Core (Test 6-4)	109
Fig. 6-6: Effect of 35 lb/Mgal Linear HPG Leakoff on the Regain Permeability of Oil Core (Test 6-5)	111
Fig. 6-7: Effect of 35 lb/Mgal Linear Guar Leakoff on the Regain Permeability of Oil Core (Test 6-6)	113
Fig. 6-8: Effect of 35 lb/Mgal Crosslinked HPG + 25 lb/Mgal FLA Leakoff on the Regain Permeability of 12 mD Oil Core (Test 6-7) Shut-in Time 12 hrs	114
Fig. 6-9: Effect of 35 lb/Mgal Crosslinked HPG + 25 lb/Mgal FLA Leakoff on the Regain Permeability of 35 mD Oil Core (Test 6-8) Shut-in Time 3 hrs	115
Fig. 6-10: Effect of Crosslinked HPG Leakoff on the Regain Permeability of a Crude Oil Saturated Core (Test 6-9)	118
Fig. 6-11: Impact of Filtered and Non-filtered Crude Oil on the Initial Crude Oil Permeability	119
Fig. 7-1: Comparison of Model and Experimental Leakoff Results of Borate Crosslinked 35 lb/Mgal HPG (Test 6-3)	125
Fig. 7-2: Comparison of Model and Experimental Leakoff Results of Borate Crosslinked 35 lb/Mgal Guar (Test 6-1)	127
Fig. 7-3: Effect of Globalized Parameters on Model Predictions (Borate Crosslinked 35 lb/Mgal HPG Leakoff)	128

Fig. 7-4: Effect of Globalized Parameters on Model Predictions (Borate Crosslinked 35 lb/Mgal Guar Leakoff).....	129
Fig. 7-5: Comparison of Model and Experimental Leak-off Results of Borate Crosslinked 35 lb/Mgal HPG in the HPS.....	131
Fig. 7-6: Comparison of Model and Experimental Leak-off Results of Borate Crosslinked 35 lb/Mgal HPG + 25 lb/Mgal Silica Flour in the HPS.....	132

ABSTRACT

Fracturing fluid leak-off characteristics have a significant impact on the final geometry and size of a hydraulic fracture. Fluid loss into the permeable fracture face reduces the overall efficiency of a fracturing fluid. In order to create a fracture with desirable flow characteristics and for the purpose of predicting fracture geometry, the ability to determine the leak-off characteristics of the fluid-formation pair is extremely important. Generally, the fluid leak-off data is obtained for a candidate fracturing fluid using formation core samples that are completely saturated with brine. In contrast to this any reservoir rock of interest has a significant movable gas/oil saturation.

The first part of this study presents the results of a series of laboratory experiments conducted to investigate the dynamic leak-off behavior of fracturing fluids in the presence of mobile gas or oil saturation. Fracturing fluid leak-off in low permeability gas saturated and high permeability oil saturated reservoir rocks is examined under conditions of varying fracturing fluid composition, formation permeability, oil composition, and fracturing pressure. The effectiveness of fluid loss additives in controlling the leak-off during multiphase flow near the fracture face is also investigated. In addition, a conceptual model to predict the leak-off in the presence of mobile gas or oil saturation at the fracture face has been developed. The model is validated using data obtained from dynamic leak-off experiments.

The results indicate that the leak-off characteristics in the presence of mobile gas or oil saturation are significantly different compared to those observed in the

presence of 100% brine saturation. In the case of mobile gas saturation, the spurt loss appears to be driven by spontaneous imbibition whereas the long time leak-off is controlled by relative permeability effects. The wall building coefficients are found to be at least an order of magnitude lower than those observed in 100% brine saturated core samples. The fluid loss additive used in this study, appears to have little or no effect on leak-off. In the case of mobile oil saturation, both oil viscosity and relative permeability effects play a role in determining the leak-off response. The spurt loss is significantly lower than that observed in 100% brine saturated core samples. In this case also, the fluid loss additive has little or no effect on leak-off. The leak-off characteristics exhibit a noticeable sensitivity to the formation permeability.

During the fracturing of high permeability formation there is a potential of reducing the permeability near the fracture face and hence the overall producibility of the formation due to fracturing fluid leak-off. In the second part of this study, the extent of impairment in formation permeability to oil due to the leak-off of fracturing fluid in oil reservoirs and subsequent recovery during production is evaluated and characterized. The experiments are conducted with a number of commonly used fracturing fluids. Effect of shut-in time, fluid loss additive, fracturing fluid composition, production rates, and oil composition on the regain permeability of oil reservoirs is investigated.

The results indicate that the recovery of permeability in the presence of oil is higher compared with that in the presence of 100% brine saturated cores. The recovery, especially for linear and crosslinked hydroxypropyl guar (HPG), is greater than 100% of the original permeability and its is dependent on the shut-in time. The

fluid loss additive does not appear to effect the regain permeability. The production rate has a positive impact on regain permeability.

A dimensionless correlation to determine the cumulative leak-off volume into the rock matrix during the dynamic filtration of a fracturing fluid is presented in the last section. The correlation is developed based on dimensional analysis. The model is validated using data obtained from dynamic leak-off experiments.

Chapter 1

Introduction and Background

1.1 Introduction

Hydraulic fracturing has been the most widely used stimulation technique in the petroleum industry for last four decades. According to Gidley *et al.*¹, 35-40% of the wells drilled in the U.S. are hydraulically fractured and economically produce 25-30% of the total U.S. oil and gas reserves. The goal of hydraulic fracturing is to increase the productivity of a well by creating a large conductive flow region, in the form of a fracture, connected to the wellbore. In order to create and propagate a fracture in the reservoir, high viscosity fracturing fluids are pumped into the wellbore at very high pressures which exceed the strength of the formation.

The most common fracturing fluids used in majority of fracturing treatments are composed of water soluble polymers, such as guar, hydroxypropyl guar (HPG), hydroxyethyl cellulose (HEC), carboxymethyl hydroxypropyl guar (CMHPG), etc. Some of these polymers (guar, HPG) can be crosslinked to enhance their viscosity. The most widely used crosslinkers are borate and zirconate. The crosslinked fluids exhibit improved proppant transport and temperature stability. A good fracturing fluid should exhibit the following characteristics¹:

- **minimizes fluid loss into the formation**
- **maintains sufficient effective viscosity to create the desired fracture geometry and transport the proppant in the fracture**
- **causes minimum damage to the formation and proppant pack**
- **exhibits good degradability so that it can be easily flowed back**
- **maintains high temperature stability**
- **offers cost effectiveness**

This study focuses on the leak-off and cleanup characteristics of fracturing fluids.

The fracturing fluids have a tendency to leak-off or filter into the formation mainly due to excess pressure in the fracture compared to the formation pressure. The leak-off of the fracturing fluid is also dependent on the permeability of the formation, shear rate imposed on the fracturing fluid, type and concentration of the polymer, and the fluid phases present in the formation. Fluid loss additives (FLAs') are added to the fracturing fluids in order to control leak-off. The FLA used are of two types, particulate and/or hydrocarbon phase. The most commonly used particulate and hydrocarbon FLAs' are silica flour and 5% diesel, respectively. Three zones are developed during leak-off and are shown in Fig. 1-1. The mechanisms which govern leak-off in individual zones are:

- 1. Wall building effects (filter cake zone) - As the fracturing fluid leaks off into the formation a filter cake starts to build up on the fracture face due to the deposition of FLA and/or polymer as shown in Fig. 1-1. The filter cake offers a significant barrier to further leak-off. The wall building coefficient (C_w) and spurt loss (V_{sp}) characterize the wall building effects. The wall building effects can be determined**

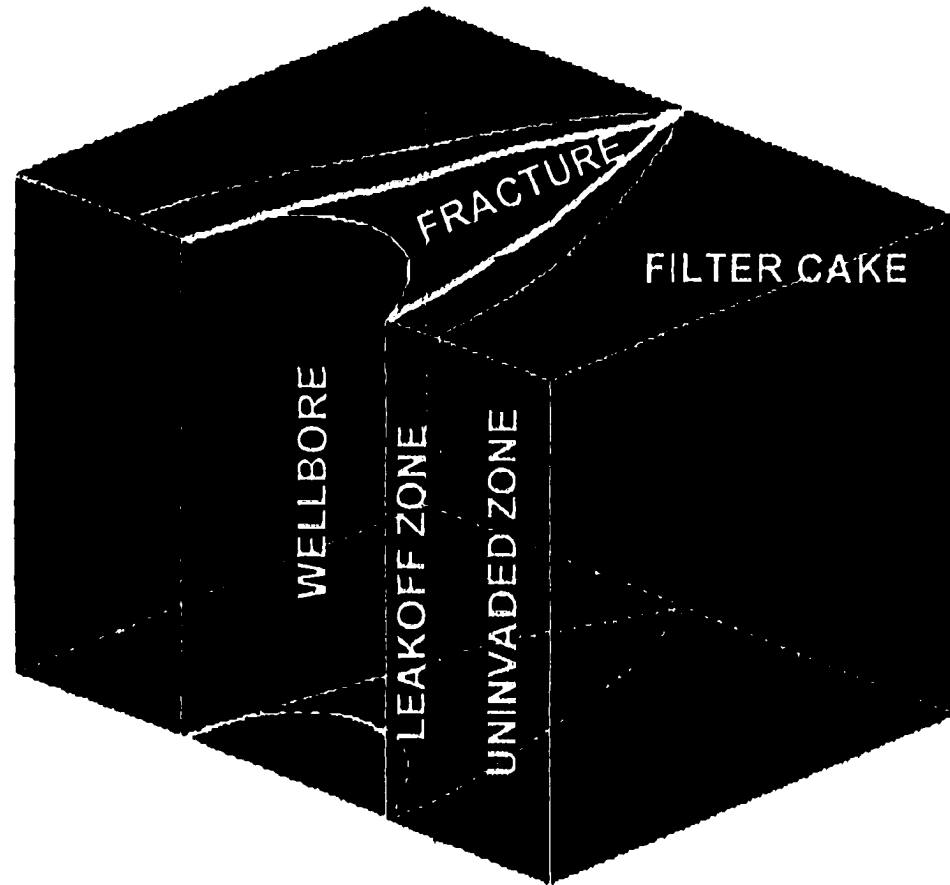


Fig. 1-1: Schematic of Fracture Propagation and Development of Zones

experimentally and analytically. When experimentally obtained leak-off volume is plotted against \sqrt{t} in Cartesian coordinates, a straight line is observed at later times as illustrated in Fig. 1-2. Based on the slope and the intercept of the straight line, the wall building coefficient and spurt loss can be determined from Eq. 1-1 and Eq. 1-2, respectively:

$$C_w = \frac{0.0164 m}{A}, \quad (1-1)$$

where m is the slope and A is cross-sectional area of the formation, and,

$$V_{sp} = \frac{0.246b}{A}, \quad (1-2)$$

where b is the intercept¹.

2. Filtrate viscosity and relative permeability effects (invaded zone) - The viscosity of the filtrate in the invaded zone is also responsible for controlling the leak-off. There are at least two fluid phases present in the invaded zone and as a result relative permeability is expected to play an important role in governing leak-off.
3. The compressibility and viscosity of the reservoir fluid in the uninvaded zone also effect the leak-off.

Traditionally, only low permeability ($k < 10$ mD) gas-bearing formations were routinely fractured hydraulically. However, recently there has been a tremendous interest in fracturing higher permeability formations. There is a vast difference in the objectives of fracturing low and high permeability formations. The goal of fracturing low permeability reservoirs is to achieve a long and narrow fracture without tip screenout. A tip screenout occurs when the concentration of the proppant near the tip of the fracture increases rapidly due to high fluid loss. In the case of fracturing high

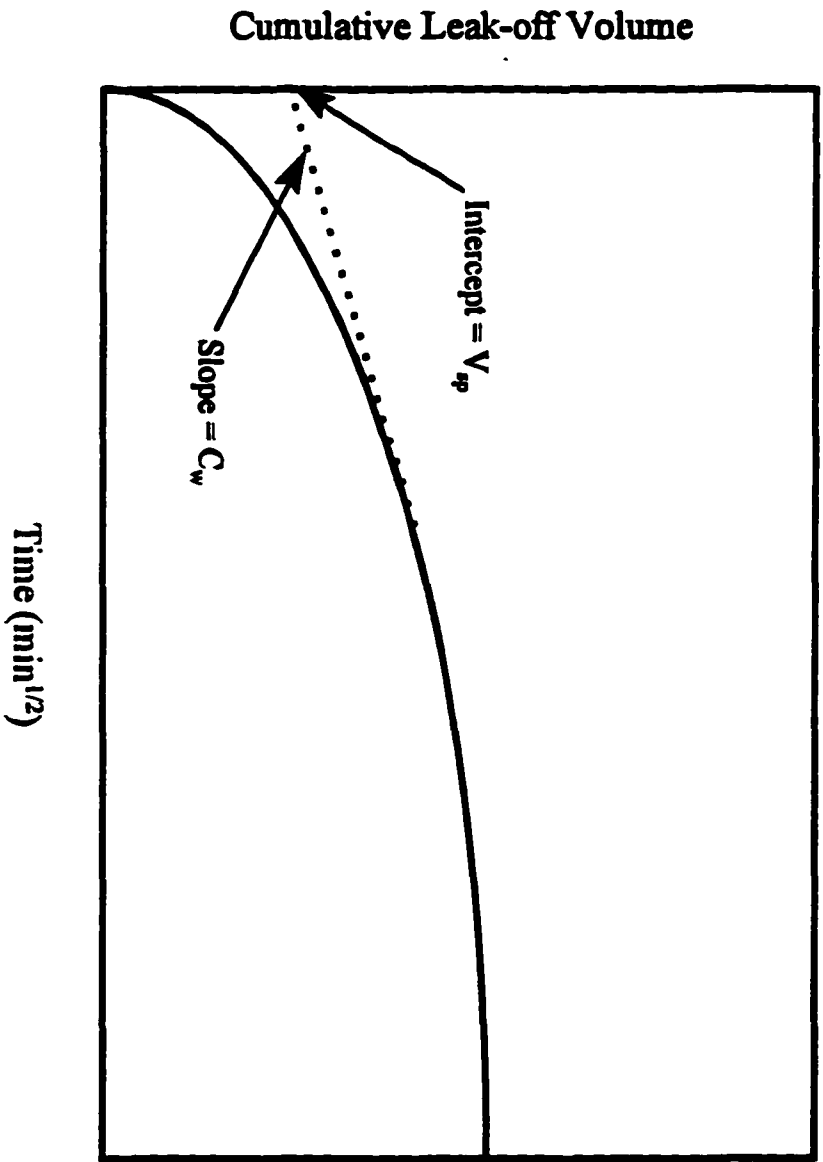


Fig. 1-2: Typical Cumulative Leak-off Plot

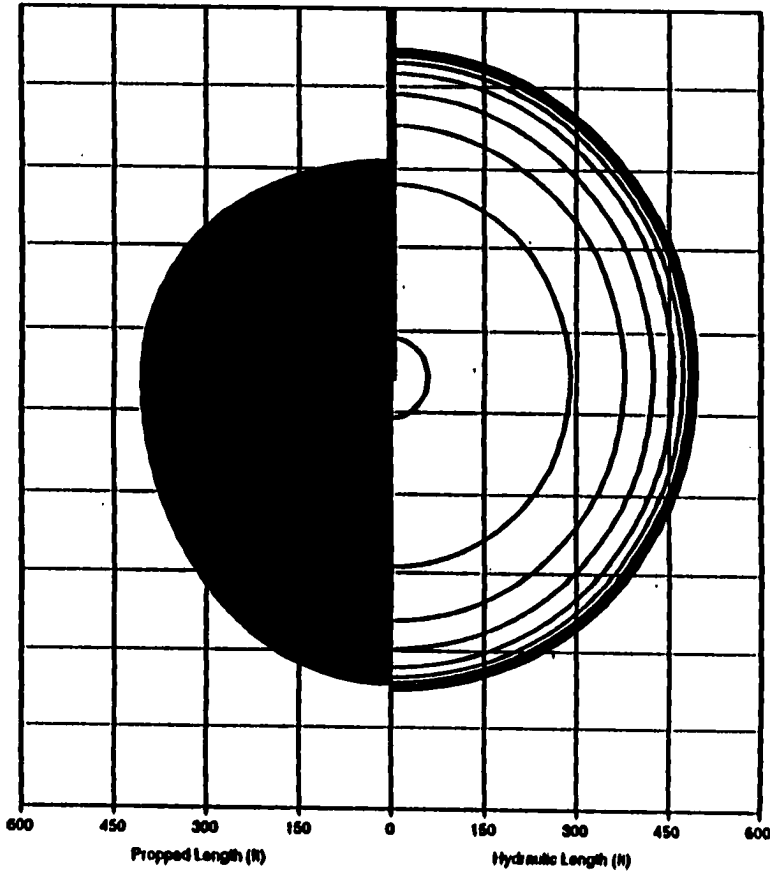
permeability formation, the objective is to maximize the fracture conductivity by creating short and wide fracture with tip screenout. In both the cases, C_w and V_p are very important parameters which govern fracture geometry and treatment performance.

While designing low and high permeability hydraulic fracturing treatments, the fracture geometry is always predetermined. The leak-off data obtained from experiments is used as an input in deciding the volume of fracturing fluid required to create a desired fracture geometry. The effect of variation in C_w on fracture length is shown in Fig. 1-3. The 3-D model in FracPro™ was used to predict the fracture length. C_w was varied and all other parameters used in the model were held fixed. It is evident from the figure that significantly longer fracture was computed for lower C_w . Therefore, an accurate understanding of fracturing fluid leak-off behavior is important for designing a successful hydraulic fracturing treatment. Inaccurate prediction of leak-off may lead to premature job termination and improper placement of proppant within the fracture.¹

Conducting laboratory fluid loss experiments on core samples is a convenient way of understanding fluid leak-off mechanisms. Fluid leak-off studies can be conducted in the laboratory either under static or dynamic conditions. The main difference is that under static conditions the fracturing fluid and thus the filter cake formed is not subjected to shear. Dynamic leak-off testing more accurately captures the essential features of the conditions existing in an actual fracture. Usually, the results obtained under static conditions underestimate the leak-off response. The review presented in this chapter is restricted to dynamic leak-off studies. A detailed review of static leak-off studies is given by McGowen *et al.*² and Penny and Conway.³

7

$C_w = 0.0001 \text{ ft}/\text{min}^{1/2}$



$C_w = 0.001 \text{ ft}/\text{min}^{1/2}$

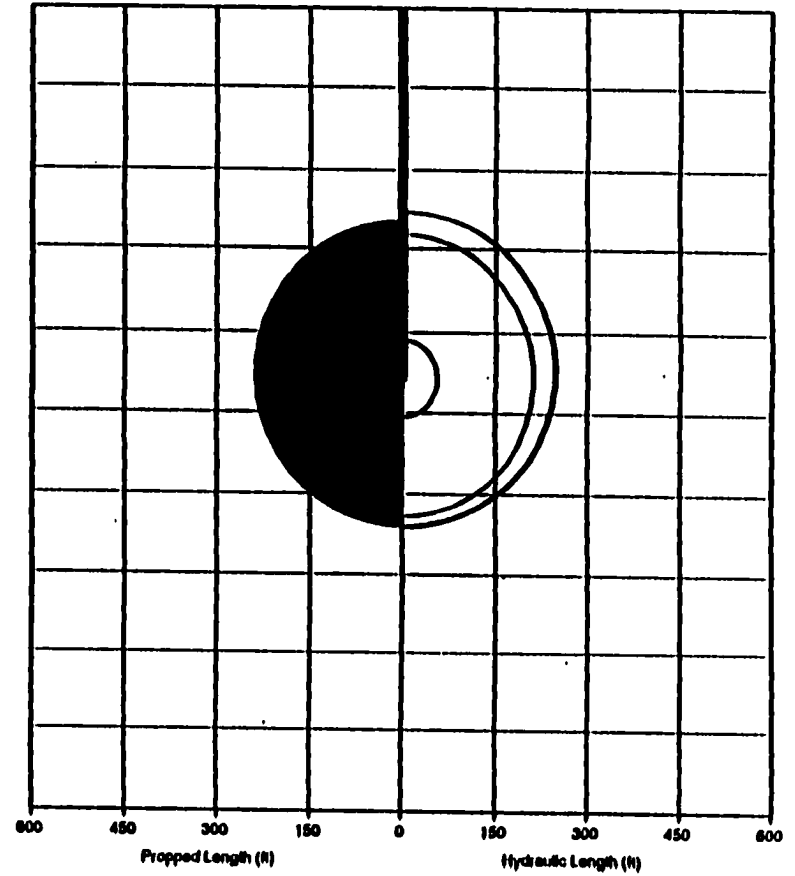


Fig. 1-3: Effect of C_w on Fracture Half Length

1.2 Review of Previous Work

Numerous dynamic leak-off studies⁴⁻²⁰ have been conducted to investigate the effect of pressure, shear rate, permeability, FLA, polymer concentration, etc. on fracturing fluid leak-off. Most of these studies focus on leak-off in low permeability formations.

Rodhart⁴, Penny⁵, and others^{6-9,15} investigated the effect of pressure, shear rate, and formation permeability on the leak-off behavior of different fracturing fluids. According to their findings, C_w is dependent on pressure drop and is also very sensitive to shear rate. Spurt loss is directly proportional to permeability whereas C_w is independent of permeability, within the range of permeability investigated. Based on the results of Rodhart⁴, C_w for both crosslinked HPG with 5% diesel and HEC with silica flour follows a $\sqrt{\Delta P}$ relationship. This indicated that the filter cake formed was incompressible (i.e. the permeability of the filter cake is independent of pressure drop). According to Ford *et al.*⁶, C_w is a function of $\Delta P^{1/6}$ and is highly dependent on shear rate. The leak-off rate increases with the increase in shear rate.

The fracturing fluid undergoes degradation in the fracture due to the variation in shear rate and temperature. McGowen *et al.*¹⁰ studied the effect of fluid degradation on leak-off. The results indicated that there was an increase in V_{sp} and a slight decrease in C_w as the fluid degrades.

Penny *et al.*³, Rodhart⁴, and several others^{6,8-9,11-14} have reported that the use of FLAs' (diesel and silica flour) drastically reduces the leak-off of both linear and crosslinked fracturing fluids. In the presence of silica flour, V_{sp} for crosslinked fluid is reduced by an order of magnitude.⁴ Based on the results of Harris *et al.*⁸, 5% diesel

had a significant effect on C_w for crosslinked fluid but less effect on linear fluid. Penny *et al.*³ examined the relative effectiveness of FLA as a function of permeability. Their results indicated that for reservoirs with permeability greater than 5 mD, particulate additives are necessary to control the spurt loss. Combination of particulate and hydrocarbon FLA provided a better control on leak-off.¹³ Recently, McGowen *et al.*¹⁴ reported that linear fluids with hydrocarbon FLA does not control leak-off. They also reported that particulate FLA is effective in reducing V_{sp} but has very little effect on C_w .

Recently, Vithal *et al.*¹⁵ reported that the leak-off of linear fluids is shear rate independent. They also reported that in very low permeability formations leak-off of linear fluids can be lower than that of crosslinked fluids. Further, they observed that filter cake formed during leak-off of both linear and crosslinked fluids is highly compressible.

Navarrete *et al.*¹⁶⁻¹⁷, Vithal *et al.*¹⁵, McGowen *et al.*¹⁸, and Parlar *et al.*¹⁹ have conducted dynamic leak-off studies with limited fluid systems in high permeability core samples. Their findings indicated that for most of the fracturing fluids, internal filter cake governs fluid leak-off. However, as opposed to Vithal *et al.*¹⁵, they observed that the leak-off of crosslinked fluids is lower compared to that of linear fluids. Navarrete *et al.*¹⁶ also demonstrated that the effectiveness of FLA increases with the increase in formation permeability and that shear rate does not significantly affect spurt loss.

Parlar *et al.*¹⁹ investigated the effect of core length, pressure drop, permeability, and polymer concentration on leak-off in high permeability core samples. Their results

showed that at least 6 inch long core samples should be used while studying leak-off in high permeability cores. The following are the findings based on their study:

- 90% of the total leak-off is due to spurt loss in the case of borate crosslinked guar
- spurt loss is directly proportional to pressure drop and permeability
- leak-off volume decreases with the increase in polymer concentration

Lord *et al.*²⁰ studied the leak-off of fracturing fluids in a large scale, high pressure fracture simulator having a total leak-off area of 3912 cm². Their findings indicated that spurt loss was higher in the simulator compared to that observed in studies having a leak-off area of 5 - 20 cm². In addition, they observed that internal pore plugging governs the leak-off of crosslinked fluids and external filter cake was formed only if the fracture surface was rough.

The core samples used in the past studies reviewed here, were completely saturated with brine. In contrast to this any reservoir rock of interest has a significant amount of movable gas and/or oil saturation. The presence of movable gas and/or oil saturation can have a significant effect on the leak-off and cleanup characteristics of fracturing fluids.

1.3 Objectives

The objectives of this study are as follows:

1. Characterize the leak-off behavior of fracturing fluids, with and without fluid loss additives, in the presence of mobile gas saturation in low permeability formations.
2. Characterize the leak-off behavior of fracturing fluids, with and without fluid loss additives, in the presence of mobile oil saturation in high permeability formations.

Study the sensitivity of leak-off behavior to fracturing fluid composition, fracture pressure, formation permeability, and oil composition.

- 3. Develop a mathematical model to predict leak-off in the presence of mobile gas or oil saturation.**
- 4. Evaluate and characterize the extent of impairment in formation permeability to oil due to the leak-off of fracturing fluids in oil reservoirs.**
- 5. Develop a dimensionless correlation to predict leak-off.**

In order to accomplish these objectives, a mathematical model was developed and dynamic filtration experiments were conducted on core samples containing mobile gas or oil saturation. The experimental results were used to validate the model.

Chapter 2 describes the experimental apparatus and procedures used in this study. In Chapter 3, formulation of a mathematical model to predict leak-off is presented. The model incorporates the current understanding of the flow of non-Newtonian fluids, filtration and cake buildup, and multiphase flow in the porous media. Chapters 4 and 5 discuss the results of dynamic leak-off in gas and oil reservoirs, respectively. The impact of fracturing fluid leak-off on return permeability of oil reservoirs is discussed in Chapter 6. The methodology followed to develop the dimensionless correlation to predict leak-off is discussed in Chapter 7. Finally, based on the findings of this study, conclusions and recommendations for future work are discussed in Chapter 8.

Chapter 2

Experimental Setup and Procedures

In order to characterize the dynamic leak-off behavior of fracturing fluids, an experimental apparatus was designed and assembled in the laboratory. In this chapter, various components of the experimental setup are described. The common procedures applied to all the experiments are also outlined here. Modifications in the procedures are discussed in respective chapters.

2.1 Experimental Setup

Schematics of the flow system for dynamic leak-off testing in the presence of mobile gas and oil are illustrated in Figs. 2-1 and 2-2, respectively. The major components of the flow system are dynamic leak-off core holder, fracturing fluid circulation system, and pressure transducer manifold.

2.1.1 Dynamic Leak-off Core Holder

A Hassler-type, multiple pressure port core holder with additional features for studying dynamic leak-off behavior is used in this study. Core samples of 2-inch diameter and up to 12-inch length can be tested in this core holder. It consists of five pressure ports at an equal spacing of 2-inch which permit measurement of differential pressure across different sections of the core sample. The pressure ports

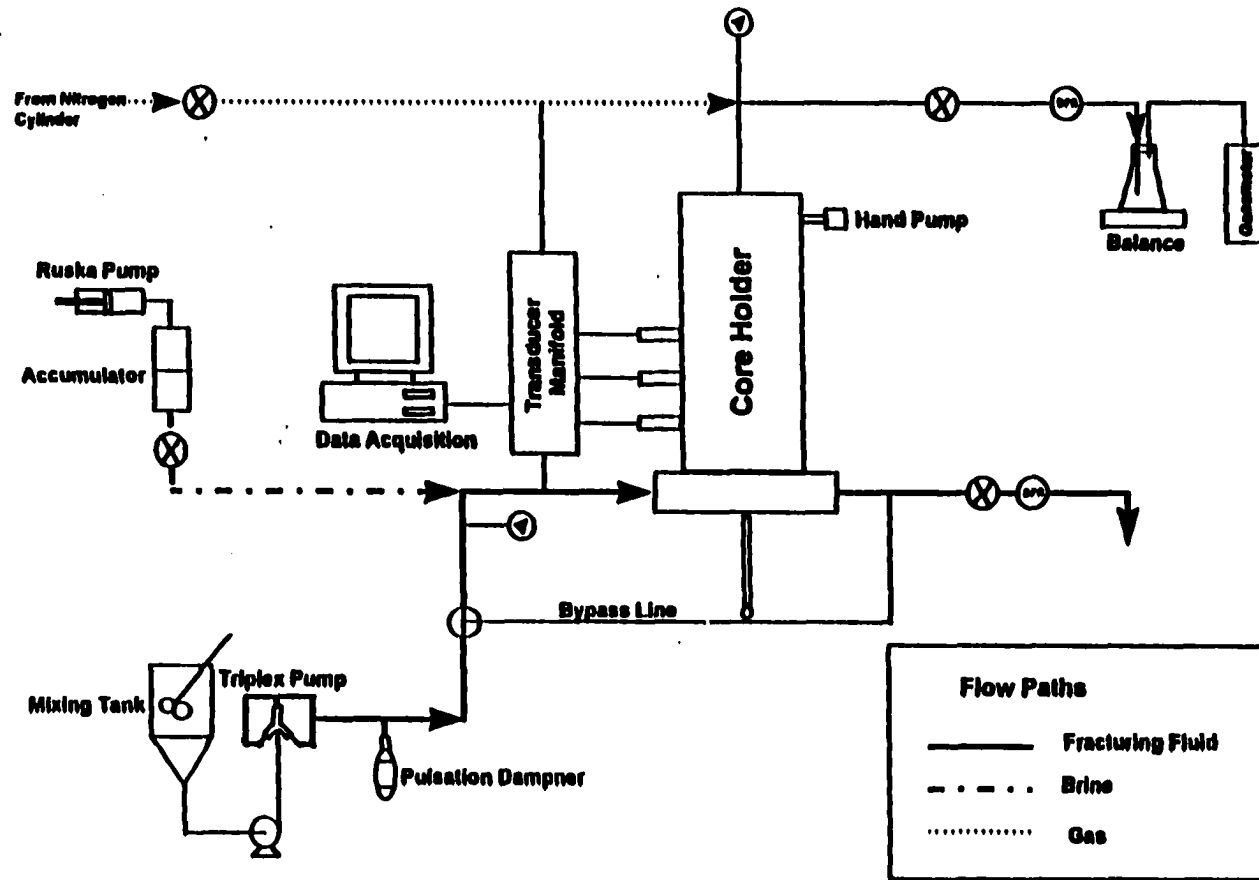


Fig. 2-1: Schematic of Experimental Setup for Gas Reservoirs

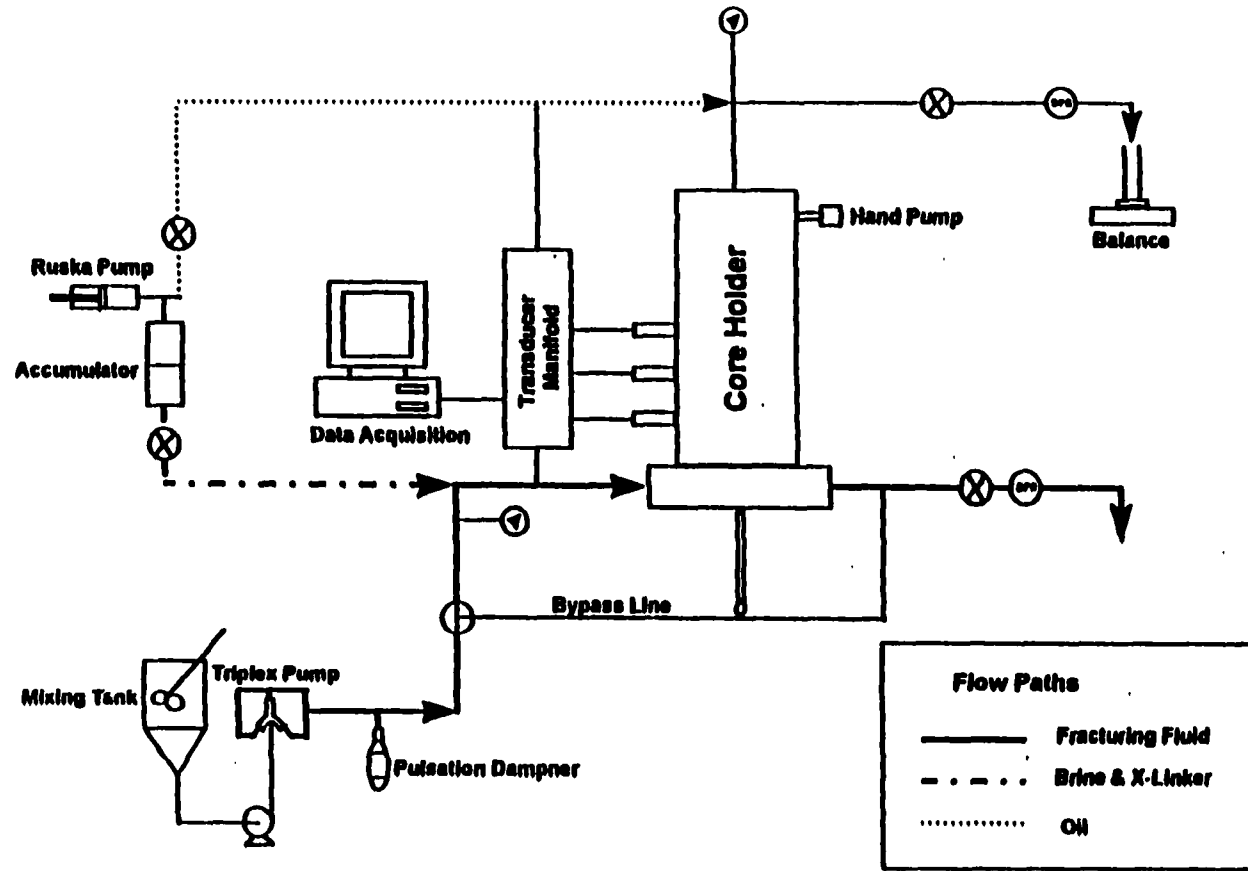


Fig. 2-2: Schematic of Experimental Setup for Oil Reservoirs

are connected to a pressure transducer manifold which facilitates the monitoring of the alteration in sectional and overall permeabilities of the core sample. The core holder has a pressure and temperature rating of 10,000 psi and 350°F, respectively.

A cross-sectional view of the core holder is shown in Fig. 2-3. The core holder is provided with a rectangular cross-section flow channel (slot) on the upstream end which simulates tangential flow across the face of the fracture. The slot is machined on a movable piston which allows for adjustable gap between the slot and the core face in order to vary the shear rate of fracturing fluid on the filter cake. The fracturing fluid flows across the face of the reservoir rock sample while the filtrate invades the sample. The core holder allows the flow of fluids in both directions.

2.1.2 Fracturing Fluid Circulation System

The circulation system consist of a triplex pump, a pulsation dampener, and a mixing tank for the fracturing fluid. The triplex pump is used for injecting the fracturing fluid through the slot at a desired flow rate while maintaining a constant pressure drop across the core sample. The triplex pump has a pressure rating of 3000 psi. A pulsation dampener is placed in the flow circuit to ensure that the pressure fluctuations generated by the triplex pump are minimal ($\pm 2\%$).

Uniform composition of the fracturing fluid is maintained throughout the experiment by continuously mixing the fracturing fluid in the mixing tank. A centrifugal pump is used for pumping the fracturing fluid from the mixing tank to the triplex pump.

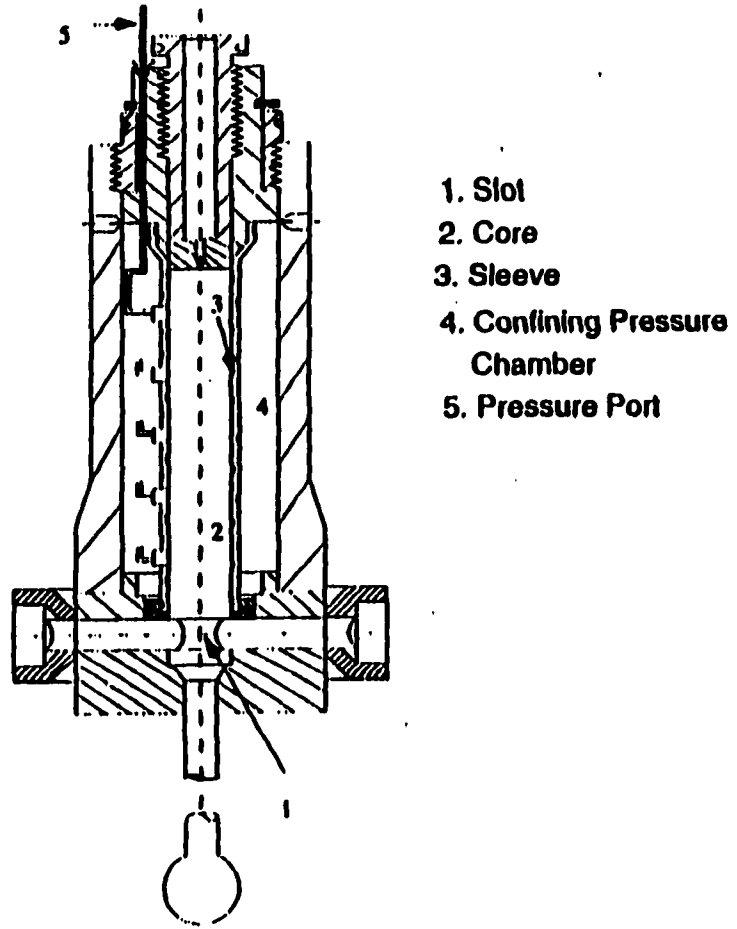


Fig. 2-3: Cross Section of the Core Holder (from Temco)

2.1.3 Proportioning Pump

A Ruska proportioning pump is used for injecting brine, mineral, and crude oil into the core sample. The available flow rate range for the pump is from 0.083 to 18.67 cm³/min. The pressure rating of the pump is 12,000 psi. This pump is also used to inject the crosslinker into the stream of polymer solution pumped by the triplex.

2.1.4 Pressure Transducer Manifold

Validyne differential pressure transducers are used for measuring sectional and overall pressure drop across the core sample. In all experimental runs, sectional pressure drops across the first three 2 inch long sections of the core sample are measured. In order to accurately measure pressure drop, transducers of varying ranges are used. A dead weight tester is used to calibrate the transducers.

2.1.5 Data Acquisition

A PC interface card is used to interface a computer directly to the transducers. A compatible data acquisition protocol is used for automatic data acquisition and storage.

2.1.6 Back Pressure Regulator (BPR)

A constant differential pressure across the core sample is maintained by installing nitrogen dome-loaded back pressure regulators in the upstream fracturing fluid flow loop and on the downstream production end as illustrated in Fig. 2-1. This ensures a convenient boundary condition for simulating the process of dynamic filtration.

2.1.7 Gas flow-meter and Balance

In the case of leak-off in the presence of mobile gas saturation, a Ruska gas flow-meter is used for measuring the cumulative production (volume) of the effluent gas. In order to separate the effluent fluid from the gas, a fluid trap is placed on a balance used for monitoring effluent fluid production.

2.2 General Experimental Procedures

A radial confining pressure of 1500 psig was applied to the core samples in all the experiments reported. The experiments were conducted at room temperature. Identical core sample preparation and initial permeability measurement procedures were followed for all the experiments.

2.2.1 Core Sample Preparation

The core samples were prepared by drilling 2-inch diameter cores using a diamond coring bit. The samples were trimmed to the required length using a diamond face grinding saw. The faces of the core sample were carefully prepared to ensure that they were perpendicular to the axis of the sample. The core samples were dried in an oven at 120° C. The weights of the core samples were recorded after drying and after vacuum saturation. The porosity of the sample was measured using Barne's fluid saturation method and the liquid permeability was measured in the core holder. Details on the type and properties of the core samples used is given in respective chapters.

2.2.2 Initial Permeability

The core sample was first vacuum saturated with the desired brine, 3% CaCl₂ brine for carbonate samples or 3% KCl brine for sandstone samples, after subjecting the sample to a vacuum for at least 12 hours. The core sample was then loaded into the

core holder and desired brine was injected at a constant flow rate, while maintaining a backpressure of 400-500 psig, until the differential pressure across various sections of the core sample stabilized and no gas bubbles were observed in the effluent. In order to verify 100% saturation of the core sample, flow rate of the brine was doubled and differential pressure across various sections of the core sample was monitored until it stabilized. The effluent brine was collected in a pre-weighed container placed on a precision balance.

Chapter 3

Model Development

3.1 Model Formulation

In order to formulate a model to simulate dynamic filtration, the core sample is considered to be isotropic and incompressible. Gravity forces are aligned with the hydrodynamic forces due to the one dimensional vertical flow in the system. Further, the filtrate, and gas or oil are considered to be immiscible, and flow of the filtrate and oil in the core sample is considered to be laminar, incompressible and isothermal. The porosity and permeability of the filter cake are assumed to be constant. The listed assumptions are reasonable for the laboratory filtration studies utilized for validation. For field applications the model can readily be modified to accommodate deviations from the assumptions. A schematic of the flow system being modeled in this study is shown in Fig. 3-1. The flow system involves interaction between various types of flow that are incorporated in the model as follows: 1) transport of fluid phases in the reservoir rock, 2) filtrate polymer mass balance, and 3) filter cake model.

3.1.1 Transport of Fluid Phases

The continuity equation for the flow of the filtrate phase in the reservoir rock is given by:

$$\phi \frac{\partial}{\partial t} (\rho_f S_f) + \frac{\partial}{\partial y} (\rho_f u_f) = 0 \quad (3-1)$$

where S_f is saturation, u_f is superficial velocity, and ρ_f is density of the filtrate. ϕ is porosity of the reservoir rock, t is time, and y is distance from the entry face.

Using Darcy's law, the superficial velocity of the filtrate is:

$$u_f = - \frac{k k_{rf}}{\mu_f} \left(\frac{\partial P_f}{\partial y} - \rho_f g \frac{\partial h}{\partial y} \right) \quad (3-2)$$

where, k_{rf} is relative permeability to the filtrate, k is absolute permeability of the reservoir rock, μ_f is viscosity of the filtrate, g is acceleration due to gravity, and h is height measured from a reference level.

Considering the pressure variations usually encountered in dynamic filtration processes, it is reasonable to treat the filtrate as incompressible and combine Eqs. (3-1) and (3-2) to obtain a relationship between pressure and saturation of the filtrate:

$$\frac{\partial}{\partial y} \left[\frac{k k_{rf}}{\mu_f} \left(\frac{\partial P_f}{\partial y} - \rho_f g \frac{\partial h}{\partial y} \right) \right] = \phi \frac{\partial S_f}{\partial t} \quad (3-3)$$

The analogous equation for gas flow where the compressibility effects cannot be ignored is:

$$\frac{\partial}{\partial y} \left[\frac{k k_{rg} \rho_g}{\mu_g} \left(\frac{\partial P_g}{\partial y} - \rho_g g \frac{\partial h}{\partial y} \right) \right] = \phi \frac{\partial (\rho_g S_g)}{\partial t} \quad (3-4)$$

Equations (3-3) and (3-4) are solved for filtrate and gas pressure and saturation variations with distance and time using the auxiliary equations, initial and boundary conditions. According to the definition of capillary pressure:

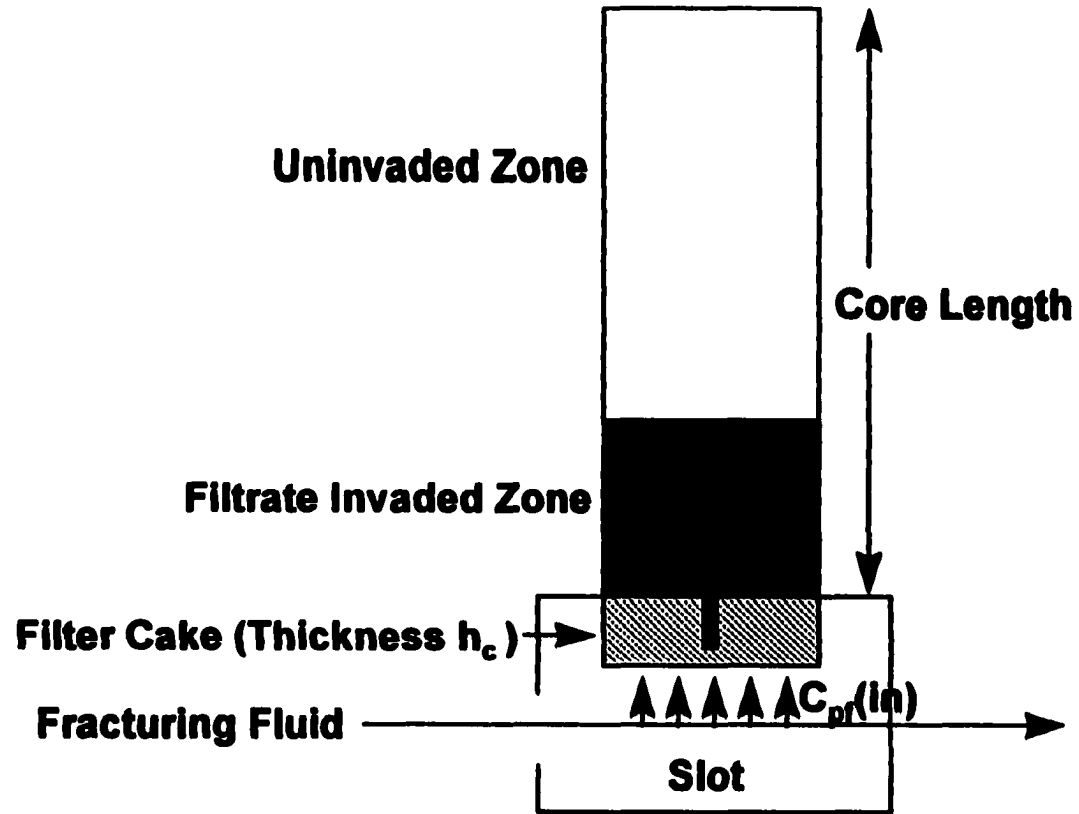


Fig. 3-1: Schematic of Model Flow System

$$P_c = P_g - P_f \quad (3-5)$$

and because gas and filtrate are the only two fluids present in the reservoir rock,

$$S_f + S_g = 1 \quad (3-6)$$

As a corollary of Eq.(3-6),

$$\frac{\partial S_f}{\partial t} + \frac{\partial S_g}{\partial t} = 0 \quad (3-7)$$

3.1.1.1 Initial Condition

The initial distribution of saturation is needed in order to predict the time and space variation of filtrate and gas saturation. For the experiments reported in this study, the residual water saturation at all locations in the core sample were stabilized before the flow of fracturing fluid was initiated. Therefore,

$$\text{At time, } t = 0, S_f = S_{wr}, 0 \leq y \leq L \quad (3-8)$$

where L is the length of the sample.

Further, no capillary pressure was imposed on the sample which indicates that initial filtrate leak-off is analogous to spontaneous imbibition.

3.1.1.2 Boundary Conditions

In the experiments reported, fracturing fluid was introduced at a constant pressure into the slot and the core outlet was maintained at atmospheric pressure. After the filtrate leak-off was initiated, zero capillary pressure was maintained at the core inlet. Therefore,

$$P_f = P_g = (P_{inj} - \Delta P_{cake}), y = 0, t > 0 \quad (3-9)$$

where P_{inj} is the injection pressure and ΔP_{cake} is pressure drop across the filter cake determined using Eq.(3-19) derived below. At the core outlet, the boundary condition is specified as:

$$P_f = 0, y=L, t>0 \quad (3-10)$$

3.1.2 Polymer Concentration in the Filtrate

During the leak-off of fracturing fluid into the reservoir rock, some of the polymer in the fracturing fluid is expected to be retained by the porous media. Assuming that the polymer transport can be accounted for by considering dispersion, the continuity equation for the transport of polymer in the filtrate is²¹

$$\phi \frac{\partial (S_f C_{pf})}{\partial t} + \frac{\partial (u_f C_{pf})}{\partial y} - \frac{\partial}{\partial y} \left(\phi S_f D \frac{\partial C_{pf}}{\partial y} \right) = 0 \quad (3-11)$$

where C_{pf} is the mass concentration of polymer in the filtrate and D is overall dispersion coefficient that is expected to account for polymer adsorption/retention in the reservoir rock.

The initial conditions for Eq. (3-11) are provided by Eq. (3-8) and Eq. (3-12).

$$C_{pf} = 0, 0 \leq y \leq L, t = 0 \quad (3-12)$$

Boundary conditions are specified by:

$$\left(u_f C_{pf} \right)_{in} = u_f C_{pf} - \phi S_f \left(D \frac{\partial C_{pf}}{\partial y} \right), y = 0, t > 0 \quad (3-13)$$

and

$$C_{pf} = 0, y=L, 0 < t < t_{bt} \quad (3-14)$$

where $C_{pf(in)}$ is the filtrate polymer concentration at the face of the filter cake, and t_{bt} is the filtrate breakthrough time at the outlet.

3.1.3 Filter Cake Model

As the leak-off of the fracturing fluid progresses an external filter cake build-up at the face of the fracture is initiated. For dynamic leak-off, the filter cake build-up is the net result of the opposing processes of deposition and erosion occurring simultaneously. Therefore, the rate of cake build-up is²¹⁻²²

$$\frac{dh_c}{dt} = \frac{u_{in} (C_{pf(in)} - C_{pf(out)}) - K_e \gamma}{(1 - \phi_c) \rho_c} \quad (3-15)$$

such that,

$$h_c = 0, \quad t = t_0 \quad (3-16)$$

In Eq.(3-15), $C_{pf(out)}$ is the concentration of polymer entering the reservoir rock, h_c is the cake thickness, K_e is the erosion rate constant, γ is shear rate on cake surface, ϕ_c is porosity of the filter cake, ρ_c is density of cake-solids, and t_0 is time when leak-off starts.

The filter cake erosion rate constant is expected to depend on the characteristics of the fracturing fluid as well as the roughness of the fracture face. As the thickness of the cake increases the width of the fracture (slot) decreases which in turn increases the shear rate and, thereby decreases viscosity. The decrease in viscosity is expected to cause an increase in leak-off rate. Assuming a power law relation for the fracturing fluid, the viscosity,

$$\mu = K\gamma^{(n-1)} \quad (3-17)$$

where K is the fluid consistency index, n is the flow behavior index, and γ is the shear rate. It can be shown that the shear rate in the fracture is¹

$$\gamma_w = \left(\frac{2n+1}{3n} \right) \frac{6q}{d(w_s - h_c)^2} \quad (3-18)$$

where d is the height of the fracture, w_s is the width of the slot, and q is the flow rate.

According to Darcy's law, the pressure drop across the filter cake is

$$\Delta P_{\text{cake}} = \frac{u_{in} \mu_f h_c}{k_c} \quad (3-19)$$

In order to predict leak-off in the presence of mobile oil saturation, a similar model presented above is used except that Eq. (3-4) was replaced by the following equation:

$$\frac{\partial}{\partial x} \left[\frac{k k_{ro}}{\mu_o} \left(\frac{\partial P_o}{\partial x} \right) \right] = \phi \frac{\partial S_o}{\partial t} \quad (3-20)$$

where subscript o denotes oil phase.

3.2 Numerical Solution

A three-point-centered, second-order approximate finite-difference scheme is used to discretize the differential equations describing the model. An implicit pressure and explicit saturation (IMPES) technique is applied for the pressure-saturation equation. The polymer transport equation is solved using an implicit scheme and the cake build-up equation is solved using an explicit scheme. Equal spacing was used for all the grid blocks in the one dimensional system, except for the first block which was as wide as the thickness of the cake. A flow chart of the model implementation is shown in Fig. 3-2.

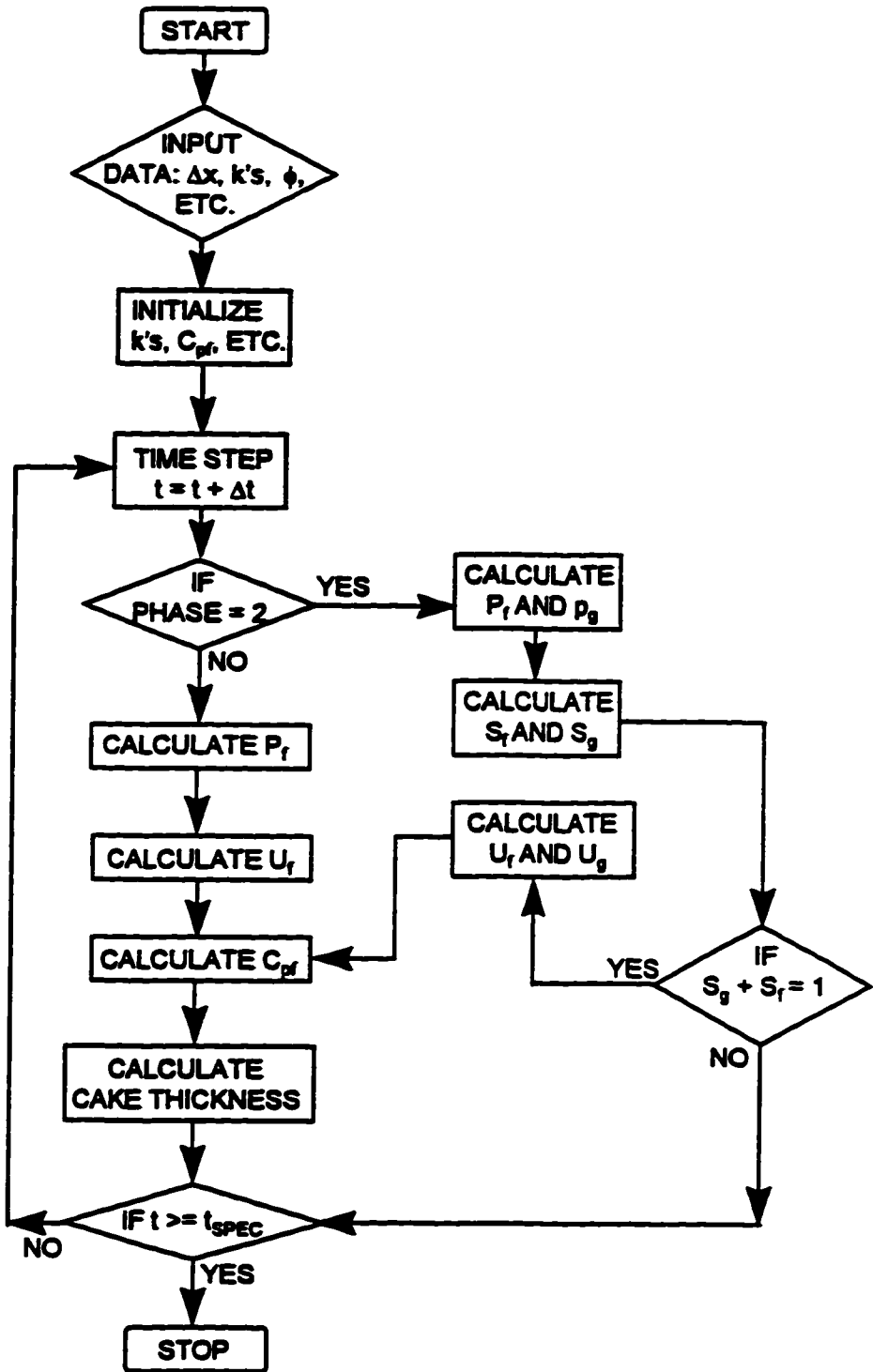


FIG. 3-2: Flow Chart Of The Model

Chapter 4

Dynamic Leak-off in Gas Reservoirs

4.1 Introduction

Hydraulic fracturing is an effective stimulation technique used to optimize the production of gas wells.²³⁻²⁴ The fractures and their flow characteristics are critical to the deliverability of many gas wells. The leak-off characteristics of a fracturing fluid have a significant effect on the gas flow characteristics of such hydraulic fractures and formation fracture interface. For a given reservoir system the leak-off of fracturing fluid into the reservoir should be minimized in order to achieve a cost effective fracture stimulation. In this chapter, the details of the study on dynamic leak-off behavior of fracturing fluids in the presence of mobile gas saturation are presented.

4.2 Experimental Procedures

The procedures followed in this study are discussed in the following sections.

4.2.1 Core Samples

Cordoba cream limestone core samples were used in this study. The core samples were prepared according to the procedure given in Chapter 2. The properties of the core samples utilized are listed in Table 4-1.

Table 4.1: Summary of core properties

	Test 4-1	Test 4-2	Test 4-3
Overall permeability (mD)	0.11	0.38	0.30
Porosity (%)	15.34	15.40	15.38
Core Length (cm)	24.28	24.84	22.76

4.2.2 Initial Permeability

The initial permeability (sectional and overall) of the core sample is determined according to the procedure described in Chapter 2. The initial, overall, and sectional permeabilities of the core sample are calculated using measured pressure drop for each section and Darcy's law, and are reported in Tables 4-1 and 4-2, respectively.

Table 4.2: Initial sectional brine permeabilities (mD)

Test	0-2 inch	2-4 inch	4-6 inch	6-outlet
4-1	0.03	0.70	0.60	0.43
4-2	0.10	1.18	1.38	1.84
4-3	0.08	1.45	3.22	1.75

4.2.3 Fracturing Fluids

Dynamic filtration characteristics of 60 lb/Mgal hydroxypropyl guar (HPG), with and without fluid loss additive are studied. The fluid loss additive used is 50 lb/Mgal silica flour.

During the leak-off testing, the pressure drop across the core samples is maintained at 1000 psid and the shear rate on the fracturing fluid is maintained at 55 sec^{-1} . The operating conditions for various experiments are summarized in Table 4-3.

Table 4.3: Operating conditions

	Test 4-1	Test 4-2	Test 4-3
Mobile phase	Brine	Gas	Gas
Leak-off pressure (psi)	1000	1000	1000
Fracturing fluid	Linear HPG	Linear HPG	Linear HPG
FLA	Silica flour	Silica flour	-

4.2.4 Leak-off in the Presence of Mobile Gas Saturation

After determining the initial permeability of the core sample, the in-situ brine is displaced with nitrogen at a constant pressure drop of 500 psid until the brine saturation reaches residual saturation. The cumulative production of effluent brine and gas is monitored continuously with the aid of a precision balance and a gas flow-meter. Complete gas-brine relative permeability curves are computed based on the production and pressure history data after gas breakthrough as illustrated in Fig. 4-1. The JBN method²⁵ was used to obtain the relative permeability curves.

Fracturing fluid is then circulated across the face of the core sample at a constant pressure drop of 1000 psid across the core sample and at a known shear rate. The cumulative leak-off volume is determined by measuring the cumulative volume of the effluent gas and the filtrate with respect to time.

4.2.4 Single-Phase Leak-off

For the purpose of comparing leak-off behavior in single-phase and two-phase flow systems, a single-phase fracturing fluid leak-off experiment is also conducted. After determining the initial permeability to the brine, the fracturing fluid is circulated across the face of the core sample using the same experimental conditions as in the case of a two-phase leak-off experiment. The effluent production is monitored using a precision balance.

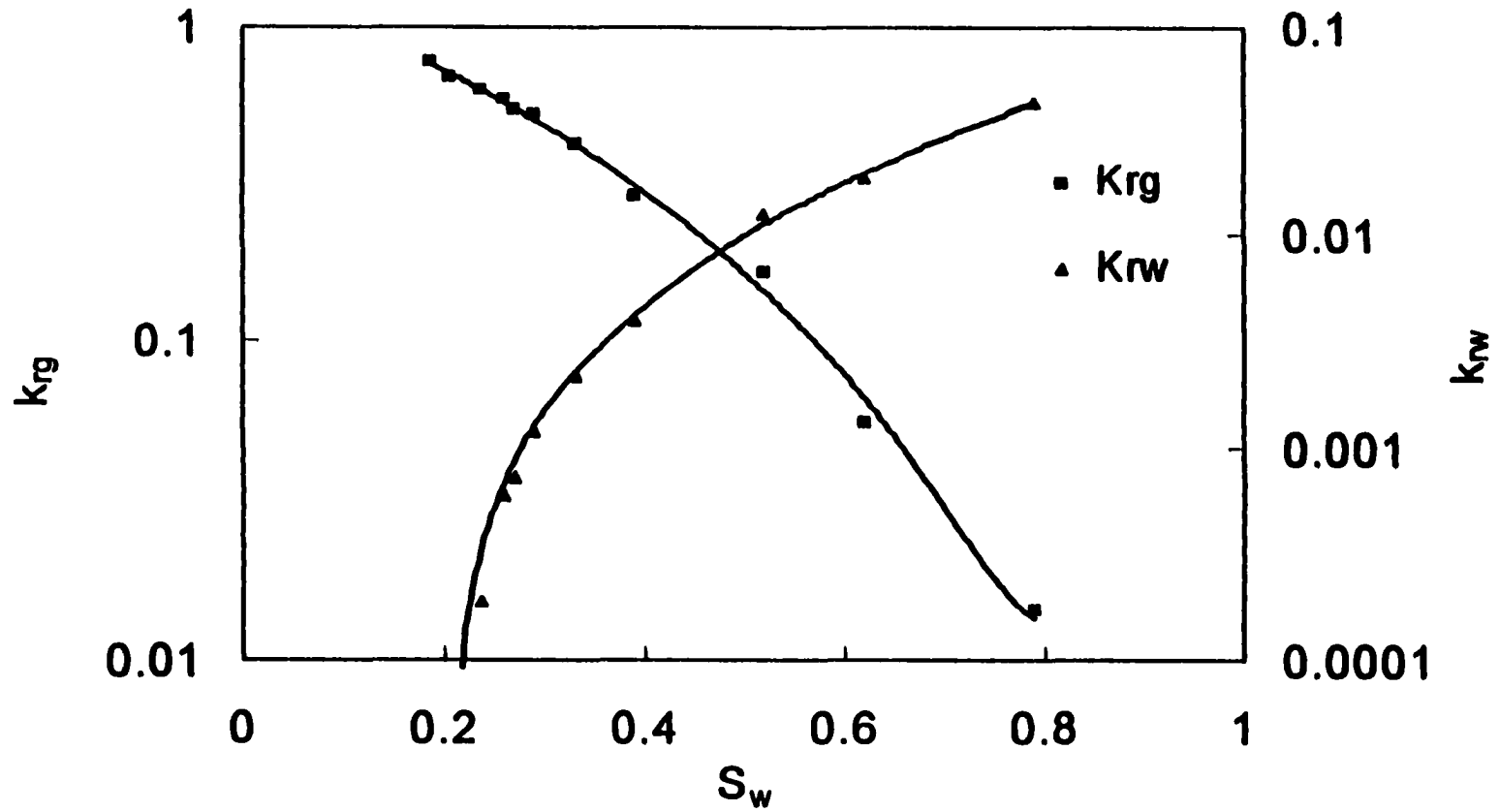


Fig. 4-1: Measured Relative Permeability Curves for Gas and Brine

4.3 Discussion of Experimental Results

The first test presented is a single-phase dynamic leak-off experiment. The other tests represent two-phase dynamic leak-off experiments in the presence of mobile gas saturation with and without fluid loss additive.

4.3.1 Comparison of Single-Phase and Two-Phase Leak-off

Figure 4-2 illustrates the comparison of single and two-phase leak-off behavior of a fracturing fluid containing 60 lb/Mgal HPG with fluid loss additive in Cordoba cream limestone. The permeability of the first section of core samples in both experiments was significantly reduced during the initial brine permeability measurements. In the case of single-phase leak-off, the data exhibited no spurt loss. This is consistent with the behavior of very tight formations. However, the leak-off behavior does not exhibit a typical variation on the plot of cumulative leak-off vs. \sqrt{t} . The plot indicates that the formation of filter cake does not reduce the leak-off. Such behavior is feasible when the permeability of the filter cake is comparable to the permeability of the first section of the core as suggested by data in Table 4-2 and interpretation of cake permeability in Table 4-5. The permeability of the filter cake is determined based on pressure profile and velocity history across the first section of the core sample. A sample calculation is shown in Appendix A.

The two-phase leak-off characteristics are noticeably different compared to the single-phase leak-off. Based on the cumulative leak-off volume plotted against \sqrt{t} , spurt loss is observed. Spurt loss occurs because of initial spontaneous imbibition of the filtrate into the sample that is initially at residual brine saturation. After the initial spurt loss, the lower relative permeability to filtrate lowers the filtrate invasion rate into

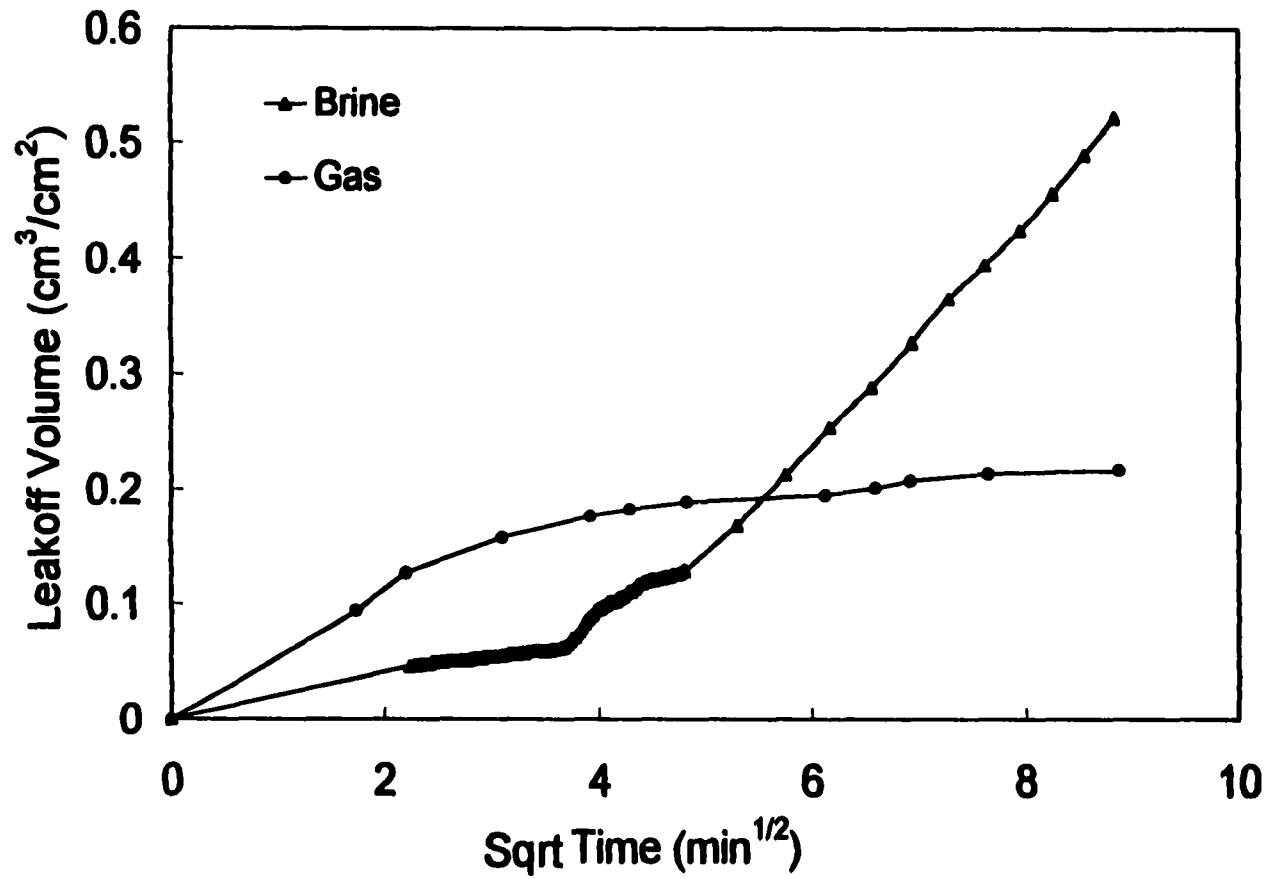


Fig. 4-2: Comparison of Leakoff Behavior of 60 lb/Mgal HPG With Fluid Loss Additive in Single Phase and Two Phase

the formation. Fluid loss starts to follow a linear behavior only after a significant time lag which indicates that the filter cake is compacted fully over a long period of time.

The C_w and V_{sp} were determined for individual experiment based on the equations given in Chapter 1 and are summarized in Table 4-4. It is evident from Table 4-4 that C_w in the presence of gas decreases approximately by an order of magnitude when compared to that observed in 100% brine saturated core sample. Therefore, if one were to design a fracturing job based on the C_w value obtained from brine cores, the fracture geometry would be under-predicted (based on Fig. 1-3).

Table 4.4: Summary of C_w and V_{sp} for linear fluids in the presence of gas

Test	Mobile Phase	C_w (ft/min ^{1/2})	V_{sp} (gal/100 ft ²)
4-1	Brine	1.73E-3	0.00
4-2	Gas	1.60E-4	3.33
4-3	Gas	1.67E-4	2.75

The pressure drop profile during single-phase and two-phase leak-off as a function of time and position is depicted in Figs. 4-3 and 4-4, respectively. The highest pressure drop in both tests occurs in the first section, which includes pressure drop across the filter cake. Further, the pressure gradients in the first section and in the other three sections in the case of single-phase leak-off do not vary in a measurable manner with time. This behavior indicates that the filtrate flow in single-phase leak-off is indistinguishable from brine flow, i.e., cake characteristics do not change with time and the filtrate has practically the same viscosity as the native brine. In the case of two-phase leak-off, a variation in the pressure drop in the last two sections is observed, providing some indication of a front propagation.

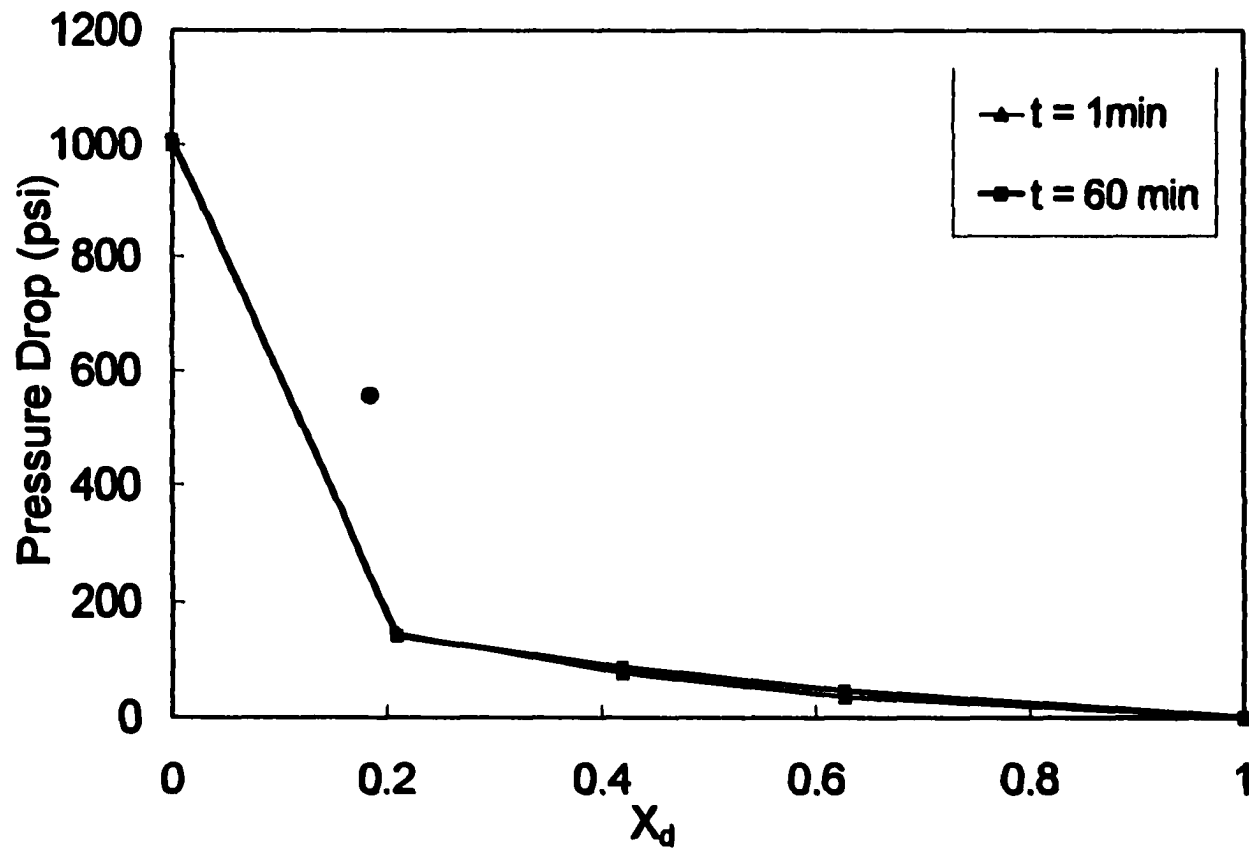


Fig. 4-3: Pressure Profile During Single Phase Leakoff

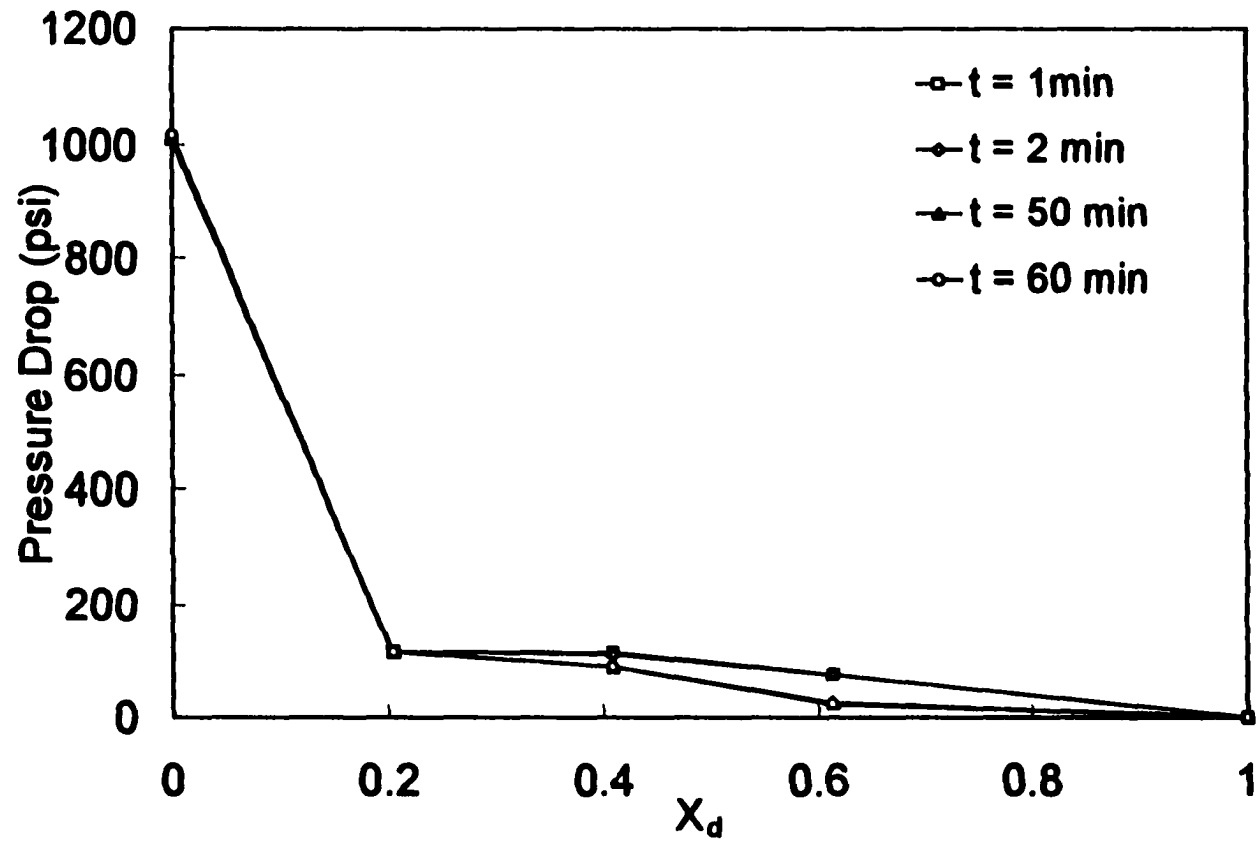


Fig. 4-4: Pressure Profile During Leakoff in the Presence of Gas Saturation

4.3.2 Effectiveness of Fluid Loss Additive During Two-Phase Leak-off

The effect of fluid loss additive (silica flour) on two-phase leak-off is shown in Fig. 4-5. In both tests, the leak-off exhibits spurt/imbibition followed by linear behavior of leak-off when plotted with the square root of time. However, the total leak-off volume is lower in the test where no fluid loss additive was added to the fracturing fluid. This anomaly may be a result of the fact that the filter cake formed in experiments with no additive is thinner but compact and the effective shear rate acting on it is less than for the filter cake with additives. Further, the permeability is slightly higher in the first section of the core sample for the test with fluid loss additive. As pointed out earlier, when the filter cake permeability is comparable to the formation permeability, the formation permeability may dominate the leak-off behavior. Therefore, a larger leak-off rate in the presence of fluid loss additive maybe a manifestation of the reservoir properties. These results contradict the general belief/assumption during fracturing treatment design that the leak-off characteristics are independent of reservoir properties.

Comparison of the fluid leak-off velocity history with and without fluid loss additive is shown in Fig. 4-6. The plot is obtained by differentiating cumulative leak-off volume with respect to time. The data shows that the spurt loss is larger in the case of fracturing fluid with additive. This may be due to the higher permeability in the first section of the core sample. The leak-off velocities at a later stage are the same for both the tests. The C_w values obtained are nearly the same and are reported in Table 4-4. This indicates that in low permeability formations, a fracturing fluid without fluid loss additive can perform as efficiently as a fluid with fluid loss additive.

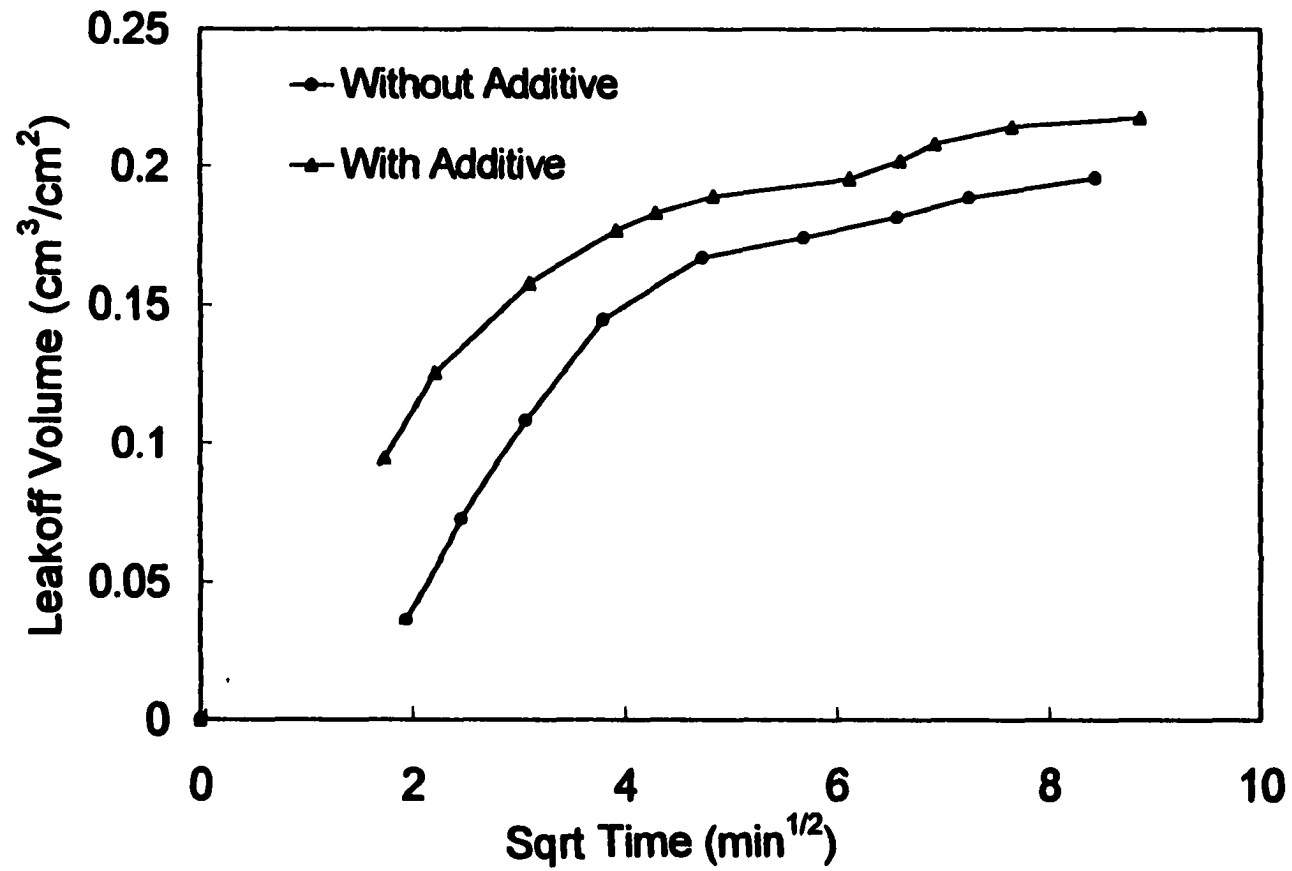


Fig. 4-5: Comparison of Fluid Loss for a 60 lb/Mgal HPG With and Without Fluid Loss Additive in the Presence of Gas Saturation

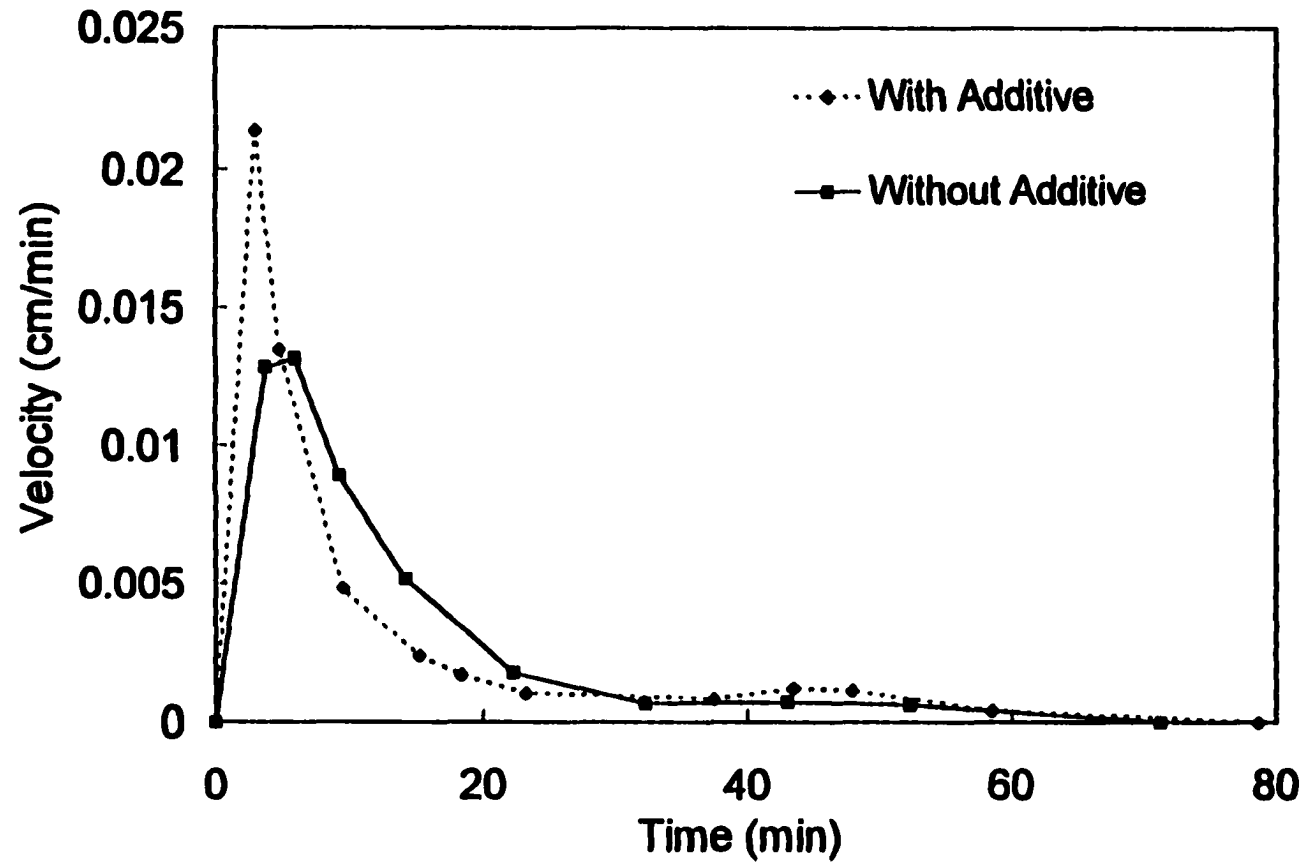


Fig. 4-6: Comparison of Leakoff Velocity for Fracturing Fluid With and Without Additive

4.4 Discussion of Model Results

The model described in the preceding chapter is validated and facilitates clearer interpretation of the experimental data including sectional pressure drop profile and cumulative leak-off history. The input to the model are the measured core properties such as sectional permeabilities (Table 4-2), relative permeability curves, porosity, length of the core; and measured fluid properties such as brine viscosity and density. Values of some of the model parameters such as filter cake erosion rate constant, dispersion coefficient, and filter cake porosity were assumed and are tabulated in Table 4-5.

Table 4.5: Input parameters for simulations

	Test 4-1	Test 4-2	Test 4-3
Cake porosity (%)	20	20	20
Cake permeability (mD)	5.69E-04	3.76E-06	2.30E-06
Cake erosion rate constant (sec/cm)	2.00E-09	4.50E-08	1.00E-09
Connate water saturation (%)	-	18.6	18.2
Inlet concentration of polymer in filtrate (gm/cm ³)	0.0129	0.0129	0.0071
Viscosity of filtrate (cP)	0.926	0.948	0.907

A comparison of the experimental and simulated cumulative leak-off volume for the single-phase experiment is shown in Fig. 4-7. The model prediction is in good agreement with the experimental data. A slight disagreement may be due to uncertainty in the estimation of filter cake permeability and in-situ viscosity of filtrate carrying polymer residues. Figure 4-8 illustrates the comparison of the experimental and simulated pressure drop profile along the length of the core after 1 minute and 60 minutes during single-phase leak-off. The model predictions are in good agreement with the experimental data.

Figures 4-9 and 4-10 illustrate the comparison of experimental and simulation results of cumulative leak-off volume and pressure drop profile, respectively, during the two-phase leak-off in the presence of fluid loss additive. A lower quality match is obtained for the leak-off behavior and pressure profile compared to the match obtained for experiments without fluid-loss additive shown in Figs 4-11 and 4-12. This indicates that the retention and transport of fluid-loss additive may not be correctly modeled by the formulation presented. The pressure drop profile predicted by the model compares well with the experimental results.

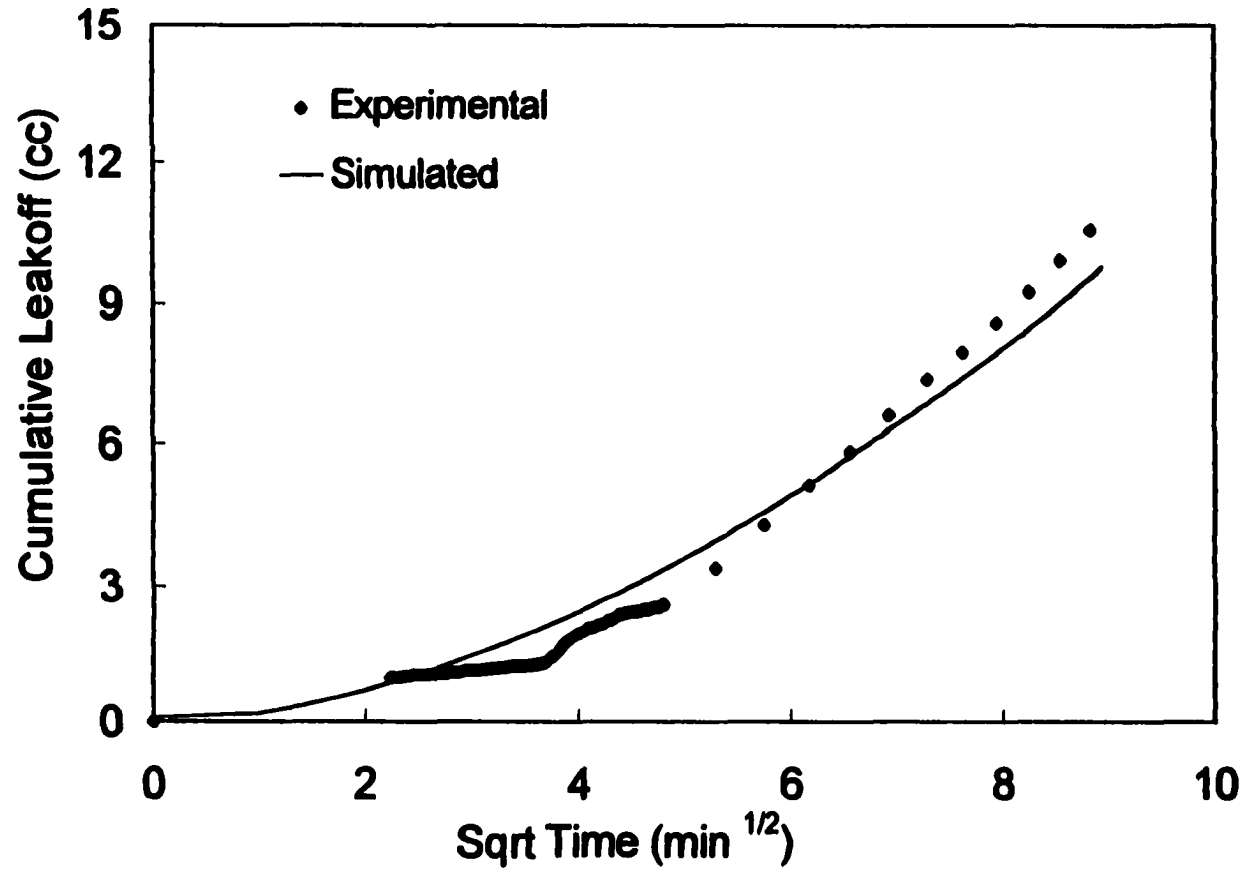


Fig. 4-7: Comparison of Experimental and Simulation Results For Single Phase Leakoff

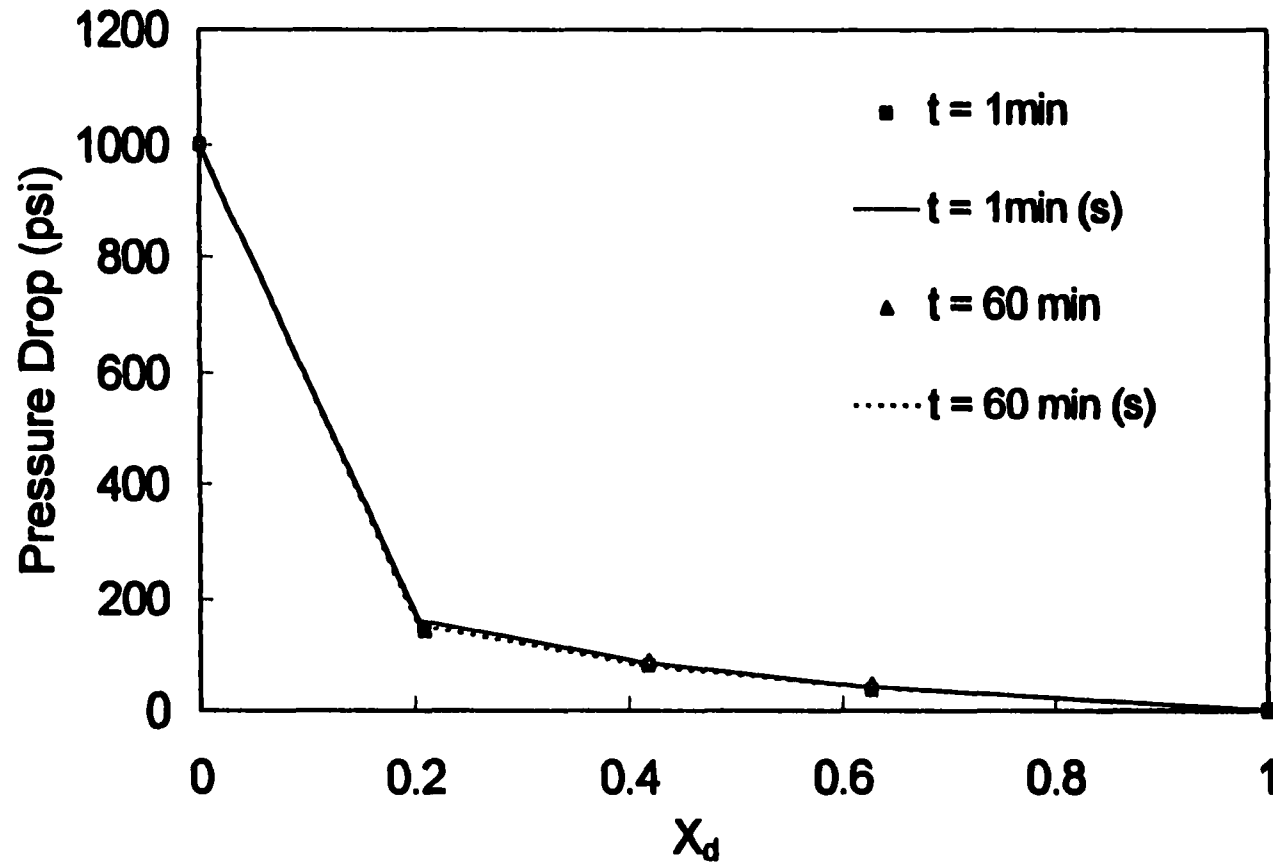


Fig. 4-8: Comparison of Experimental and Simulated Pressure Profile During Single Phase Leakoff

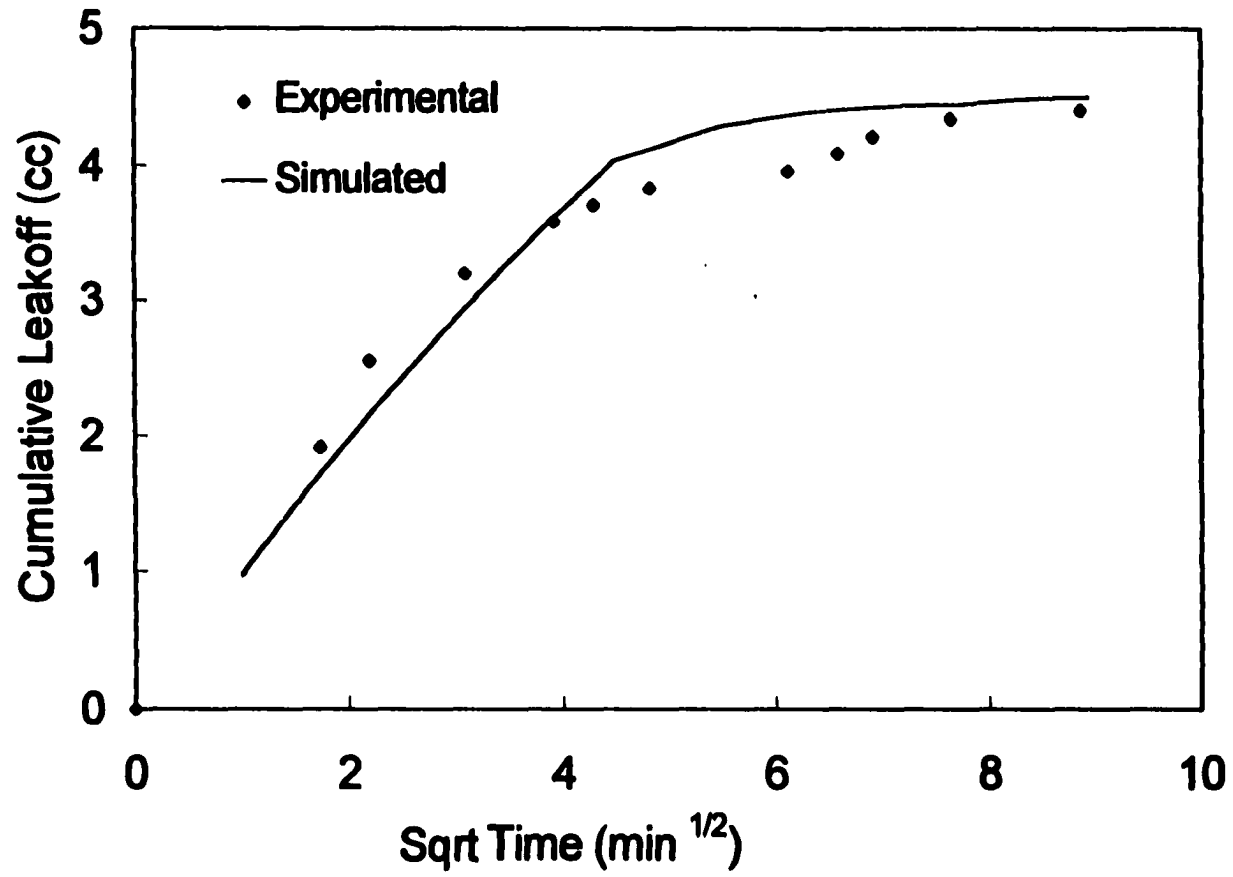


Fig. 4-9: Comparison of Experimental and Simulation Results During Two Phase Leakoff

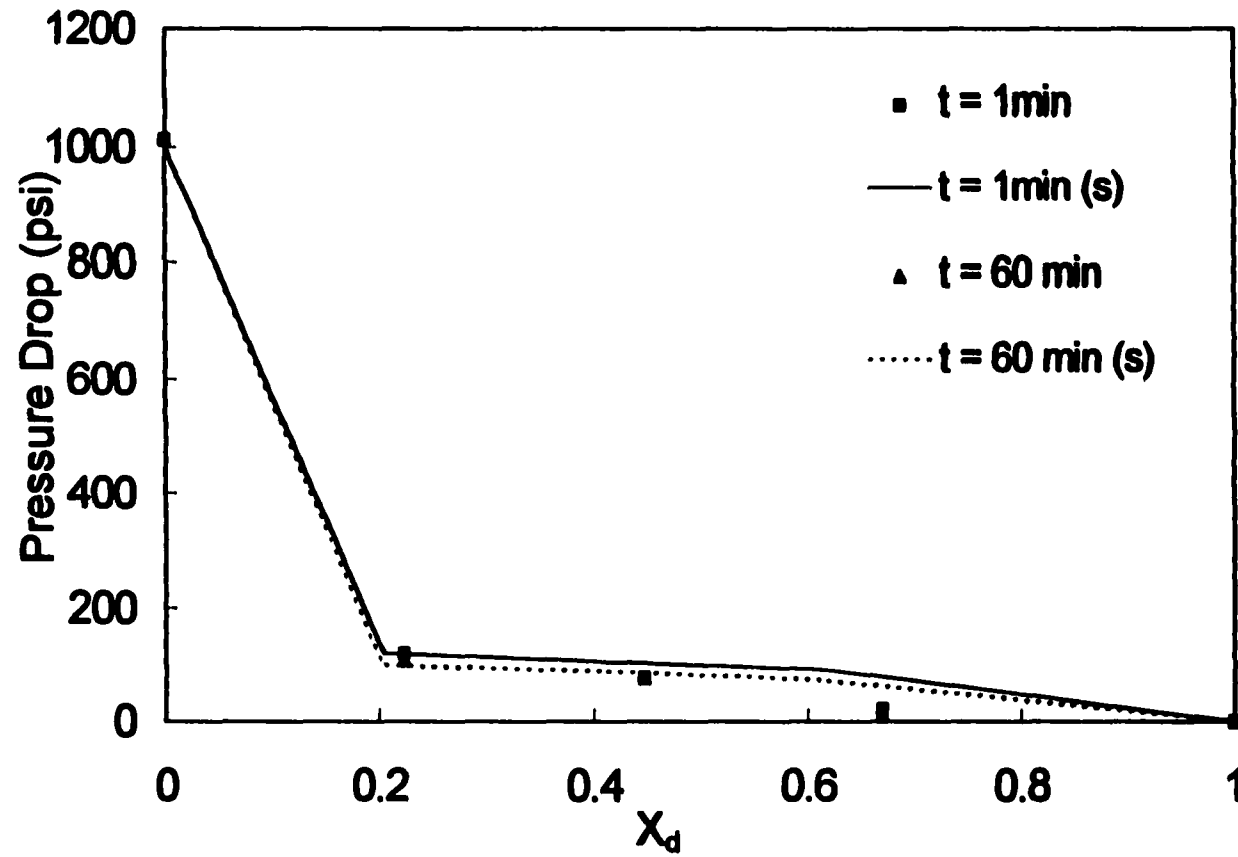


Fig. 4-10: Comparison of Experimental and Simulated Pressure Profile During Leakoff in Presence of Gas

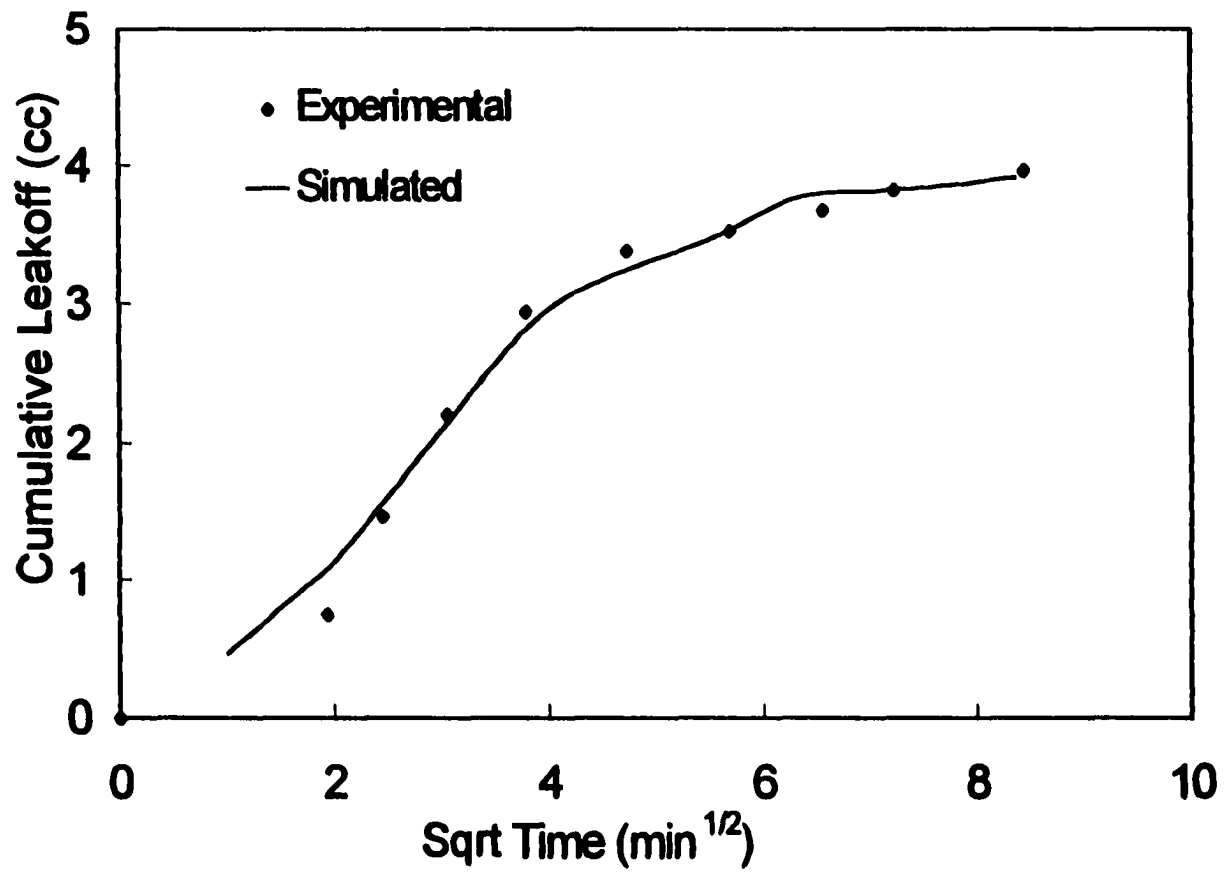


Fig. 4-11: Comparison of Simulation and Experimental Results During Two Phase Leakoff in the Absence of Additive

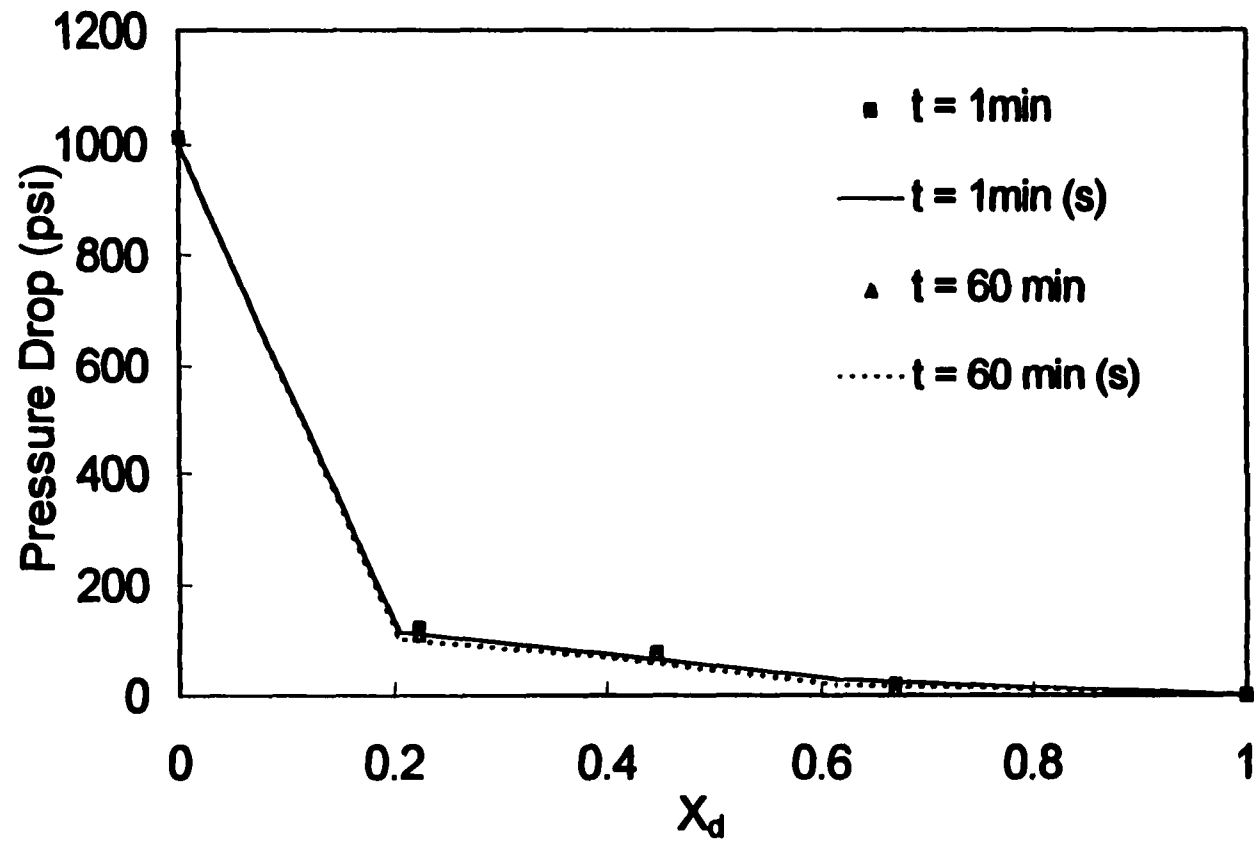


Fig. 4-12: Comparison of Experimental and Simulated Pressure Profiles During Leakoff in the Presence of Gas (without Additive)

Chapter 5

Dynamic Leak-off in Oil Reservoirs

5.1 Introduction

In recent years, increasingly higher permeability formations are being hydraulically fractured (frac-pack) to overcome formation damage and/or prevent sand production problems.²⁶⁻²⁸ Generally, it is believed that during the initial stages of frac-pack treatments, a large amount of spurt loss occurs, which contributes to low fluid efficiency and high pumping cost.¹⁷ Spurt loss should be controlled in order to reduce the pumping cost and improve the economics of frac-pack treatments. Fluid loss additives are expected to reduce spurt loss by blocking the pore throats of the reservoir rock in the vicinity of the fracture face.

In the design of fracturing fluid the presence of oil in the reservoir is usually ignored, which can significantly affect spurt loss and the performance of fluid loss additives. This chapter focuses on the results of dynamic leak-off experiments conducted in the presence of mobile oil saturation. The leak-off behavior of both linear and crosslinked fracturing fluids has been investigated.

5.2 Experimental Procedures

In this study, Berea sandstone core samples 2 inch diameter and 10-11 inch in length were used. The samples were prepared according to the procedure given in Chapter 2. Mercury injection capillary pressure curve was measured in order to determine the pore-throat size distribution of the core sample as shown in Fig. 5-1. The core sample exhibits a pore-throat size ranging from 1 to 30 μm as compared to 20-100 μm for silica flour used as a fluid loss additive.

The dynamic leak-off experiments in the presence of mobile mineral or crude oil were conducted in the following sequence:

1. Initial brine permeability of the core sample was determined according to the procedure given in Chapter 2.
2. After determining the initial permeability of the core sample, the in-situ brine was displaced with mineral or crude oil at a constant flow rate, until the brine saturation reached residual saturation. At least two pore volumes of oil was injected to ensure that the water saturation was immobile. Based on the stabilized pressure drop data, the initial, sectional and overall oil permeability of the core sample were calculated.
3. Fracturing fluid was then injected across the face of the core sample at a shear rate of 55 sec^{-1} and a constant pressure drop of 500 or 1000 psid was maintained across the core sample. The cumulative leak-off volume was determined by measuring the cumulative volume of effluent oil and filtrate with respect to time.

In addition to two-phase fracturing fluid leak-off experiments, 3 single-phase leak-off experiments were conducted for the purpose of comparing the leak-off behavior in single-phase and two-phase flow systems. After determining the initial

permeability to brine, the fracturing fluid was injected across the face of the core sample, using the same experimental conditions as in the case of a two-phase leak-off experiments.

5.3 Results and Discussion

This section has been divided into two parts. In the first part, the impact of oil saturation on the leak-off of linear fluids is discussed and the second part discusses the impact of mobile oil saturation on the leak-off of crosslinked fluids.

5.3.1 Impact of Mobile Oil Saturation on the Leak-off of Linear Fluids

In order to investigate the effect of mobile oil saturation on the leak-off behavior of linear fracturing fluids, mineral oil was used as an oil phase. The mineral oil utilized in the studies is a hydrocarbon lubricant (hydraulic oil). The primary components of the oil are heavy paraffinic petroleum distillates. The specific gravity and viscosity of the oil at room temperature are 0.865 and 35 cP, respectively. It was observed that the core sample wettability shifted towards oil-wet after contact with this oil. This may have resulted from surface-active chemicals in mineral oil that are added to improve the lubrication properties of the oil. Such additives make it easier for the oil to spread on and form a very stable film on the surface it contacts, i.e., these additives tend to make a surface oil-wet. During leak-off, a constant pressure drop of 1000 psid was maintained across the length of the core sample. The fracturing fluid and FLA used were 40 lb/Mgal HPG and 50 lb/Mgal silica flour (SF), respectively. The diameter of the silica flour particles ranged from 20-100 μm .

The core sample and fluid properties and operating conditions for all the experiments are summarized in Table 5-1. The initial, sectional brine permeability of

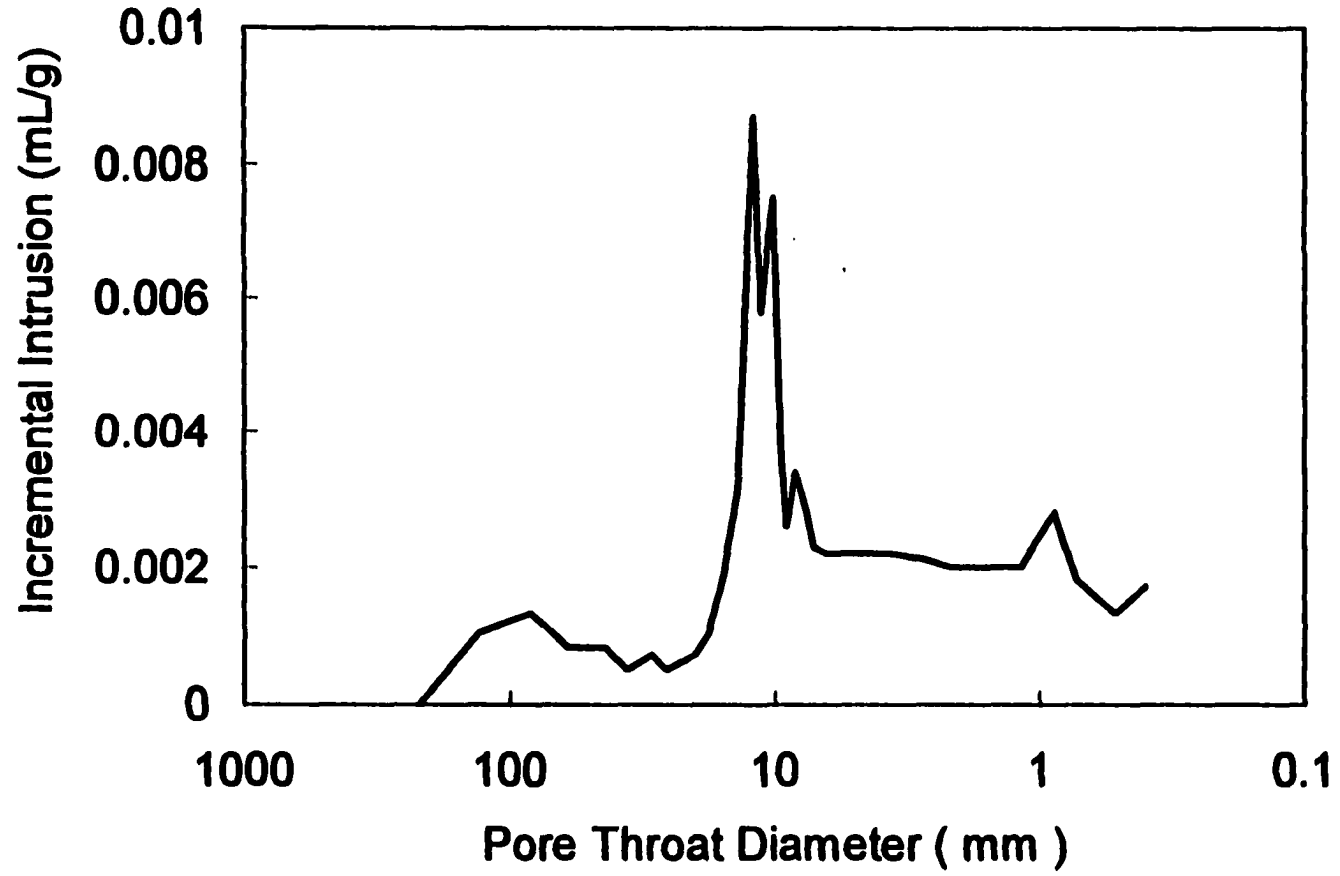


Fig. 5-1: Measured Pore Throat Size Distribution of Berea Sandstone Core Sample

the core samples are reported in Table 5-2. The filtrate obtained during the leak-off was separated from the effluent oil and the viscosity of the filtrate was measured using a Bohlin viscometer. The viscosity measurements for the filtrate are listed in Table 5-3. Test 5-1 was a single-phase leak-off experiment whereas Tests 5-2 through 5-4 were two-phase leak-off experiments.

Table 5.1: Core and fluid properties and operating conditions

	Test 5-1	Test 5-2	Test 5-3	Test 5-4
Permeability (mD)	83.99	23.7	49.66	144.46
Porosity (%)	15.07	15.31	15.1	17
Core length (cm)	26.19	25.68	25.4	27.94
Initial water saturation (%)	100	17.8	18.05	19.5
Fracturing fluid (lb/Mgal)	40# HPG	40# HPG	40# HPG	40# HPG
FLA (lb/Mgal)	50# SF	50# SF	50# SF	50# SF
Leak-off pressure drop (psi)	1000	1000	1000	1000
Oil density (g/cc)	-	0.87	0.87	0.87
Brine density (g/cc)	1.06	1.06	1.06	1.06
Oil viscosity at 77 °F (cP)	-	35	35	35
Brine viscosity at 77°F (cP)	1.04	1.01	1.04	1.0

Table 5.2: Initial sectional permeability to brine (mD)

Test	0-2 inch	2-4 inch	4-6 inch	6-outlet
5-1	55.95	76.34	88.67	113.59
5-2	7.63	31.82	60.1	60.1
5-3	19.43	75.99	77.22	86.49
5-4	62.56	106.0	175.79	294.3

Table 5.3: Apparent viscosity of the effluent filtrate (cP)

Shear Rate (sec ⁻¹)	Test 5-1	Test 5-2	Test 5-3	Test 5-4
1	-	15	-	-
50	-	1.01	15.67	47.02

5.3.1.1 Comparison Between Single-Phase and Two-Phase Leak-off

Figure 5-2 clearly depicts the considerable difference between single-phase (Test 5-1) and two-phase (Test 5-4) leak-off in core samples with comparable permeabilities. Although, the overall permeabilities of the core samples used in Tests 5-1 and 5-4 were different, the permeabilities for their first section (0-2 inch) were approximately the same as shown in Table 5-2. In the case of single-phase leak-off, a significant amount of spurt loss occurs during initial stages of leak-off which controls the formation of the filter cake and the leak-off rate after the spurt loss. This behavior is consistent with that reported by Navarrete and Mitchell.¹⁷ However, in the case of two-phase leak-off, there is a significant reduction in initial spurt loss (although the overall spurt loss is high) which could be attributed to the higher viscosity of the formation oil and low relative permeability for the filtrate at the initiation of leak-off. Thus, for two-phase leak-off the filter cake formation appears to be slow and leads to higher steady-state leak-off rate. This suggests that the presence of mobile oil saturation delays the formation of a good quality filter cake. The C_w and V_{sp} for individual experiment are reported in Table 5-4.

Table 5.4: Summary of C_w and V_{sp} for linear fluids in the presence of oil

Test	Mobile Phase	C_w (ft/min ^{1/2})	V_{sp} (gal/100 ft ²)
5-1	Brine	3.25E-3	71.93
5-2	Mineral oil	9.22E-3	0.0
5-3	Mineral oil	1.30E-2	0.0
5-4	Mineral oil	5.04E-3	185.85

Figure 5-3 shows the variation of the pressure profile along the core sample at different time values for single-phase leak-off. Sectional pressure drop was measured between 0-2 inch, 2-4 inch and 4 inch to outlet. The data shows that the pressure

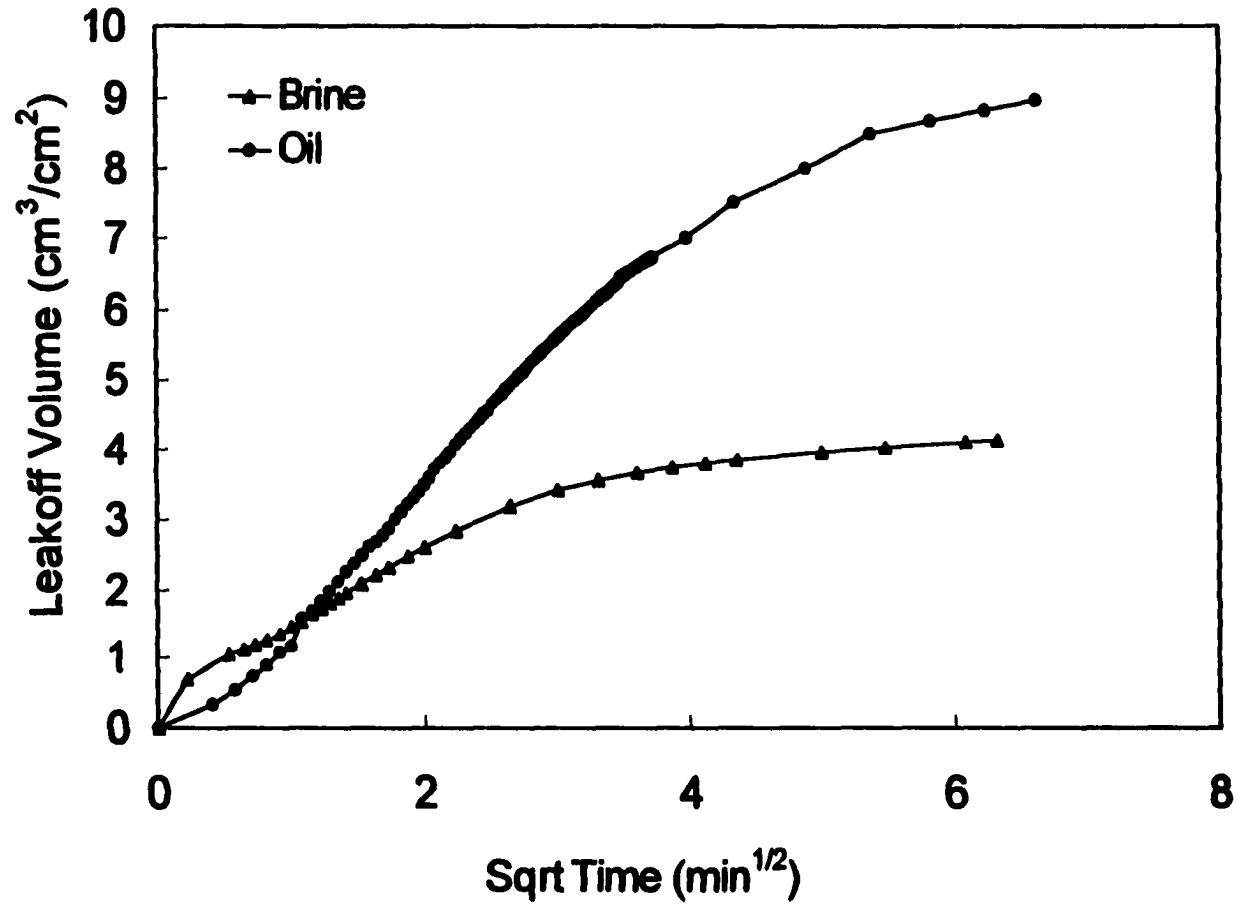


Fig. 5-2: Comparison of Single and Two Phase Dynamic Leakoff Behavior of 40 lb/Mgal HPG with Silica Flour

profile stabilizes within the first ten minutes of leak-off, the pressure drop across the first section of the core sample increasing from approximately 894 psi to 973 psi indicating the formation of an internal filter cake in addition to an external one. After ten minutes the pressure gradient across the entire core sample attains a stable value. As shown by the estimated cake permeability tabulated in Table 5-5, determined using the procedure given in Appendix A, a stable filter cake which controls the leak-off has been formed.

Table 5.5: Estimated filter cake permeabilities (mD)

Time (min)	Test 5-1	Test 5-2	Test 5-3	Test 5-4
5	1.1E-2	-	2.2E+0	8.9E+0
10	4.6E-3	-	5.1E-1	6.0E-1
20	6.1E-4	-	1.1E-1	6.7E-1
30	5.3E-4	9.4E-2	9.3E-2	9.7E-2
40	5.2E-4	4.0E-2	3.9E-2	3.6E-2

The variation of the pressure profile at various time values for two-phase leak-off, shown in Fig. 5-4, exhibits an interesting behavior. As before, the pressure drop was measured for sections between 0-2 inch, 2-4 inch, 4-6 inch and 6-10 inch. The pressure drop across the first section of the core sample increases gradually over 30 minutes from 445 psi to 875 psi. The pressure profiles in Fig. 5-4 and the leak-off history in Fig. 5-2 suggest that a poorer quality cake has formed even after an extended period of time. Such behavior may be attributed to the poor adhesion of water-wet polymer molecules and fluid loss additives to the oil covered fracture face and pore internal surface. This hypothesis is supported by the anomaly in pressure profile at 20 minutes (Fig. 5-4) which suggests a sudden shearing of the cake. Pressure history for

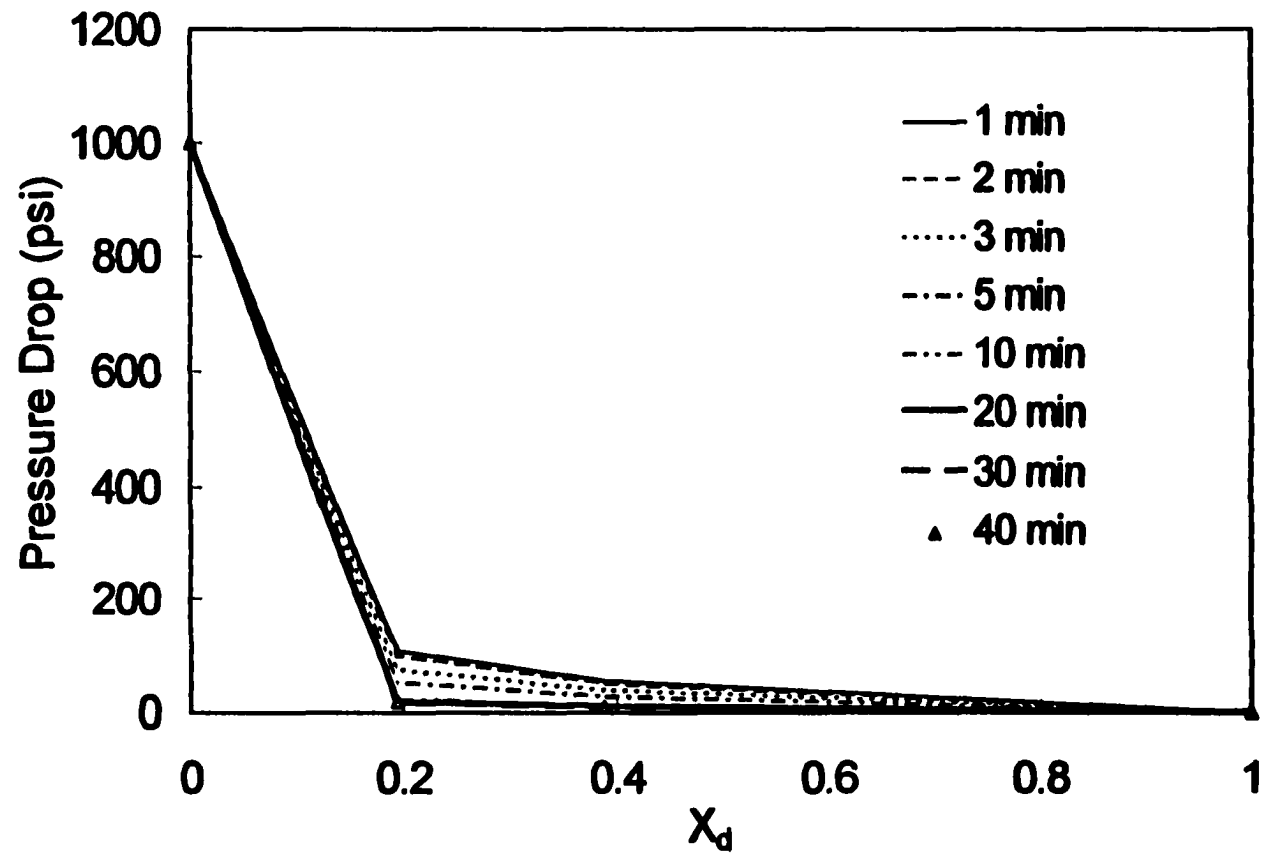


Fig. 5-3: Pressure Profile During Single Phase Leakoff (Test 5-1)

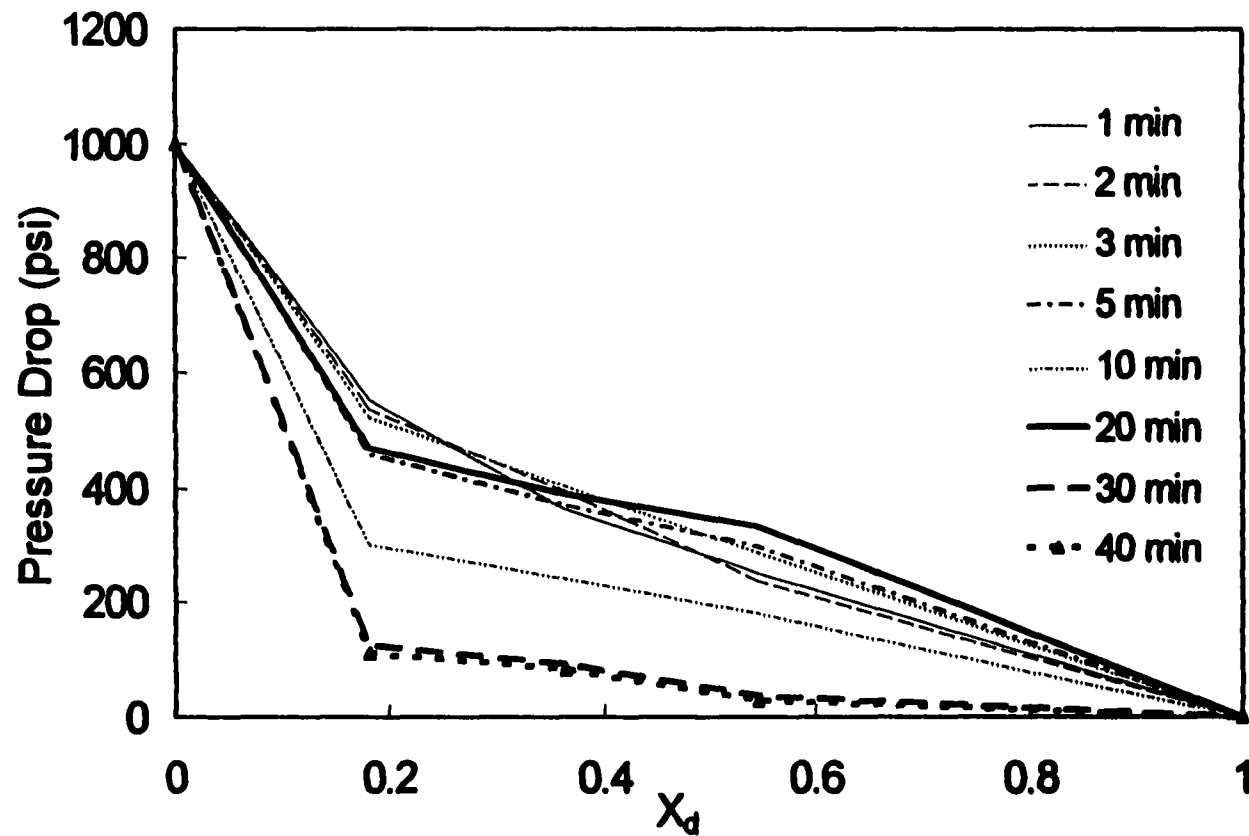


Fig. 5-4: Pressure Profile During Two Phase Leakoff (Test 5-4)

the same test (Fig. 5-8) also shows anomalous fluctuations in pressure suggesting a cake with poor adhesion to the fracture face.

5.3.1.2 Effect of Sectional Permeability on Two-Phase Leak-off

Figure 5-5 compares the cumulative leak-off volume vs. square root of time for Tests 5-2, 5-3, and 5-4 conducted with samples of varying permeabilities. The brine permeability of the first section (0-2 inch) in Tests 5-2, 5-3, and 5-4 were 7.63 mD, 19.43 mD, and 62.56 mD, respectively. It is observed that the initial spurt loss and cumulative leak-off volume increase with the first section permeability of the core sample. For example, after 16 minutes the cumulative leak-off volumes were 27.27 cm³, 52.31 cm³, and 143.19 cm³ in Tests 5-2, 5-3, and 5-4, respectively. Interestingly, the cumulative leak-off volume at different time values is a linear function of the first section (0-2 inch) permeability as depicted in Fig. 5-6. Thus, in the presence of mobile oil saturation the permeability of the fracture face appears to be an important factor controlling the leak-off rate of linear fluids.

5.3.1.3 Effectiveness of Fluid Loss Additives During Two-Phase Leak-off

The purpose of the fluid loss additives is to minimize the leak-off after initial spurt loss by contributing to the formation of an impermeable external and/or internal filter cake. In all the experiments reported, silica flour was used as a fluid loss additive. A comparison of leak-off velocity as a function of time for core samples of different permeabilities is shown in Fig. 5-7. For the purpose of comparison, leak-off velocity variations during the single-phase flow test is also shown in Fig. 5-7. Maximum spurt velocity occurs in the 144 mD sample and the minimum in the 24 mD core sample. The data indicates that until approximately 30 minutes the leak-off rate is highest in the 144

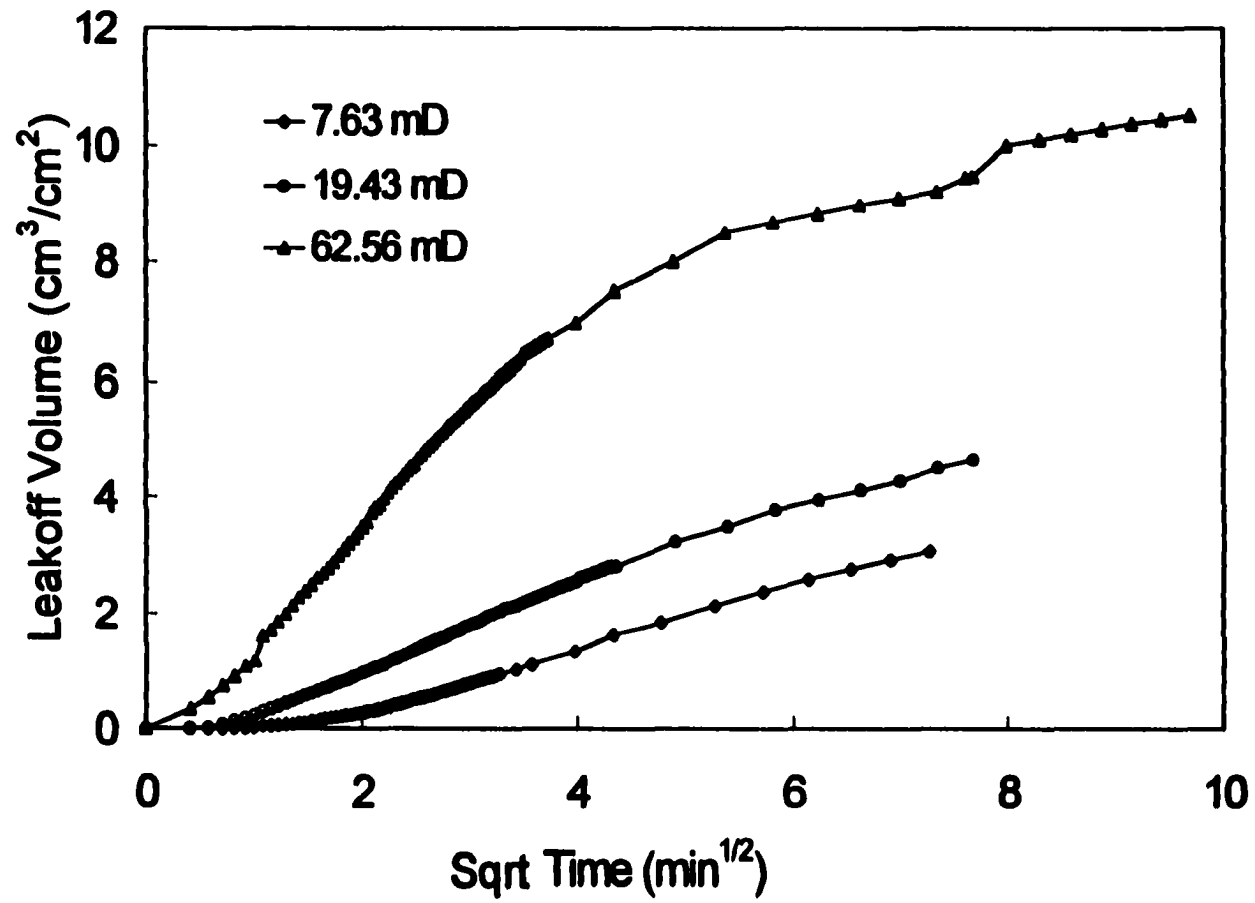


Fig. 5-5: Effect of First Section Permeability on Two Phase Leakoff

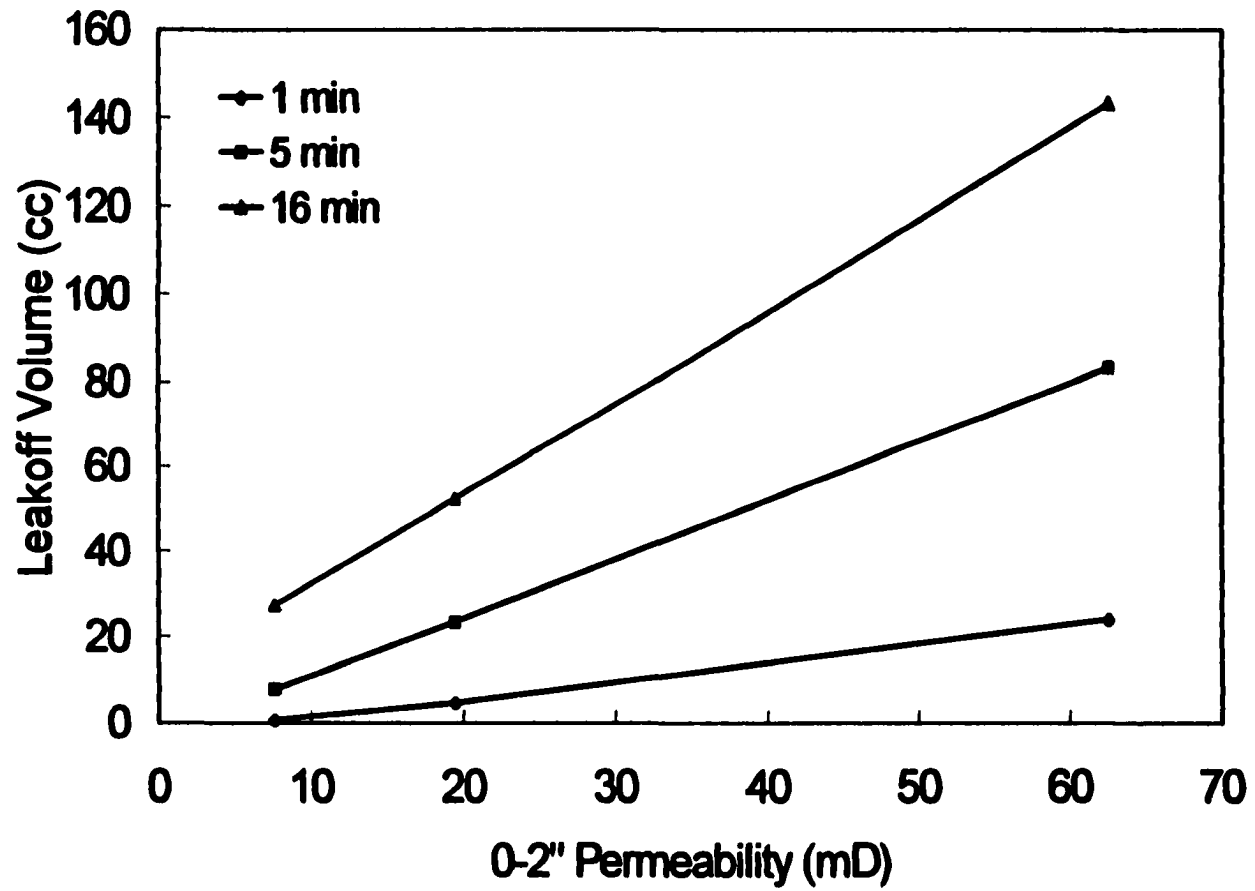


Fig. 5-6: Functional Dependency of 40 lb/Mgal Linear HPG Leakoff on Fracture Face Permeability

mD sample as compared to the leak-off rates in the other two samples. For single-phase leak-off, even though the initial filtrate velocity was the highest, the velocity falls below that of all two-phase tests just after ten minutes, indicating the formation of a low permeability filter cake. This demonstrates that the effectiveness of fluid loss additives is significantly reduced in the presence of mobile oil saturation. As mentioned earlier, the presence of oil in the core sample may prevent the water-wet fluid loss additive from plugging the pore throats of the core sample, thereby delaying the formation of a filter cake. After 30 minutes, the leak-off velocity in all two-phase leak-off samples was approximately the same indicating the filter cake stabilization and similar quality of the filter cake in all three core samples.

These results demonstrate the conclusion by Navarrete *et al.*¹⁶⁻¹⁷, that the effectiveness of fluid loss additives increases as the initial permeability of the formation increases is not valid for leak-off in the presence of mobile oil.

It is generally believed that fluid loss additives lead to the formation of an external and/or internal cake that is effective in preventing the invasion of any polymer dispersed in fracturing fluid into the reservoir.¹⁶⁻¹⁷ With this belief, the produced filtrate which would be a mixture of in-situ brine and carrier water filtered from fracturing fluid is expected to have viscosity close to 1 cP. However, in the tests involving two-phase flow, the produced filtrate exhibited turbidity and viscosity values significantly higher than 1 cP (Table 5-3). This indicates that the filter cake formed in two-phase tests allowed significant amount of polymer to invade the reservoir. This further supports the hypothesis that filter cake formed in presence of oil saturation is of poor quality and the presence of oil prevents the retention of polymer by the reservoir rock.

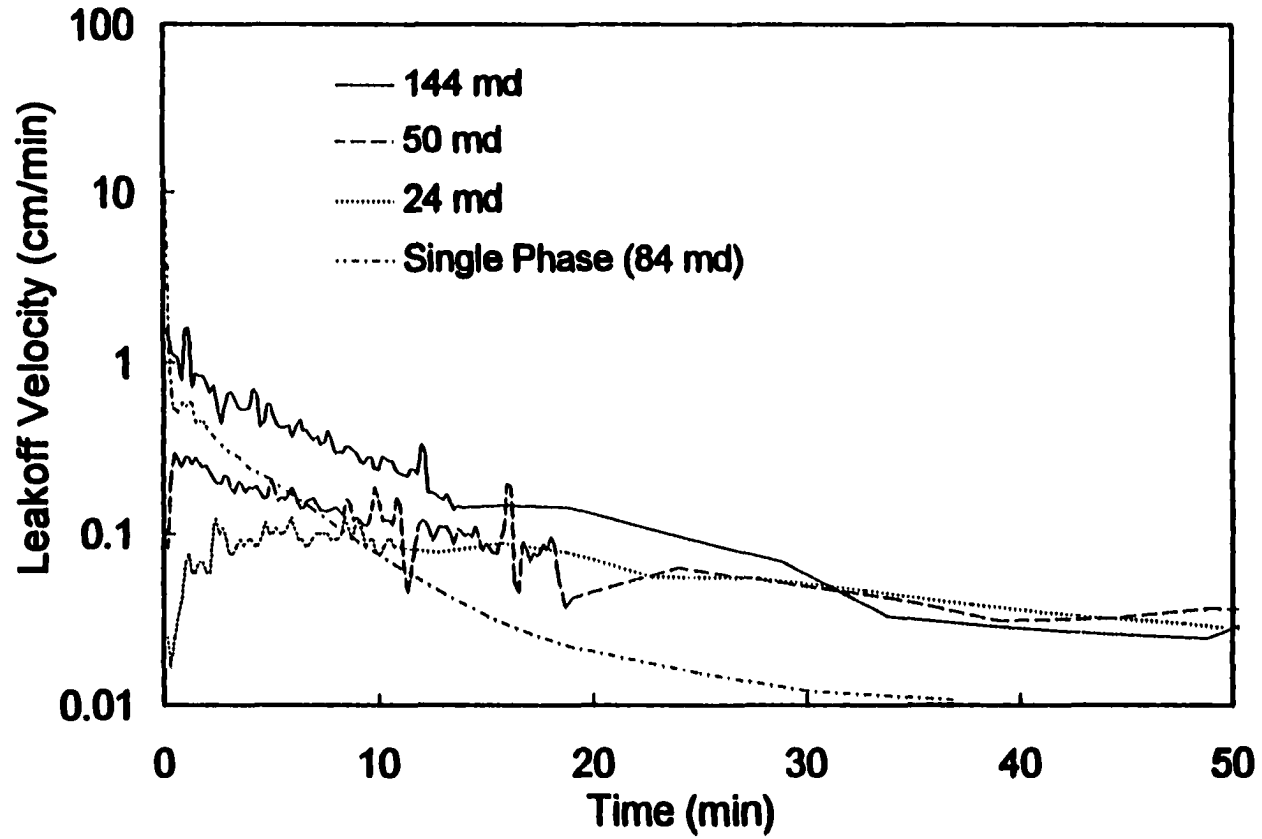


Fig. 5-7: Effect of Fluid Loss Additive on Leakoff During Single and Two Phase Dynamic Leakoff

Variation in sectional pressure gradients as a function of time during two-phase leak-off (Test 5-4) is illustrated in Fig. 5-8. In this experiment, all of the movable oil in the core sample was completely displaced by the filtrate as indicated by the produced filtrate volume (Fig. 5-2) which was more than one pore volume. The data shows that a good quality filter cake is not formed (Table 5-5) until all the oil has been displaced by the filtrate. The frequent anomalies in pressure gradients in all the sections appears to be due to the instability (erosion) of the filter cake.

5.3.1.4 Simulation Results

The model described in Chapter 3 is validated and facilitates clearer interpretation of the experimental data. The input to the model were the measured core properties such as sectional permeabilities (Table 5-2), porosity, length of the core; and measured fluid properties such as brine, oil, and filtrate viscosities (Tables 5-1 and 5-3). Some of the model parameters such as cake erosion rate constant and dispersion coefficient were iterated upon to improve the quality of match.

Figures 5-9 through 5-11 illustrate a qualitative agreement between experimental results and the model predictions.

5.3.1.5 Post-treatment Leak-off Behavior

The fracturing fluid may continue to undergo static leak-off into the formation even after the treatment has been terminated and the well shut-in due to excess pressure in the fracture. This can have an effect on the fracture geometry, pressure decay in the fracture, and the closure time.¹ Therefore, it is important to understand the leak-off behavior after the fracture treatment has been terminated.

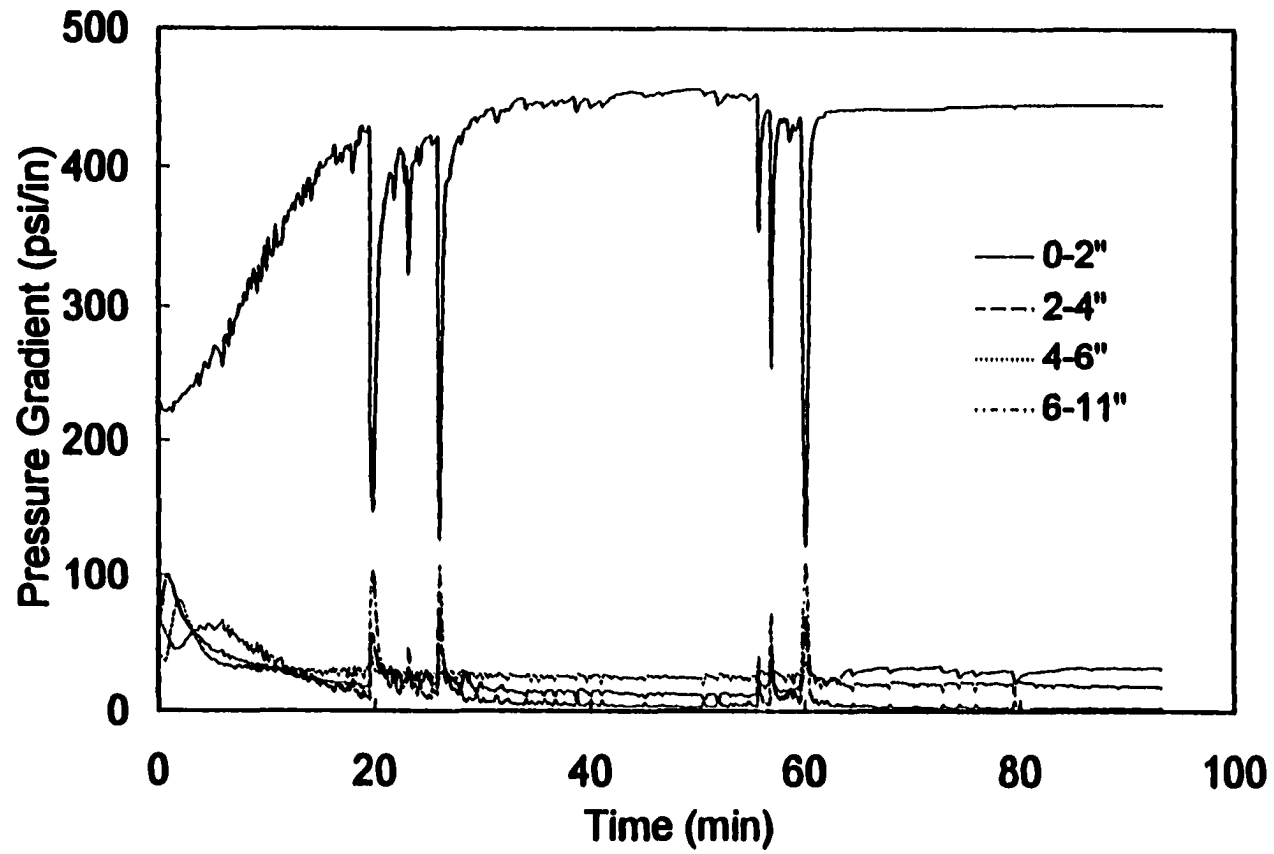


Fig. 5-8: Sectional Pressure Gradient During Two Phase Leakoff (Test 5-4)

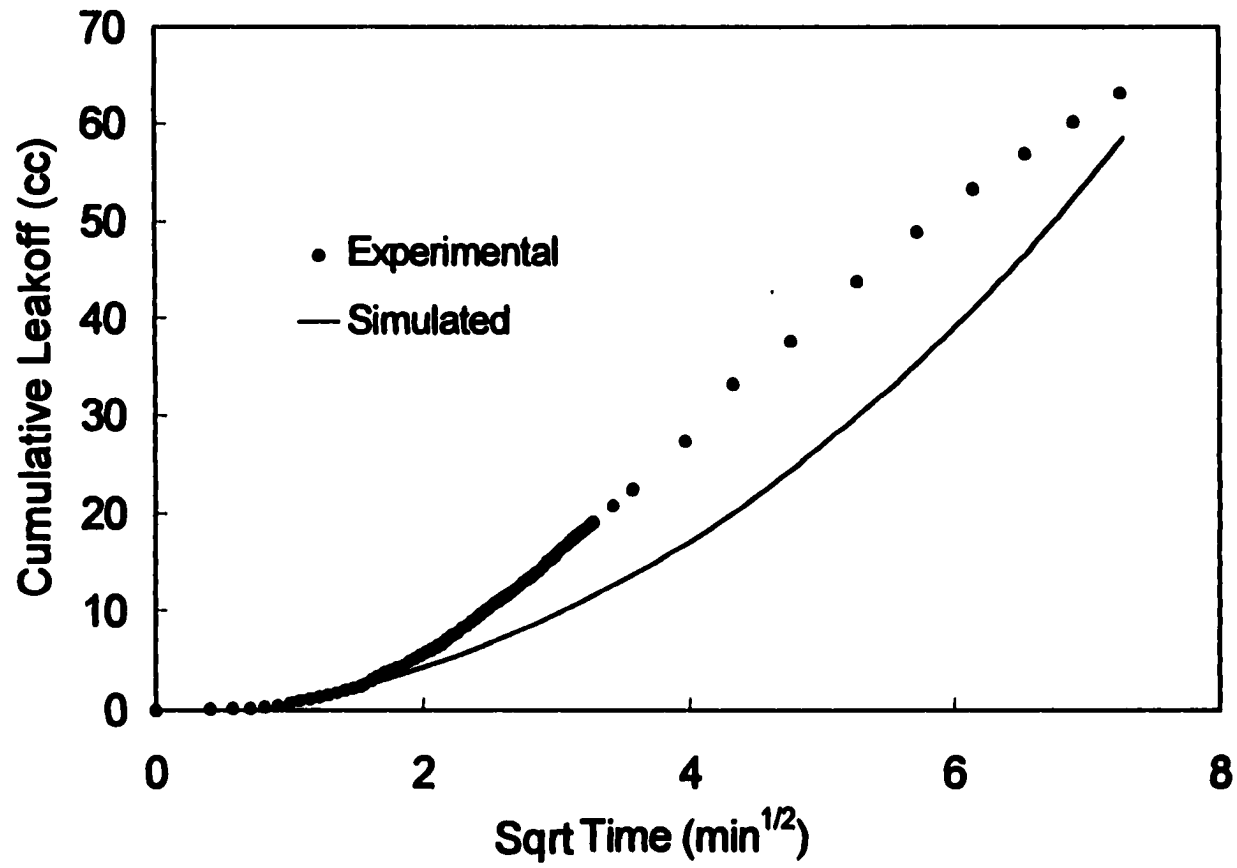


Fig. 5-9: Comparison of Experimental and Simulated Leakoff in the Presence of Mobile Oil Saturation (Test 5-2)

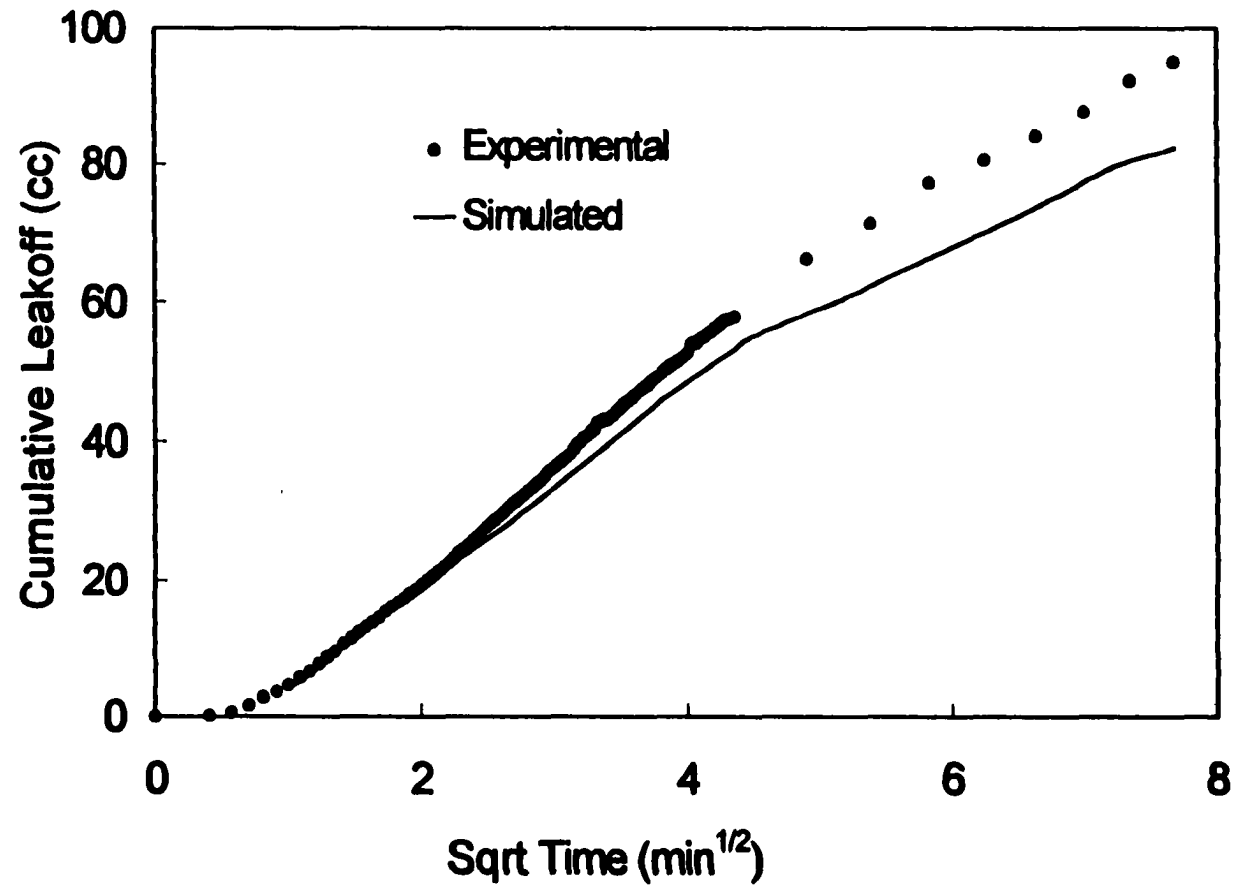


Fig. 5-10: Comparison of Experimental and Simulated Leakoff in the Presence of Mobile Oil Saturation (Test 5-3)

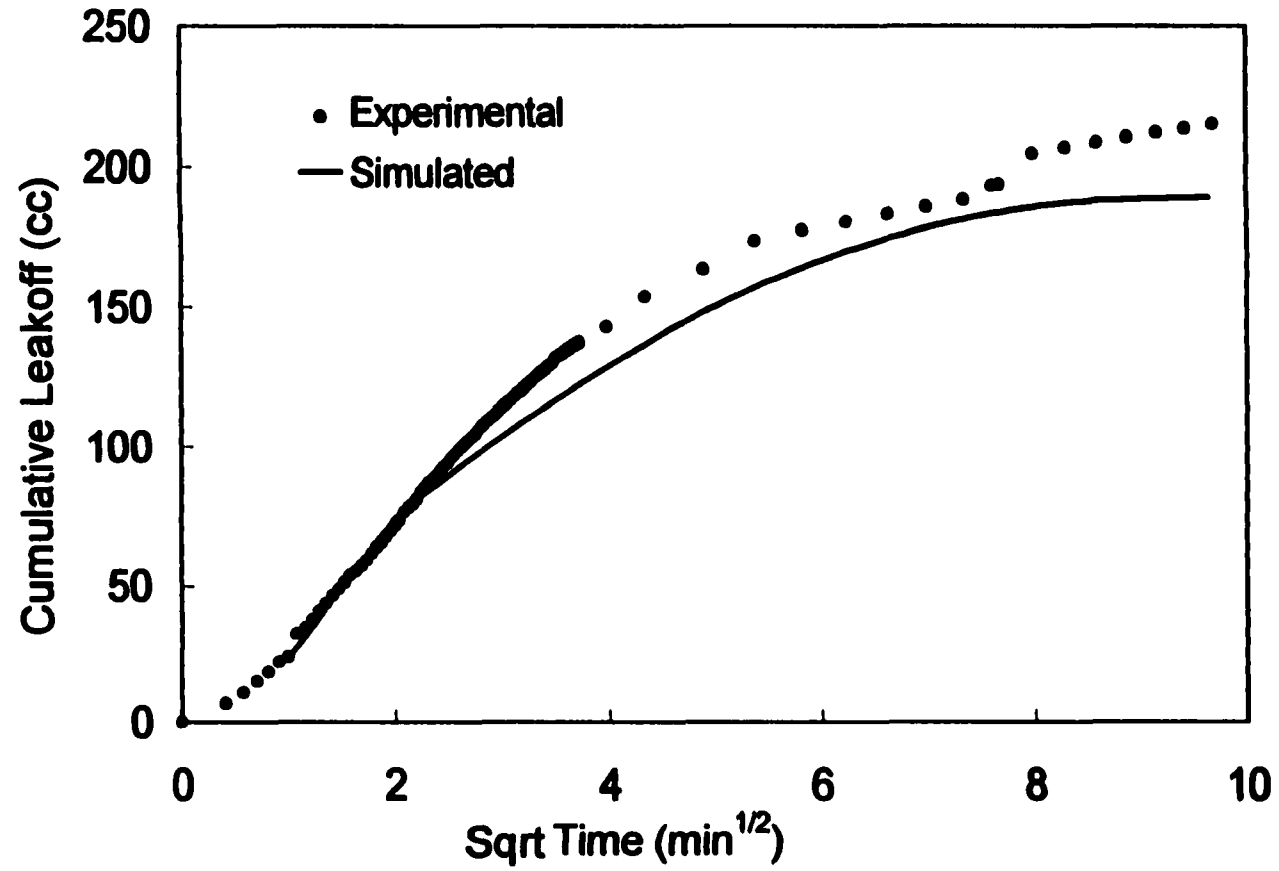


Fig. 5-11: Comparison of Experimental and Simulated Leakoff in the Presence of Mobile Oil Saturation (Test 5-4)

In order to study the leak-off behavior during shut-in, the injection of fracturing fluid in a sample of the experiments (Tests 5-3, 5-4, & 5-5) was stopped after a certain time. However, the fracturing fluid was still subjected to static leak-off conditions. The filtrate volume and the decline in pressure drop across the length of the core sample was continuously monitored for at least 20 minutes.

Figure 5-12 compares the dynamic and static (shut-in) leak-off behavior of 35 lb/Mgal HPG with 25 lb/Mgal silica flour in a core sample saturated with mineral oil (Test 5-5). The 0-2 inch, 2-4 inch, 4-6 inch, 6-10 inch, and 0-10 inch brine permeabilities are 1.93 mD, 2.1 mD, 5.34 mD, 15.48 mD, and 3.81 mD, respectively. The pressure drop during dynamic leak-off was maintained at 500 psi. It is evident from the figure that there is a difference in static and dynamic leak-off behavior. The static leak-off rate is lower than the dynamic leak-off rate. The dynamic and static C_w values are $4.3E-3$ and $1.1E-3$ ft/min^{1/2}, respectively. The difference provides an insight into the contribution of fluid shear on the erosion of the filter cake.

The effect of shut-in on the leak-off behavior of 40 lb/Mgal HPG with 50 lb/Mgal silica flour (Tests 5-3 & 5-4) is shown in Fig. 5-13. In both tests, the oil saturation near the fracture face had been reduced to residual oil saturation. It is evident from the figure that the leak-off volume is a linear function of shut-in time in both tests. This implies a constant leak-off rate and hence a fully compact filter cake has been formed. The static C_w values in the case of Tests 5-3 and 5-4 are $1.8E-3$ and $1.2E-3$ ft/min^{1/2}, respectively. The static C_w values correspond approximately to the dynamic C_w value obtained in the case of 100 % brine saturated core sample.

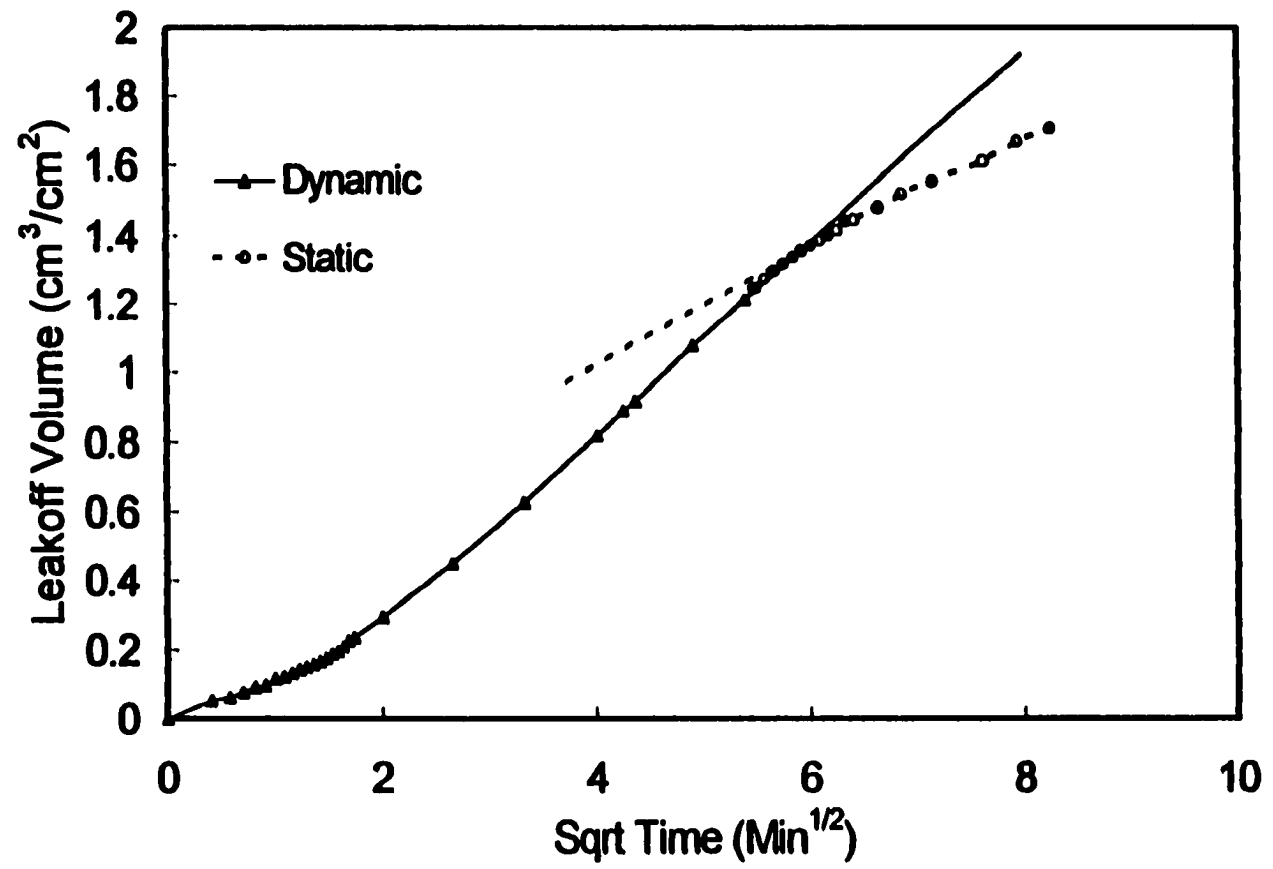


Fig. 5-12: Effect of Shut-in on the Leakoff Behavior of 35 lb/Mgal HPG + 25 lb/Mgal Silica Flour (Test 5-5)

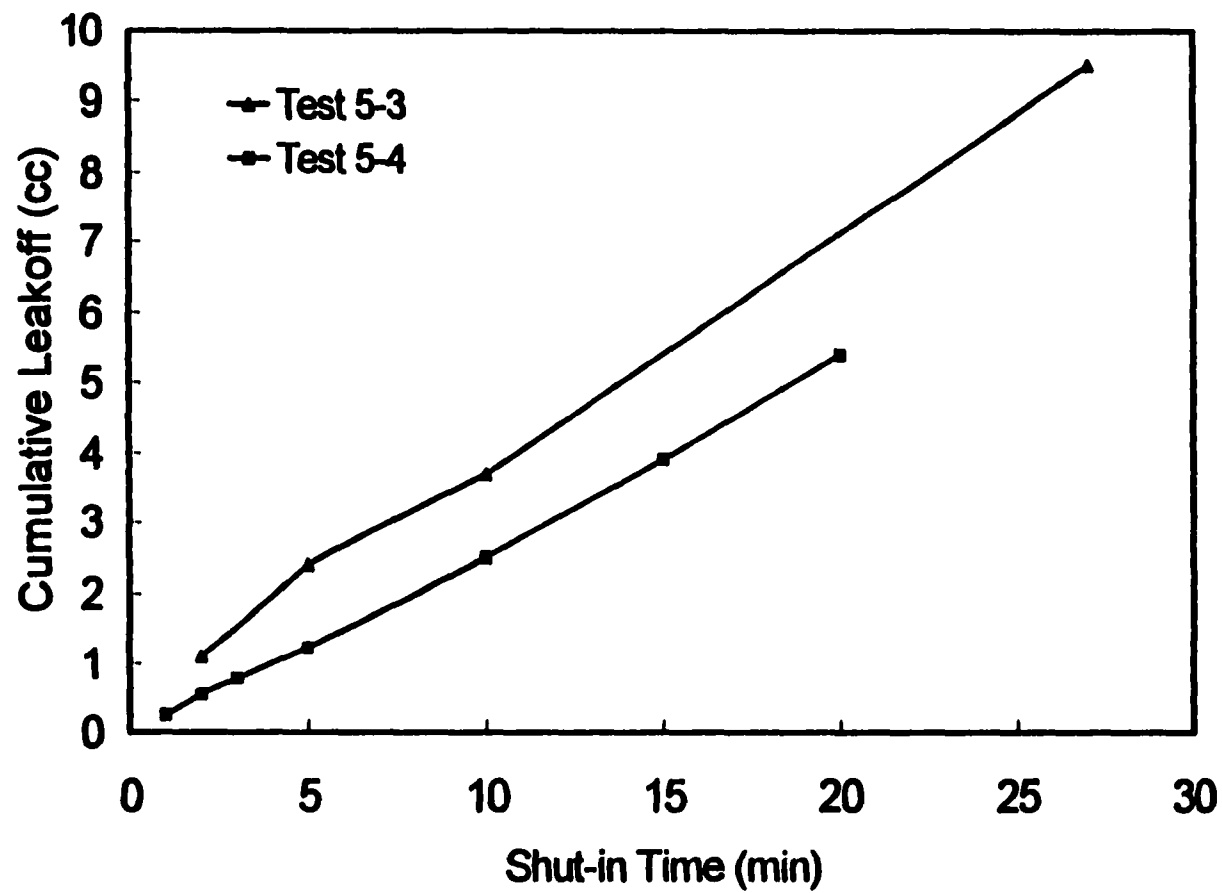


Fig. 5-13 : Effect of Shut-in on the Leakoff Behavior of 40 lb/Mgal HPG + 50 lb/Mgal Silica Flour (Test 5-3 & 5-4)

5.3.2 Impact of Mobile Oil Saturation on the Leak-off of Crosslinked Fluids

In order to investigate the effect of mobile oil saturation on the leak-off behavior of crosslinked fracturing fluids, mineral and crude oil were used as the oil phase. The viscosities of mineral and crude oil used were 35 and 6 cP, respectively. A constant pressure drop of 500 or 1000 psi was maintained across the length of the core sample during the leak-off test. For the purpose of comparison, leak-off experiments with linear fracturing fluids were also conducted. The fracturing fluids studied were 35 lb/Mgal guar (borate crosslinked and linear) and 35 lb/Mgal HPG (borate crosslinked and linear). The length of the core samples in all the experiments was 10 inch. The initial, sectional and overall brine and oil permeability of the core samples are reported in Table 5-6. The operating conditions for all the experiments are summarized in Table 5-7. The C_w and V_{sp} calculated for all the experiments are listed in Table 5-8.

Table 5.6: Initial sectional and overall brine and oil permeability (mD)

Test	Fluid Phase	0-2"	2-4"	4-6"	6-10"	0-10"
6-1	Brine (k)	44.2	96.3	144.1	19.6	35.5
6-2	Brine(k)	106.3	72.3	167.4	169.1	121.8
	Mineral oil (kk _{ro})	79.6	55.2	114.6	131.7	101.7
6-3	Brine (k)	25.0	74.7	5.9	12.8	13.2
6-4	Brine(k)	28.3	66.9	99.7	94.5	61.3
	Mineral oil (kk _{ro})	22.6	55.6	78.9	68.5	48.0
6-5	Brine(k)	44.3	35.4	60.7	53.5	47.8
	Mineral oil (kk _{ro})	33.4	27.2	43.5	44.8	37.2
6-6	Brine(k)	99.2	117.7	159.2	188.9	141.1
	Mineral oil (kk _{ro})	76.9	82.6	118.8	148.3	106.4
6-7	Brine(k)	12.9	12.7	16.3	23.0	16.4
	Mineral oil (kk _{ro})	9.9	9.6	11.6	15.7	11.9
6-8	Brine(k)	24.4	27.5	146.8	90.5	47.1
	Mineral oil (kk _{ro})	17.6	21.0	114.9	72.2	35.5
6-9	Brine(k)	22.5	29.0	32.2	37.7	30.7
	Crude oil (kk _{ro})	4.9	7.0	12.6	4.3	5.7
6-10	Brine(k)	16.6	17.4	19.6	18.5	18.0
	Mineral oil (kk _{ro})	13.2	14.0	15.9	15.5	14.6
6-11	Brine(k)	20.5	30.7	19.5	19.7	21.3
	Crude oil (kk _{ro})	17.8	25.4	17.0	13.7	16.6

Table 5.7: Summary of operating conditions

Test	Fluid	FLA	S_w	Leak-off Press. Drop (psi)
6-1	X-linked Guar	None	100%	500
6-2	X-linked Guar	None	S_{wc}	500
6-3	X-linked HPG	None	100%	500
6-4	X-linked HPG	None	S_{wc}	500
6-5	Linear HPG	None	S_{wc}	500
6-6	Linear Guar	None	S_{wc}	500
6-7	X-linked HPG	Silica flour	S_{wc}	500
6-8	X-linked HPG	Silica flour	S_{wc}	500
6-9	X-linked HPG	None	S_{wc}	500
6-10	X-linked HPG	None	S_{wc}	500
6-11	X-linked HPG	None	S_{wc}	1000

Table 5.8: Summary of C_w and V_{sp} for crosslinked fluids in the presence of oil

Test	Mobile Phase	C_w (ft/min ^{1/2})	V_{sp} (gal/100 ft ²)
6-1	Brine	1.9E-3	33.35
6-2	Mineral oil	2.6E-3	5.35
6-3	Brine	2.7E-3	19.36
6-4	Mineral oil	3.2E-3	2.48
6-5	Mineral oil	7.8E-3	0.0
6-6	Mineral oil	8.3E-3	0.0
6-7	Mineral oil	1.6E-3	0.43
6-8	Mineral oil	2.3E-3	0.46
6-9	Crude oil	2.6E-3	1.85
6-10	Mineral oil	2.1E-3	0.58
6-11	Crude oil	2.6E-3	5.59

5.3.2.1 Leak-off of Crosslinked Guar

A comparison between the leak-off of 35 lb/Mgal borate crosslinked guar in brine and mineral oil core is depicted in Fig. 5-14. In both the cases, the total leak-off time was 20 minutes. It is evident from the figure that there is a significant difference in the leak-off behavior. Although the permeability of the brine core was lower compared to that of the oil core (Table 5-6), the cumulative leak-off volume in the brine core was nearly twice of that obtained in the oil core. In the case of oil core, the

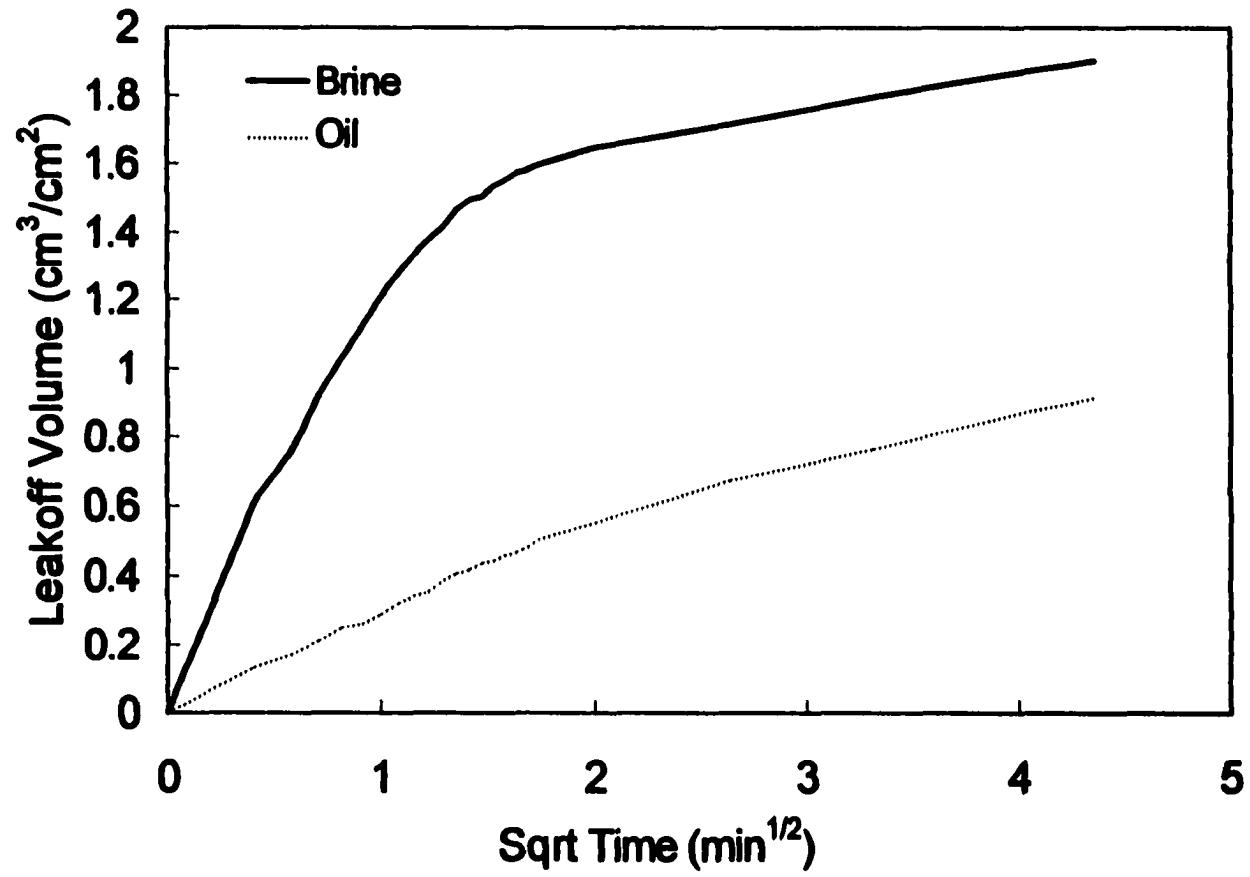


Fig. 5-14: Comparison Between Leakoff of crosslinked 35 lb/Mgal Guar in Brine and Oil Cores

spurt loss was reduced more than six times when compared to that observed in the brine core (Table 5-8). This behavior could be due to the dominance of viscous forces in the oil core that tends to resist initial leak-off. The leak-off in a brine core is governed by spurt loss and the formation of an external and/or internal filter cake. However, in the presence of mobile oil, the oil viscosity and to some extent the near fracture face permeability controls the spurt loss and relative permeability governs the long term leak-off

The presence of oil can restrict the formation of a compact filter cake. Figure 5-15 illustrates the effect of this phenomenon on the pressure gradient in the 0-2 inch section of the core sample during the leak-off of 35 lb/Mgal borate crosslinked guar in brine and oil core. In the case of brine core, the pressure gradient increases steeply (230 psi/in after 1 minute) as soon as leak-off is initiated. The pressure gradient stabilizes after about 2 minutes and simultaneously the leak-off rate also starts declining as observed in Fig. 5-14. This indicates that a fully compacted filter cake has developed. However, in the case of the oil core, the pressure gradient increases steadily. It takes approximately 7 minutes for the pressure gradient to reach 230 psi/in and even after that it does not stabilize. This proves that in the presence of oil it takes a very long time for a compact filter cake to develop. In addition, it confirms that in an oil core it is not the filter cake which governs leak-off, but it is indeed the oil viscosity and relative permeability which control leak-off.

5.3.2.2 Leak-off of Crosslinked HPG

The leak-off behavior of 35 lb/Mgal borate crosslinked HPG in brine and oil core is shown in Fig. 5-16. The leak-off characteristics of crosslinked HPG are similar

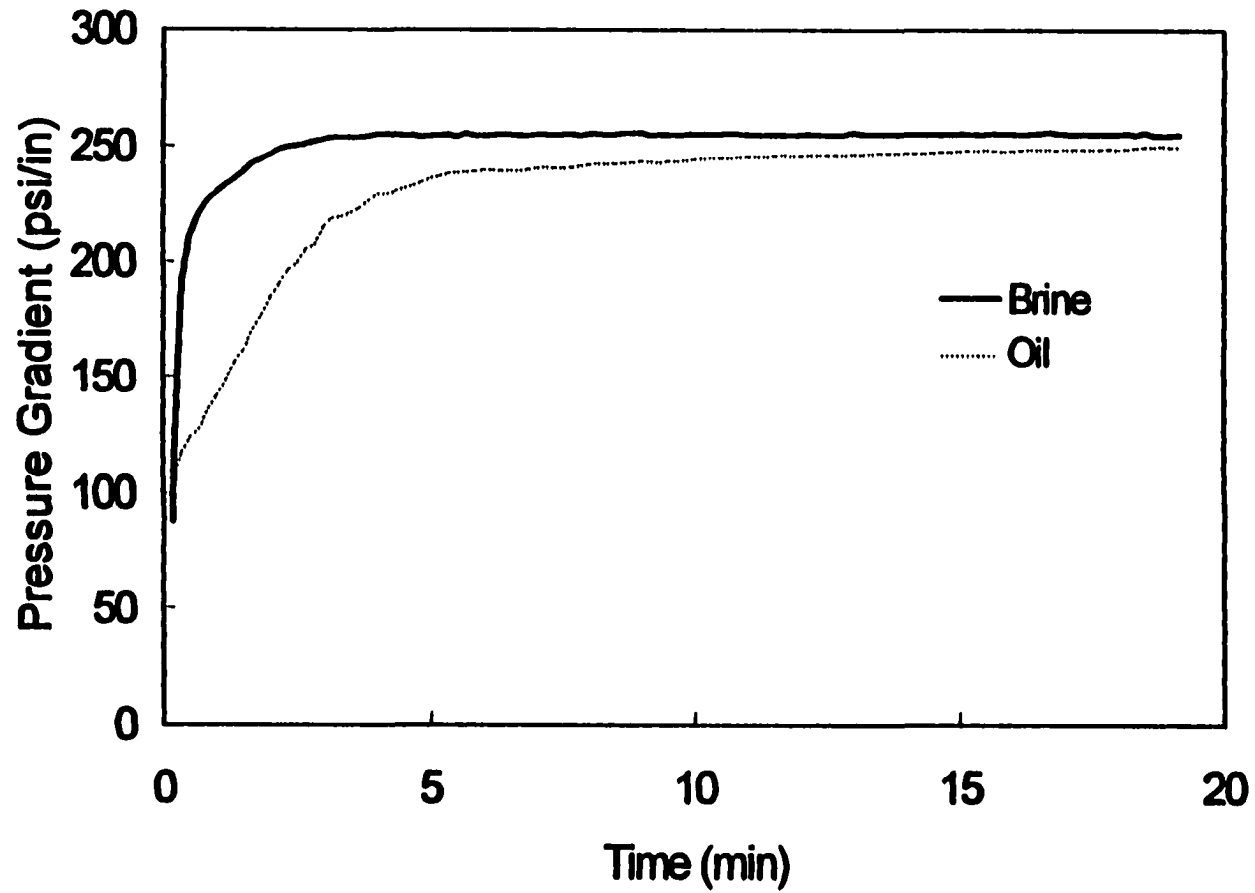


Fig. 5-15: Pressure Gradient Profile in the 0-2" Section of Brine and Oil Cores During the Leakoff of crosslinked Guar

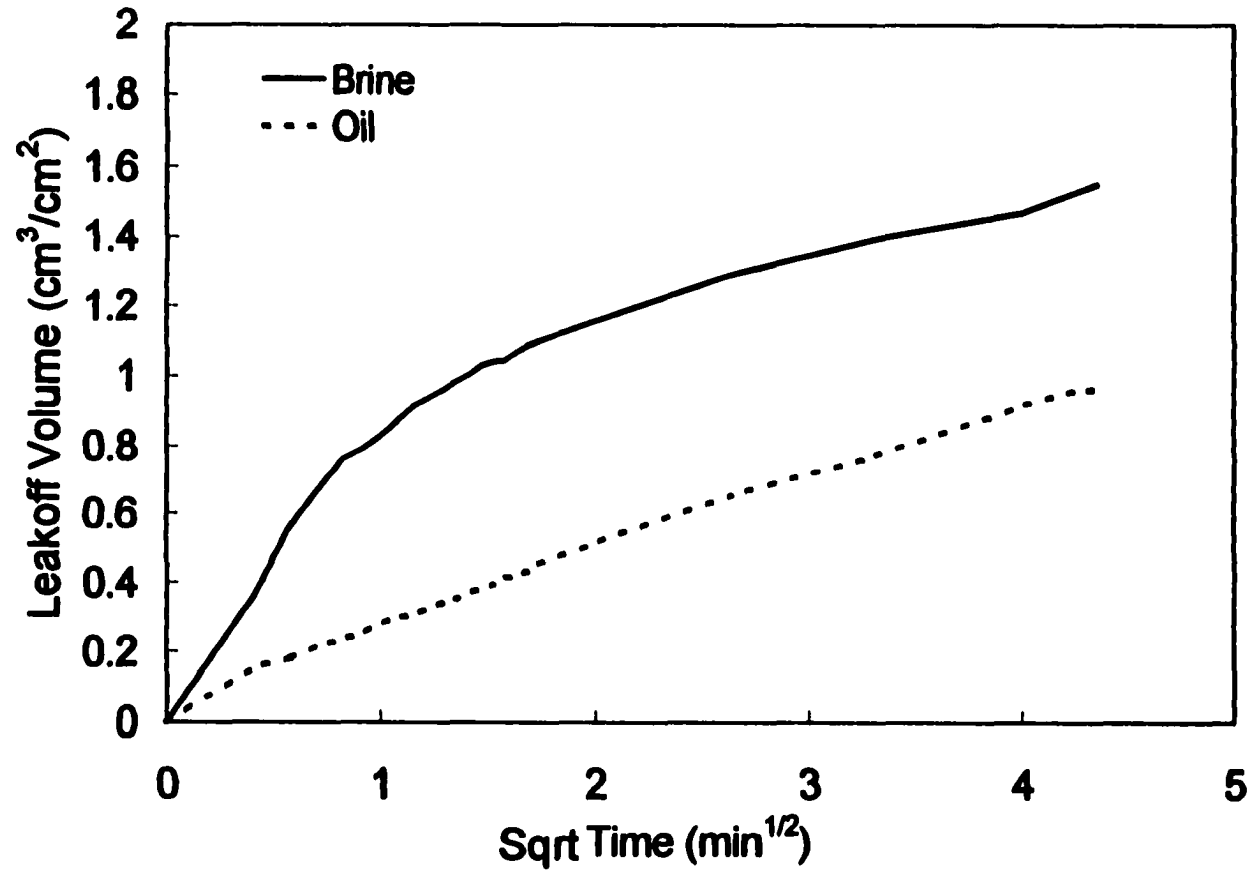


Fig. 5-16: Comparison Between Leakoff of crosslinked 35 lb/Mgal HPG in Brine and Oil Cores

to that of crosslinked guar. In this case also, the leak-off in the oil core was significantly lower than that observed in the brine core. The spurt loss in oil core was approximately 9 times lower than that obtained in brine core as indicated in Table 5-8.

5.3.2.3 Effect of FLA on Leak-off

Figure 5-17 portrays the leak-off behavior of 35 lb/Mgal borate crosslinked HPG, with and without FLA in oil cores. It has been shown by several researchers¹⁴⁻¹⁸ that FLA has a significant impact on leak-off in 100% brine saturated core samples. It promotes the reduction of spurt loss and to some extent enhances the wall building coefficient by forming an internal and/or external filter cake. However, in the case of oil cores it is evident from Fig. 5-17 and Table 5-8 that FLA has practically no effect on leak-off. The FLA used was 25 lb/Mgal silica flour. Within the range of permeability investigated, the spurt loss and C_w obtained with FLA are comparable to those obtained without FLA as indicated in Table 5-8. The slight variation in spurt loss and C_w could be attributed to the difference in permeability.

The sectional pressure gradient variations during the leak-off of 35 lb/Mgal crosslinked HPG, with and without FLA is shown in Fig. 5-18 and Fig. 5-19, respectively. Had the FLA been effective in controlling the leak-off, one would expect a steep increase in pressure gradient in the 0-2 inch section of the core sample as soon as leak-off was initiated. However, that was not the case as illustrated in Fig. 5-18. The pressure gradient in the 0-2 inch section of the core gradually increases and the trend is comparable to that observed when no FLA was used (Fig. 5-19). This indicates that the presence of oil prevents the FLA from firmly adhering to the face of the core.

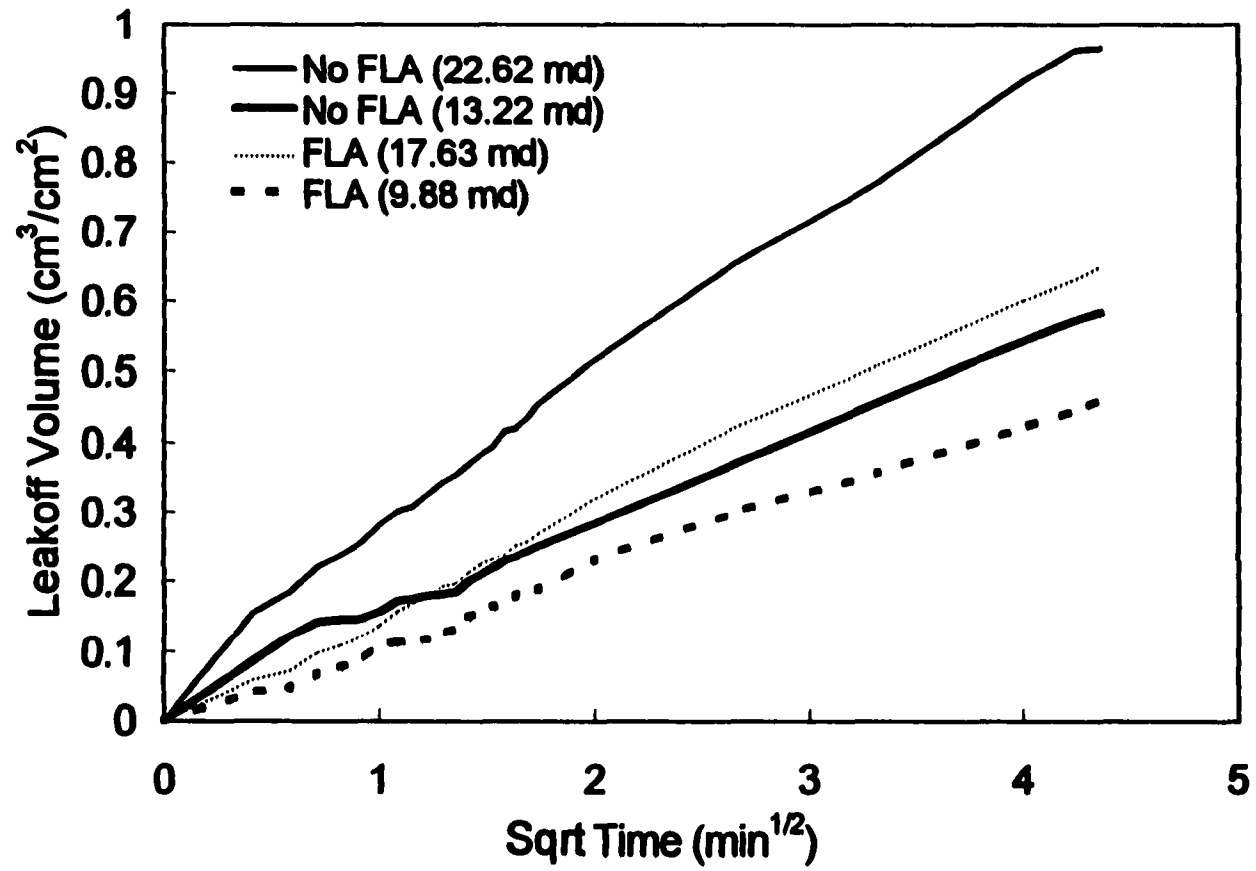


Fig. 5-17: Effect of Fluid Loss Additive (FLA) on the Leakoff of crosslinked 35 lb/Mgal HPG in Oil Cores

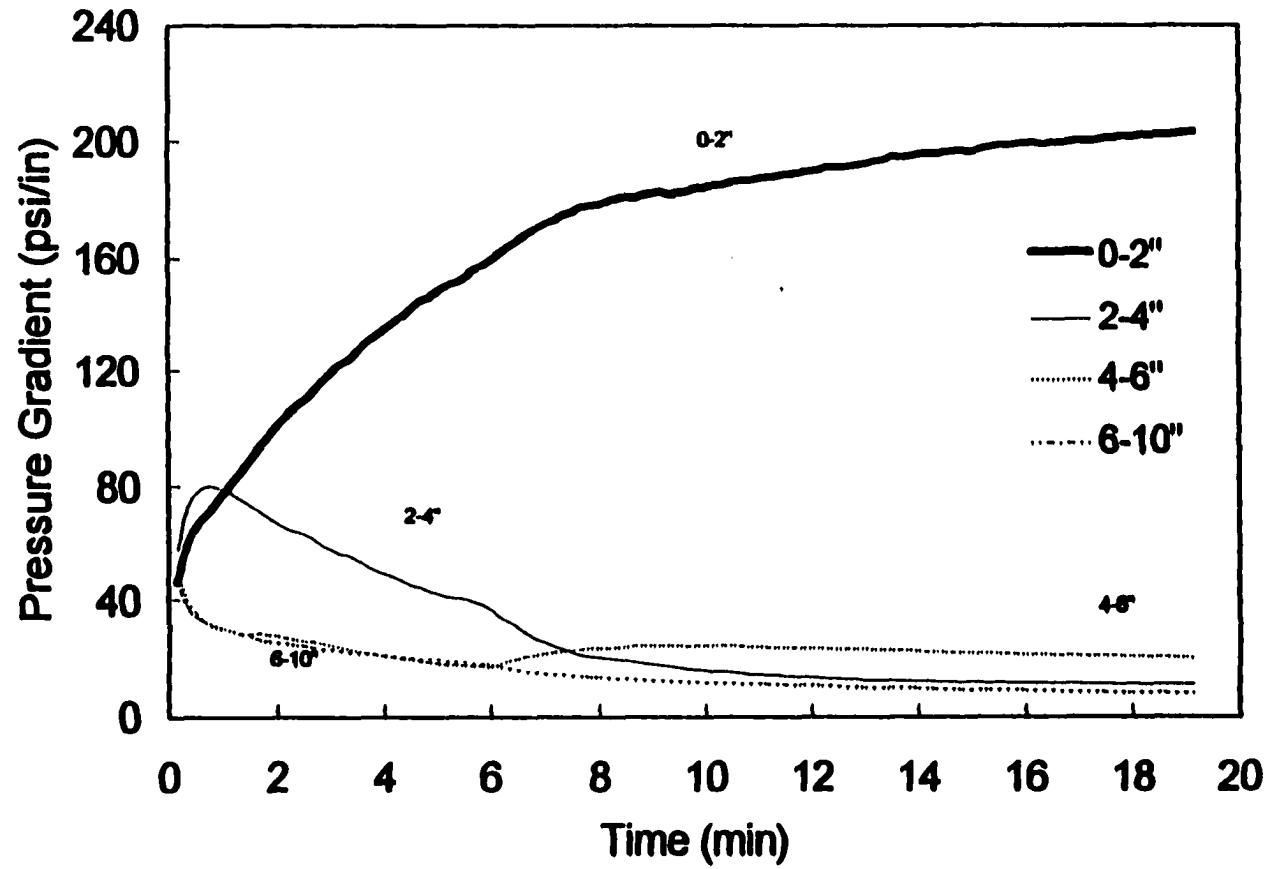


Fig. 5-18: Sectional Pressure Gradient During Leakoff of 35 lb/Mgal crosslinked HPG + FLA In Oil Core

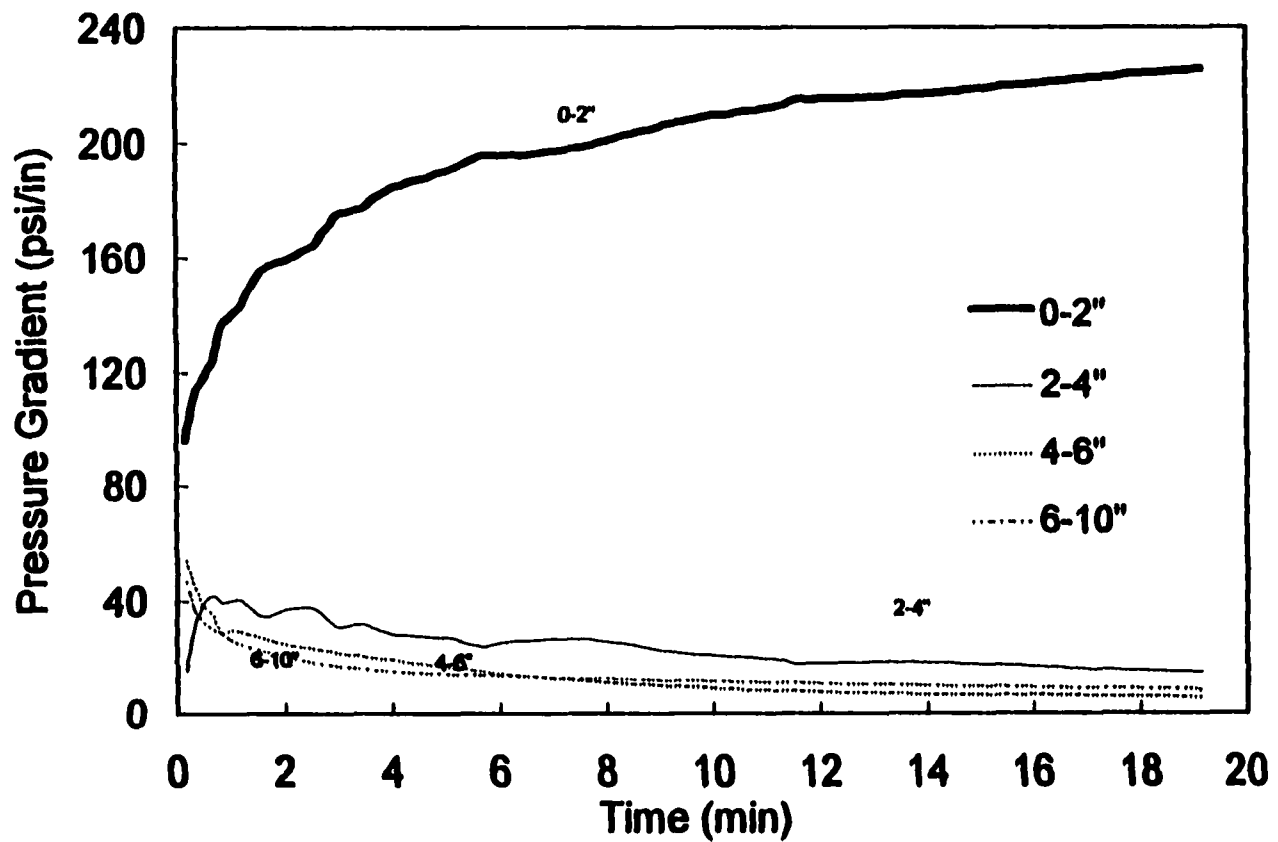


Fig. 5-19: Sectional Pressure Gradient During Leakoff of 35 lb/Mgal crosslinked HPG in Oil Core

5.3.2.4 Leak-off of Linear Fluids

Figure 5-20 compares the leak-off behavior of 35 lb/Mgal linear and borate crosslinked fluids (HPG and guar) in oil cores. Comparable early time leak-off volume was noticed for all the fluids. The slight variation could be attributed to the difference in permeability. However, after approximately one minute the leak-off behavior of linear fluids significantly deviates away from that of crosslinked fluids. The possible explanation for this could be that the pore throat size is large enough to allow the polymer molecules to enter the core as a result of which no external filter cake is being formed. There is also a possibility that the relative permeability of the linear fluid filtrate is higher compared to that of the crosslinked filtrate. Figures 5-21 and 5-22 illustrate the variation in sectional pressure gradient during the leak-off of linear 35 lb/Mgal linear HPG and guar, respectively. In both the cases, the pressure gradient in the 0-2 inch section of the core decreases with time. This indicates that there is a front propagation and no external filter cake is formed. However, the pressure gradient in the 2-4 inch section of the core gradually increases with time, indicating gradual plugging in that section.

5.3.2.5 Effect of crude oil on the Leak-off of Crosslinked HPG

The leak-off of 35 lb/Mgal borate crosslinked HPG in mineral and crude oil core samples is shown in Fig. 5-23. Identical early time leak-off trend was observed in both the cases. In the case of crude oil sample, the spurt loss was slightly higher whereas the C_w was lower when compared to that observed in mineral oil sample. The increase in spurt loss in the case of crude oil, can be attributed to the lower viscosity of crude oil (6 cP) as opposed to that of mineral oil (35 cP). In addition, one would have

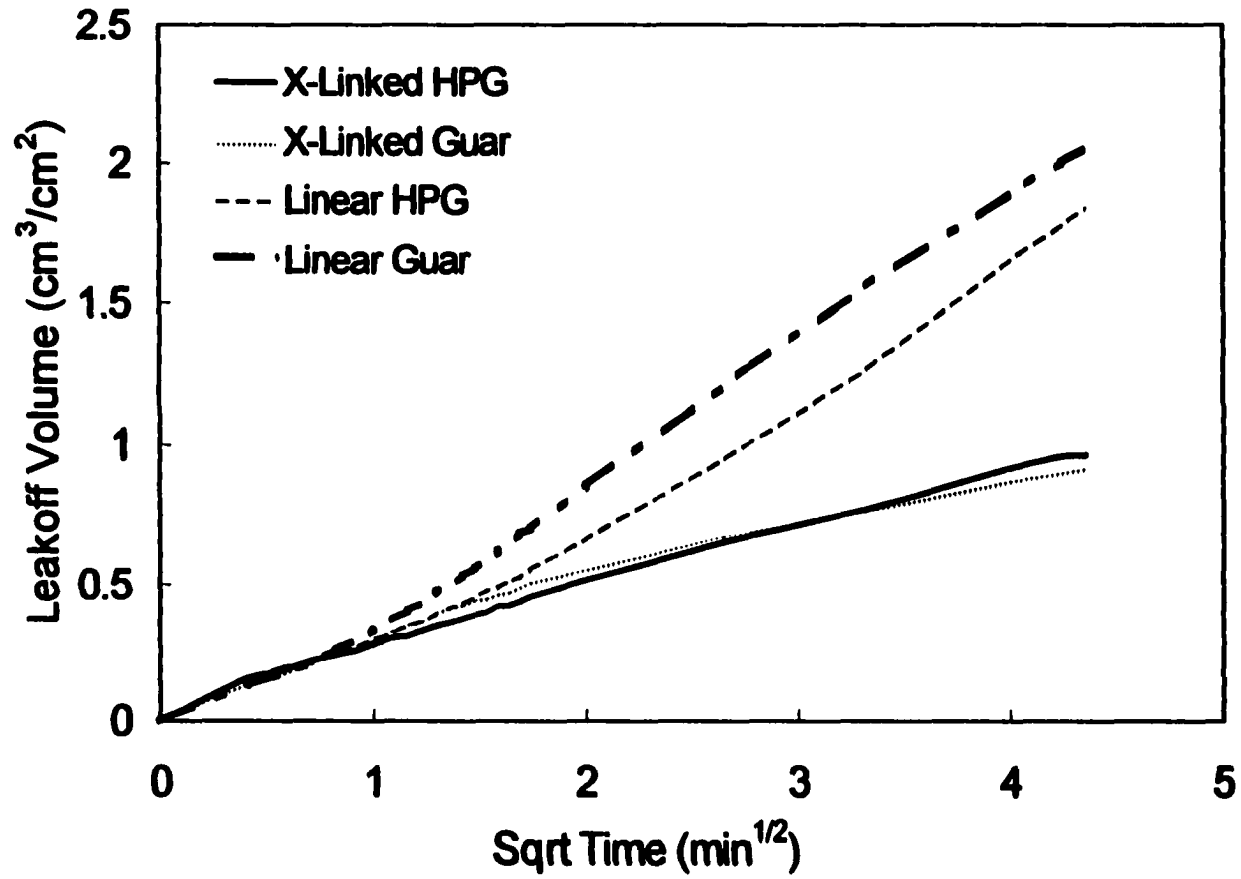


Fig. 5-20: Comparison Between Linear and crosslinked 35 lb/Mgal Guar and HPG Leakoff in Oil Cores

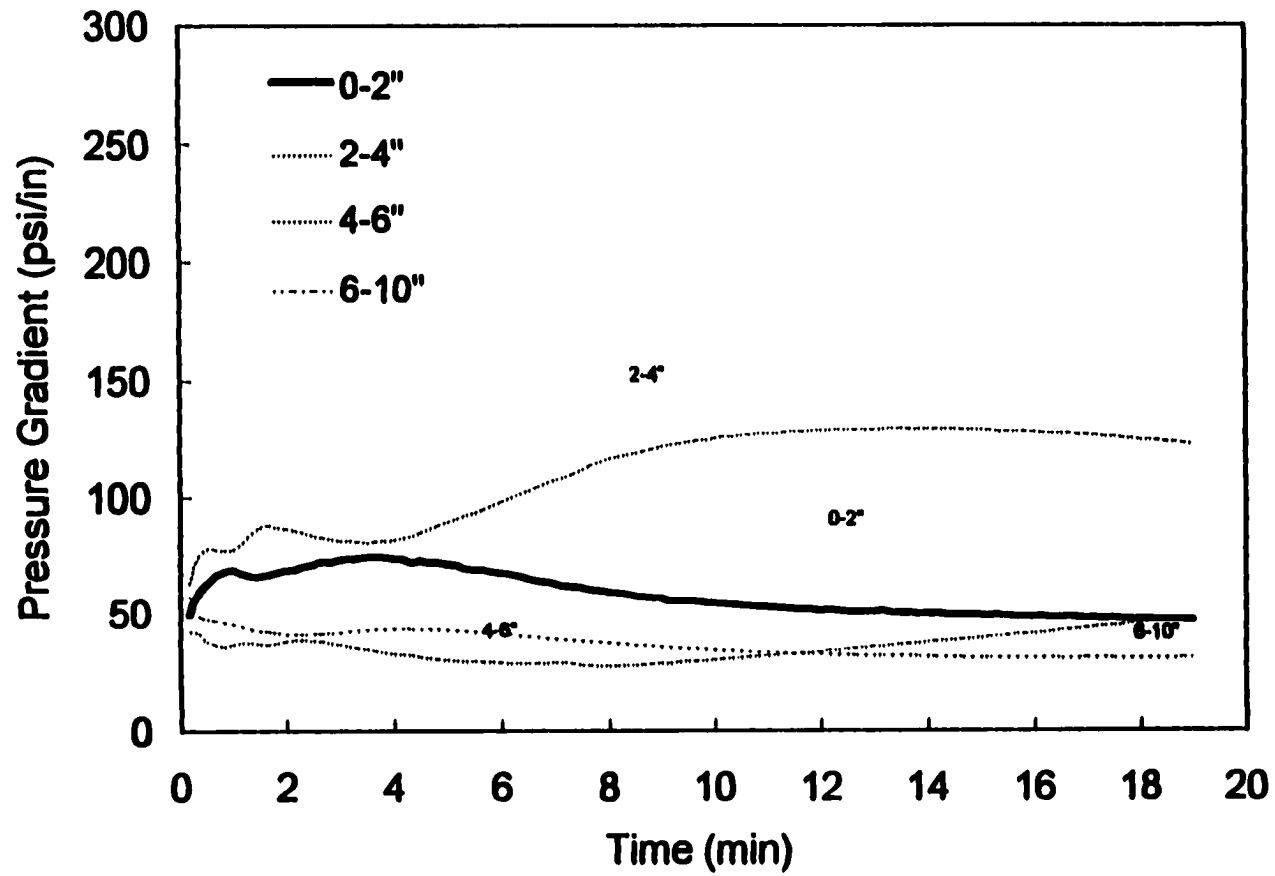


Fig. 5-21: Sectional Pressure Gradient During Leakoff of 35 lb/Mgal Linear HPG in Oil Core

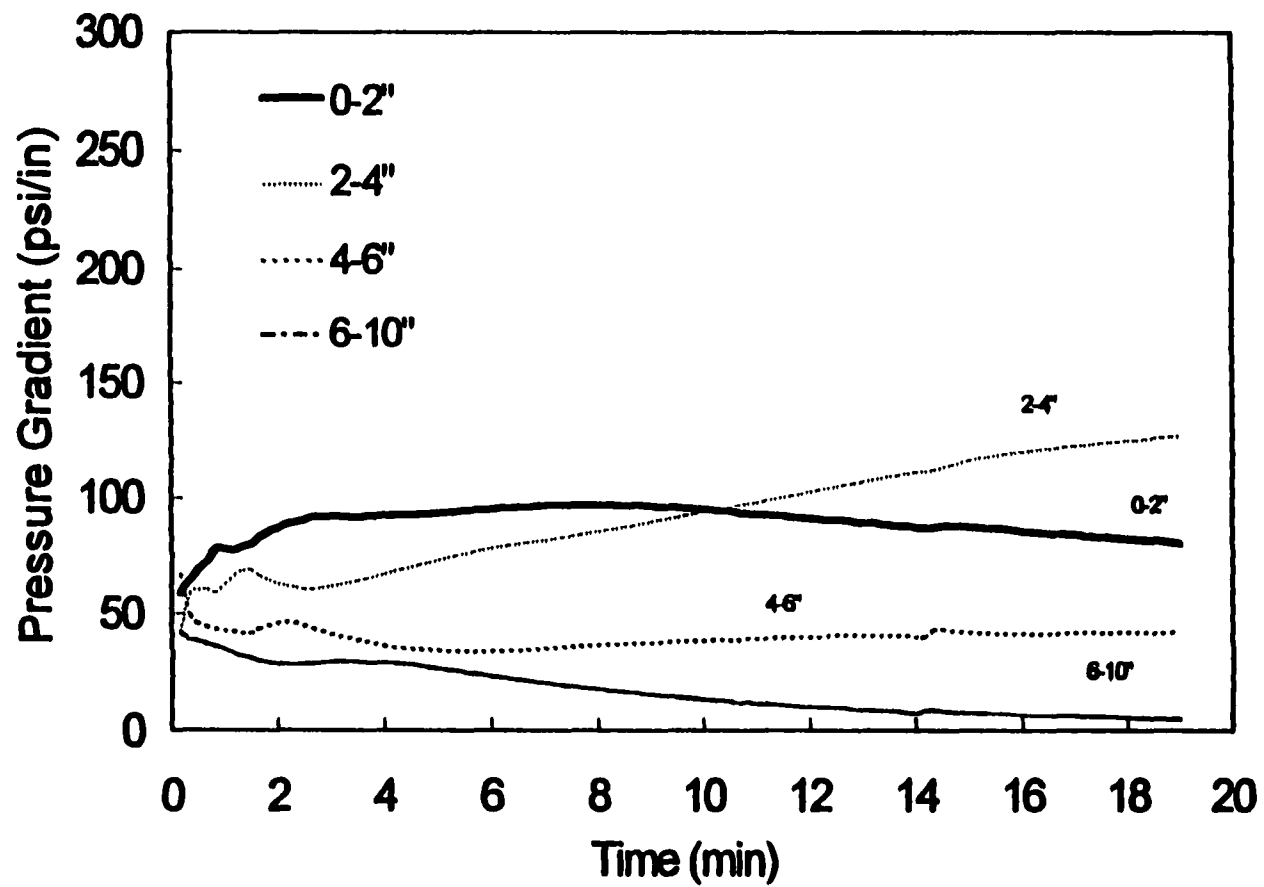


Fig. 5-22: Sectional Pressure Gradient During Leakoff of 35 lb/Mgal Linear Guar in oil core

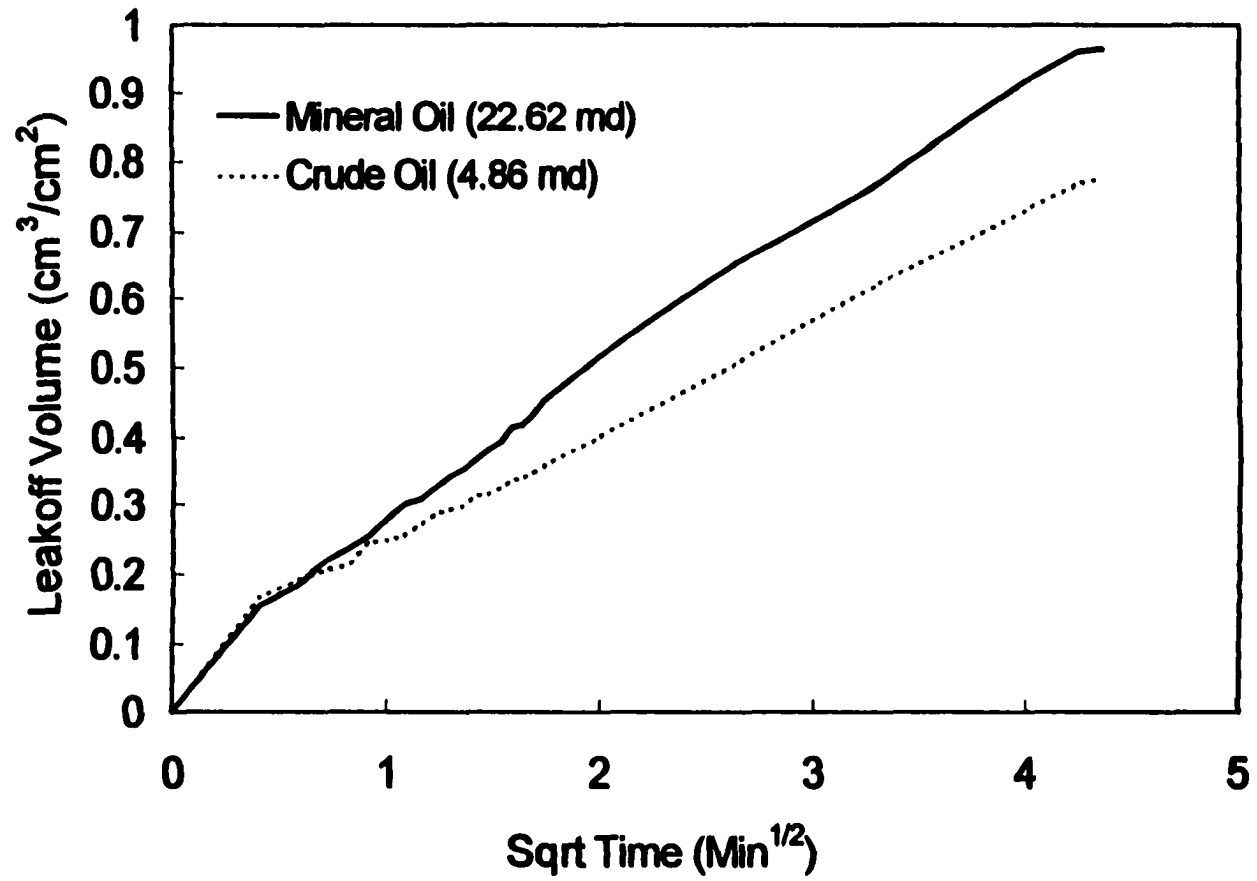


Fig. 5-23: Comparison Between Leakoff of crosslinked 35 lb/Mgal HPG in Mineral and crude oil core

also expected the C_w in the case of crude oil sample to be higher due to lower crude oil viscosity. However, that was not the case since C_w is a function of fracture face permeability as illustrated in Fig. 5-25. The fracture face permeability of crude oil sample was lower than that of mineral oil sample, therefore the C_w was lower in the case of crude oil sample.

5.3.2.6 Effect of pressure drop on leak-off

The effect of pressure drop on the leak-off behavior of 35 lb/Mgal borate crosslinked HPG in crude oil core samples is portrayed in Fig. 5-24. The pressure drop during leak-off was maintained at 500/1000 psid. It is evident from the figure that increase in pressure gradient only increased the spurt loss (Table 5-8) but there was no effect on C_w (identical slopes). This clearly shows that initial leak-off is pressure gradient dependent and later time leak-off is independent of the pressure gradient. This suggests that the filter cake stabilization provides a stepped pressure profile that accommodates most of the pressure gradient across the system.

5.3.2.7 Effect of First Section Permeability on C_w

Fig. 5-25 illustrates the effect of 0-2 inch permeability on C_w of borate crosslinked 35 lb/Mgal HPG in mineral oil core samples. Within the range of permeability investigated, it is evident from the figure that C_w is directly proportional to the first section permeability.

5.3.2.8 Simulation Results

In all the cases, the viscosity of the filtrate was assumed to be 1 cP. Figures 5-26 and 5-27 compare the model's prediction of the leak-off volume and pressure gradient variations, respectively, with the experimental data during the leak-off of 35

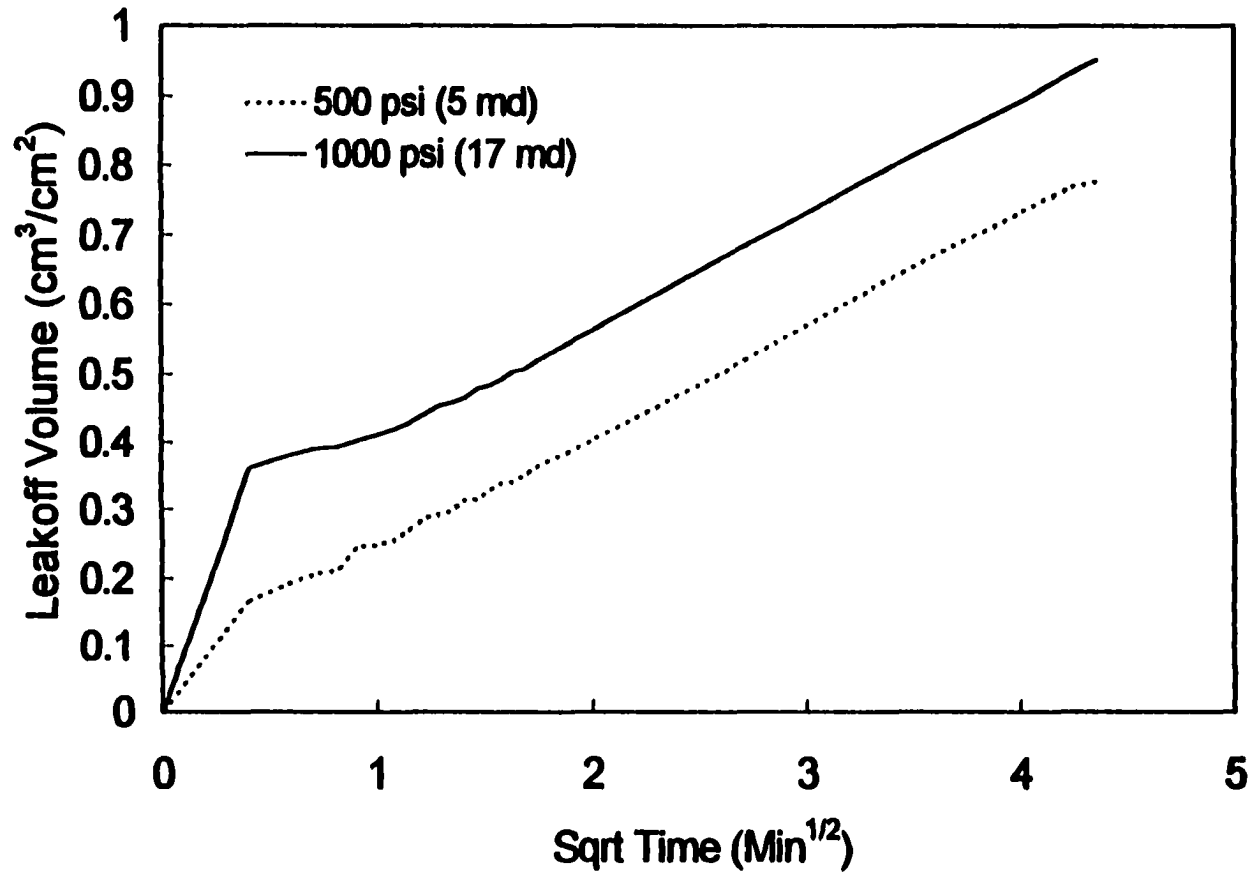


Fig. 5-24: Effect of Pressure Drop on the Leakoff of 35 lb/Mgal crosslinked HPG in Crude Oil Saturated Core Samples

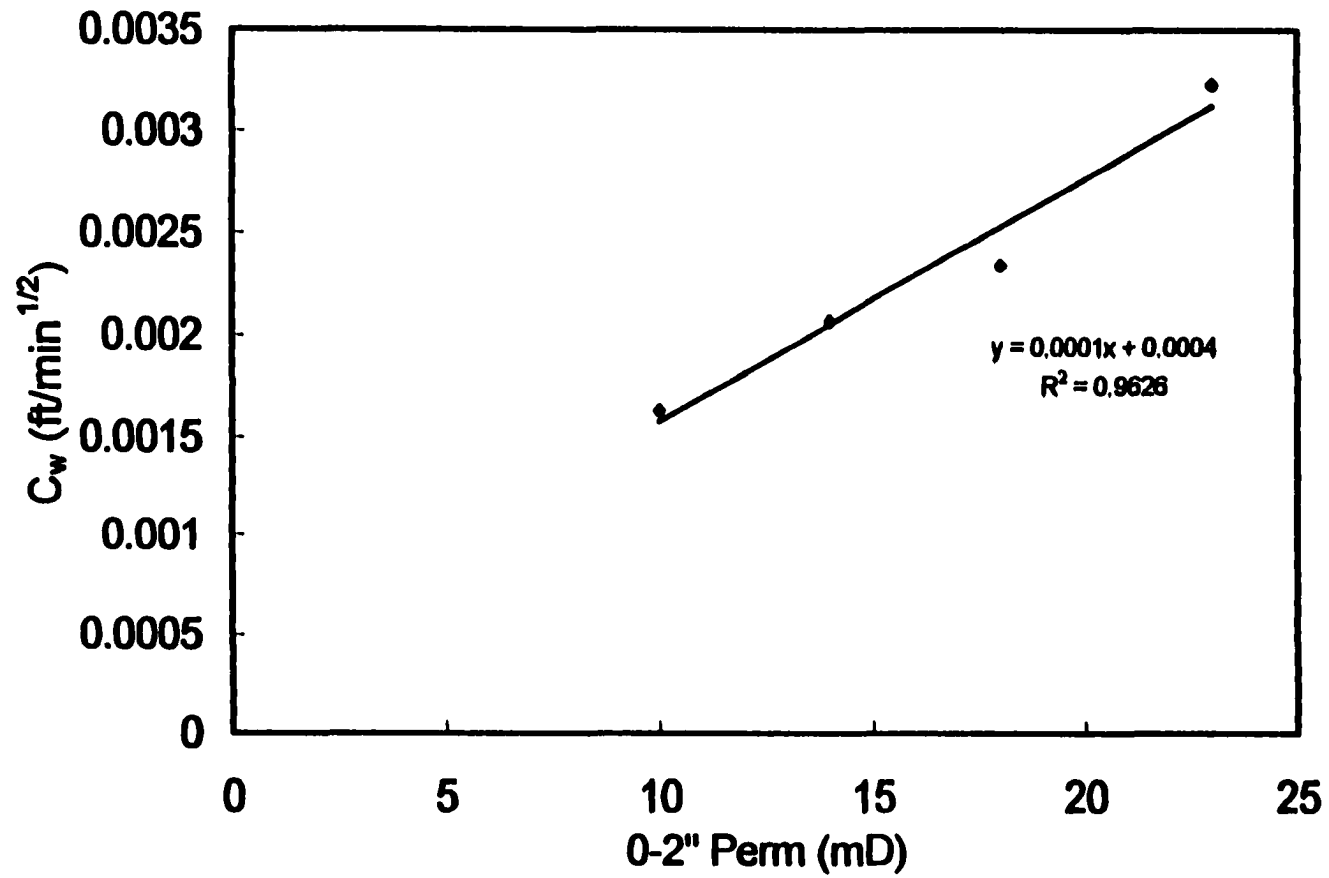


Fig. 5-25 : Effect of Fracture Face Permeability on C_w of 35 lb/Mgal crosslinked HPG In Mineral Oil Saturated Core Samples

lb/Mgal borate crosslinked guar in 100% brine saturated core. A good match is obtained between the model predictions and the experimental data as observed in the figures.

A comparison between the predicted and experimentally measured leak-off of borate crosslinked 35 lb/Mgal HPG in a core sample saturated with mineral oil is illustrated in Fig. 5-28. In this case also, a good match is obtained between the model predictions and the experimental data. Also, the sensitivity of the model prediction to filtrate viscosity is shown in Fig. 5-28. It is evident from the figure that the model is quite sensitive to the filtrate viscosity. A fairly good match for pressure gradient profile is also obtained as shown in Fig. 5-29.

Figures 5-30 and 5-31 compare the predicted and experimentally measured leak-off of borate crosslinked 35 lb/Mgal HPG with 25 lb/Mgal silica flour in mineral oil saturated core samples. In both cases, only a qualitative agreement between the experimental results and model predictions is achieved for early time leak-off. Also, the model is unable to match the pressure gradient profile as depicted in Fig. 5-32.

A comparison between the model predicted and experimentally measured leak-off of borate crosslinked 35 lb/Mgal HPG in a crude oil saturated core sample is illustrated in Fig. 5-33. As seen in the figure, the model under-predicts early time leak-off, however at later times a good match was achieved.

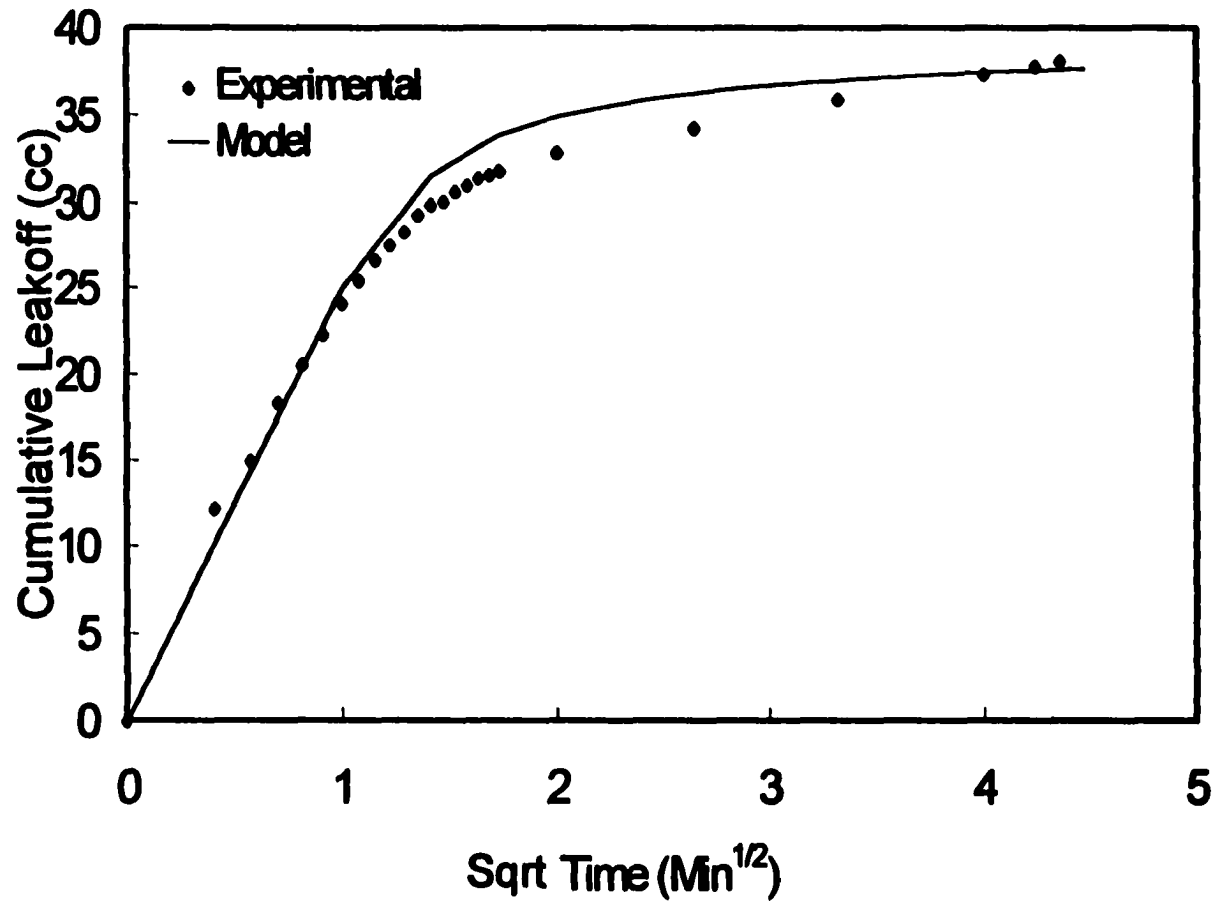


Fig. 5-26: Comparison of Model Predicted and Experimentally Measured Leakoff Volume (Test 6-1)

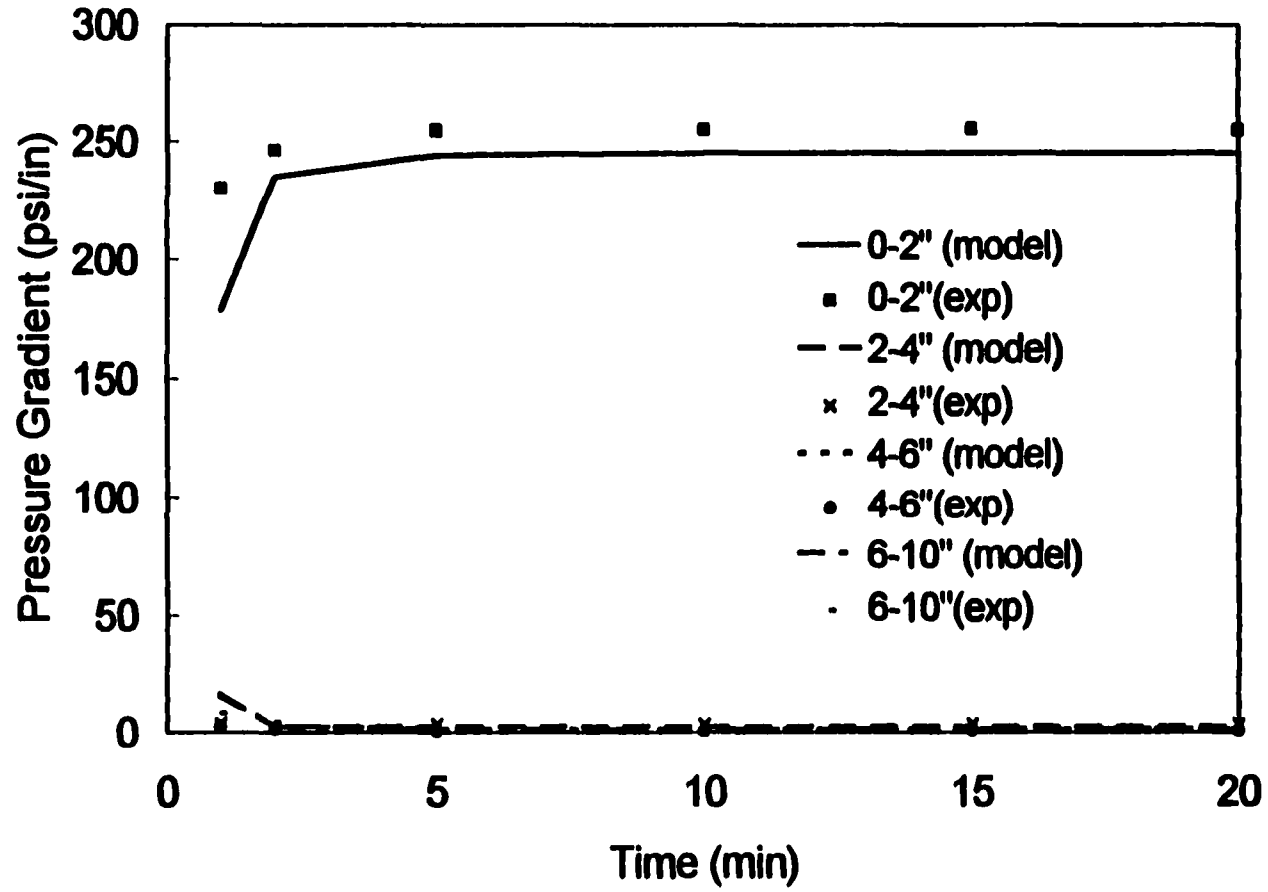


Fig. 5-27: Comparison of Predicted and Observed Pressure Gradient Profile (Test 6-1)

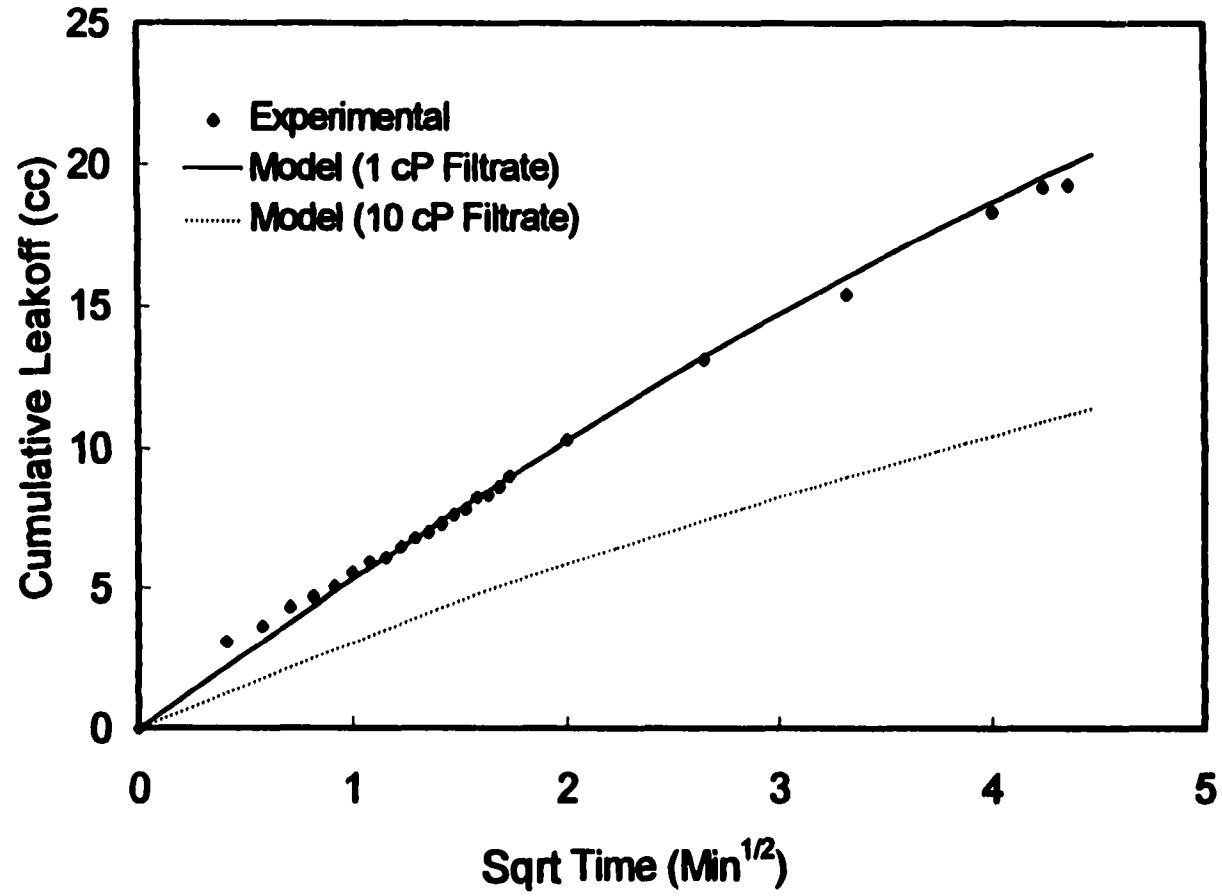


Fig. 5-28: Comparison of Model Predicted and Experimentally Measured Leakoff Volume (Test 6-4)

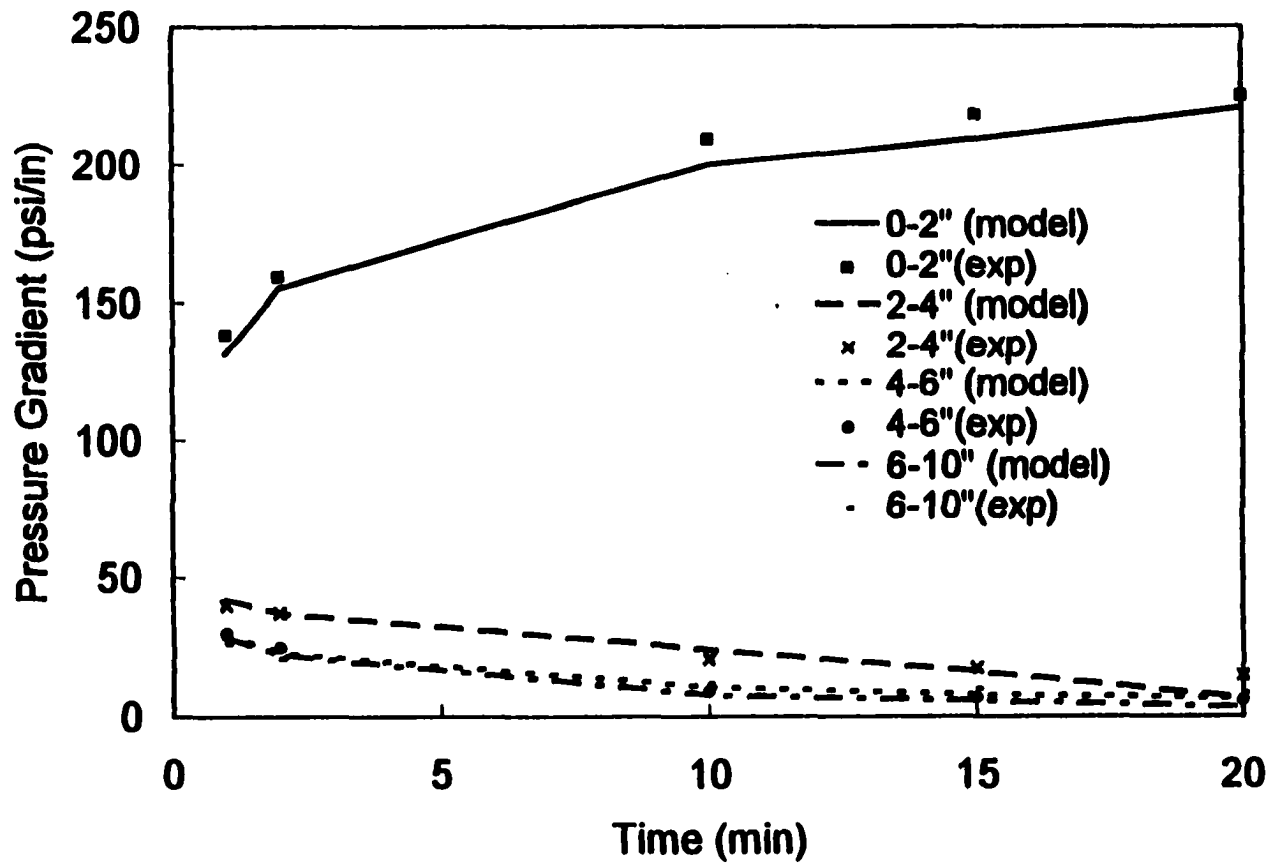


Fig. 5-29: Comparison of Predicted and Observed Pressure Gradient Profile (Test 6-4)

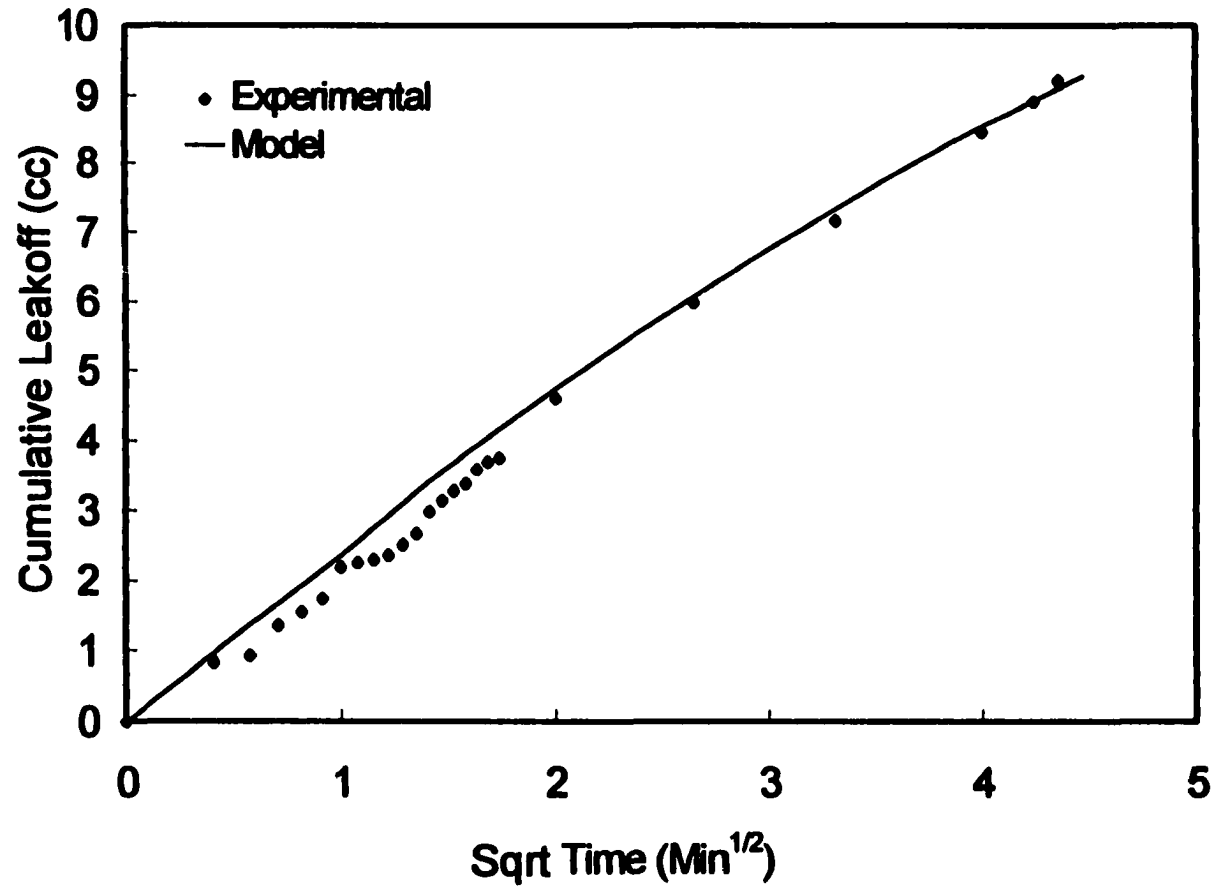


Fig. 5-30: Comparison of Model Predicted and Experimentally Measured Leakoff Volume (Test 6-7)

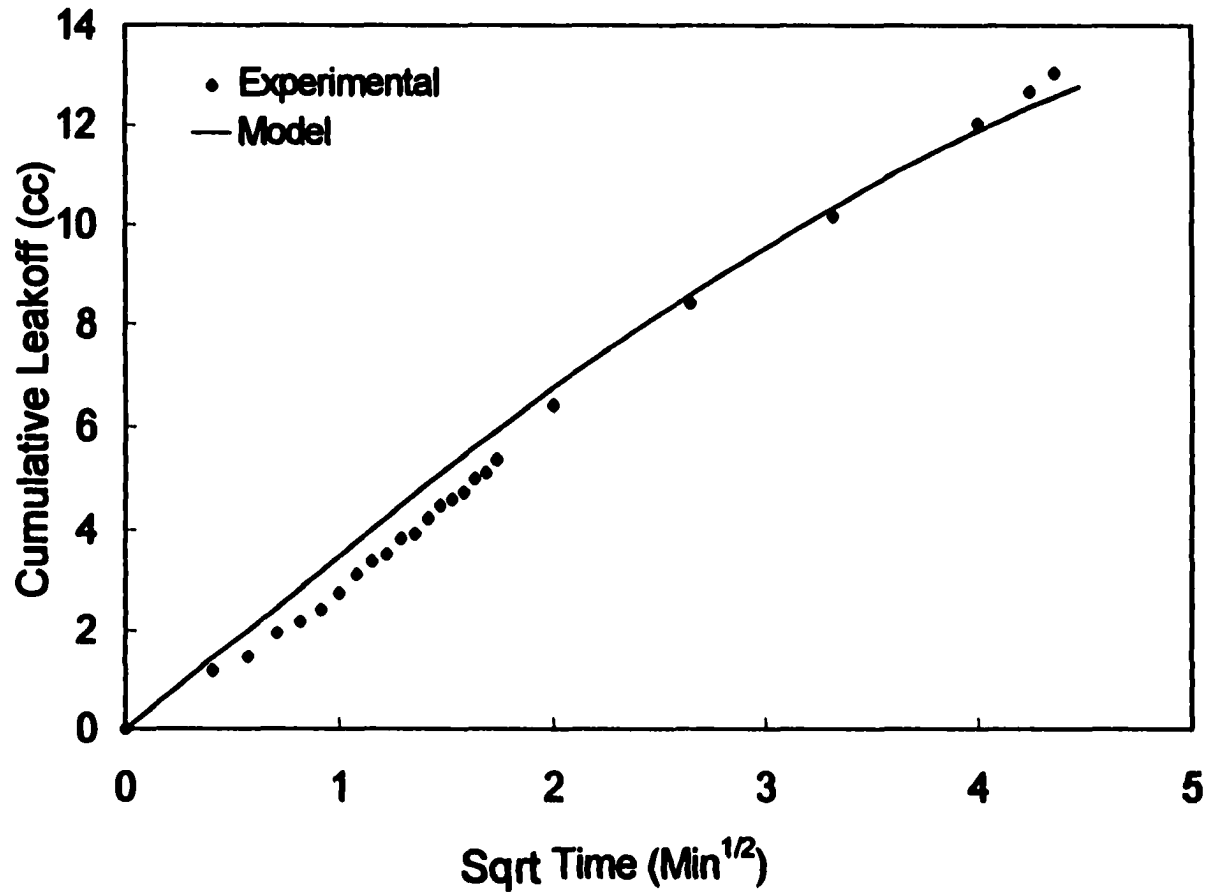


Fig. 5-31: Comparison of Model Predicted and Experimentally Measured Leakoff Volume (Test 6-8)

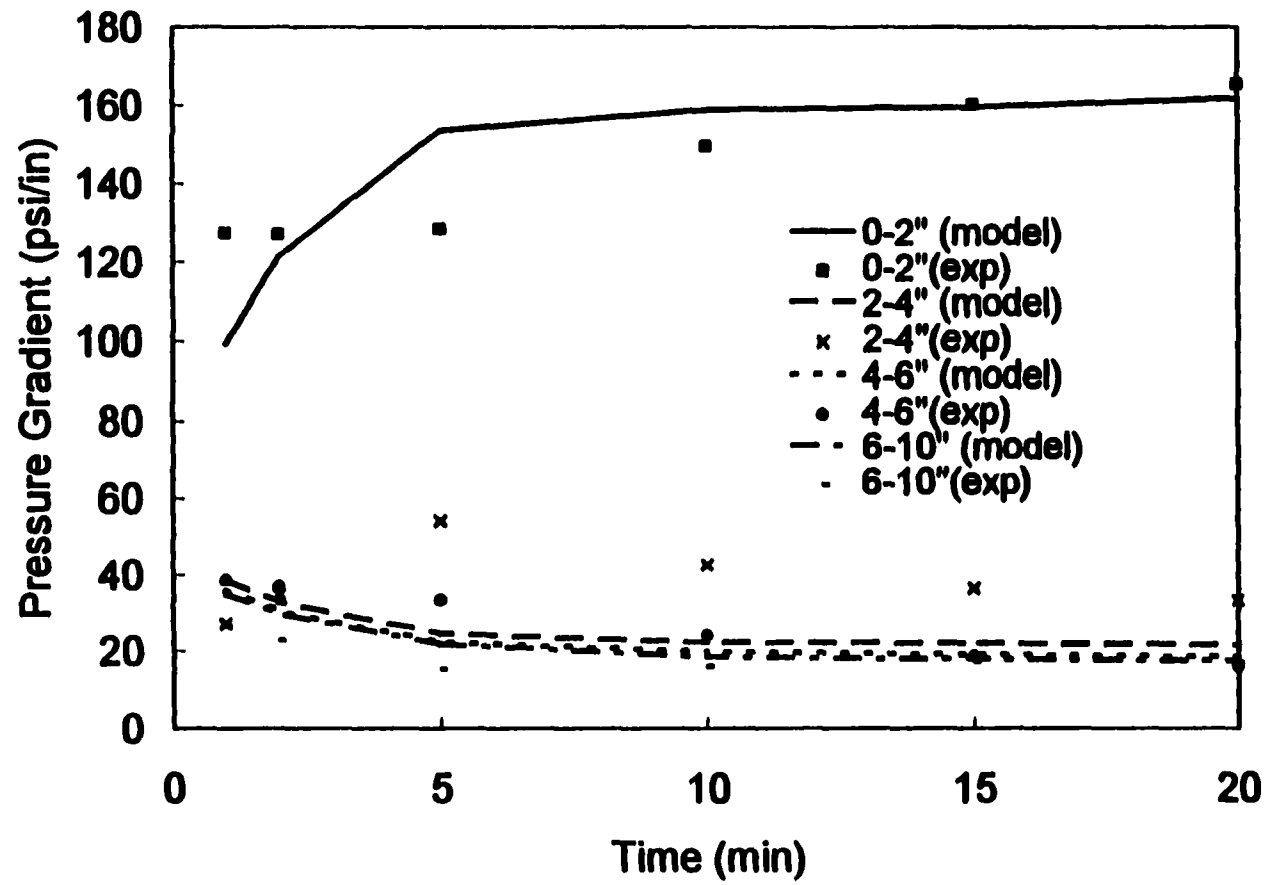


Fig. 5-32: Comparison of Predicted and Observed Pressure Gradient Profile (Test 6-7)

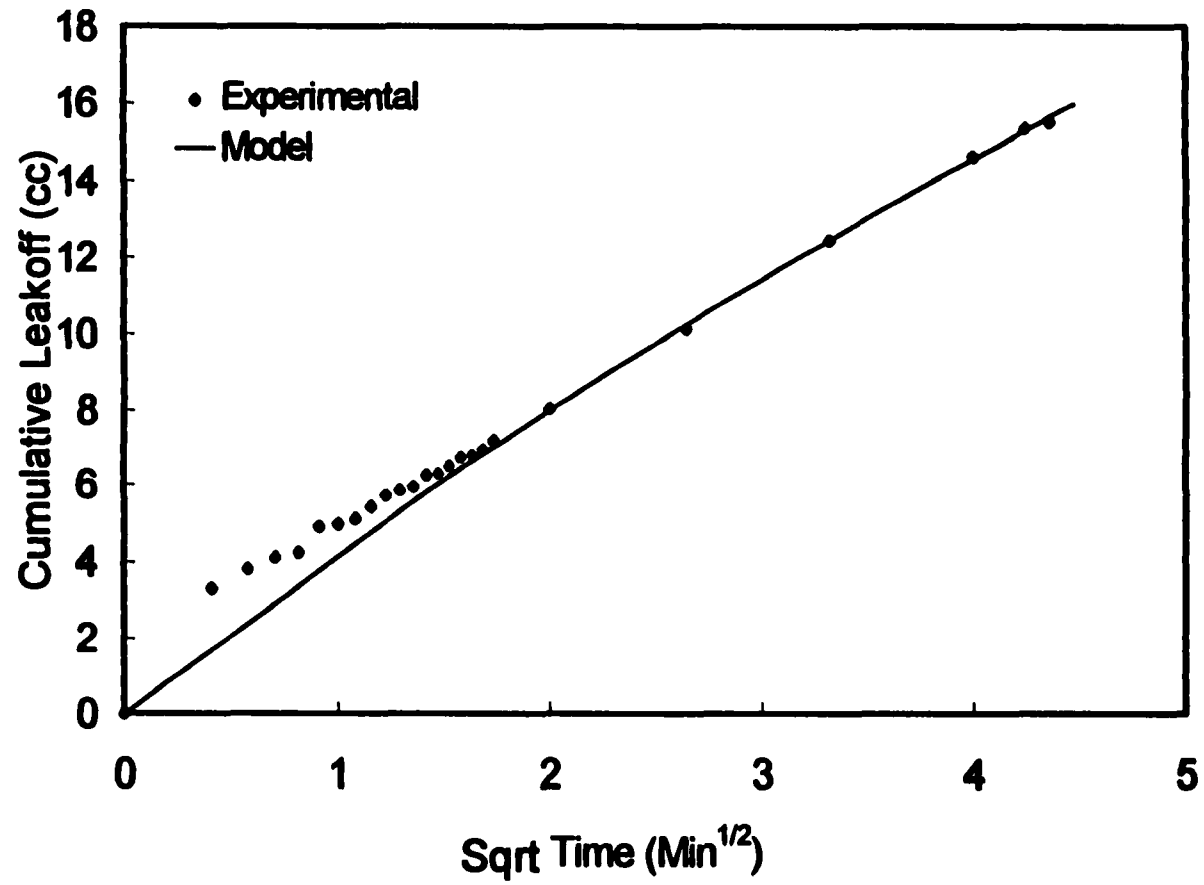


Fig. 5-33: Comparison of Model Predicted and Experimentally Measured Leakoff Volume (Test 6-9)

Chapter 6

Return Permeability Testing for Oil Reservoirs

6.1 Introduction

During the hydraulic fracturing of high permeability reservoirs there is always a concern that the fracturing fluid leak-off may cause a reduction in permeability, thereby seriously affecting the well producibility. One important criterion of a successful fracturing treatment is a limited formation damage. The leak-off can be controlled with the aid of fluid loss additives. But, the addition of fluid loss additives may also severely reduce the fracture face permeability.

Very few researchers^{17-18,29} have investigated the impairment in formation permeability caused due to fracturing fluid leak-off in high permeability reservoirs. Further, all of the past studies were conducted in 100% brine saturated core samples. However, the formations that are hydraulically fractured contain movable oil and/or gas in addition to brine. It has been shown in Chapter 5 that the presence of movable oil significantly alters the leak-off behavior of the fracturing fluids. Therefore, one would expect the return permeability and its recovery after leak-off in oil core to be different compared to that observed in 100% brine saturated core sample.

The objective of this study is to investigate the effect of fracturing fluid leak-off on formation permeability in the presence of movable oil saturation. The variation of permeability with distance from the fracture face and its subsequent recovery as a function of production from the reservoir is investigated.

6.2 Experimental Procedures

In this study, Berea sandstone core samples 2 inch in diameter and 10 inch long were used. The average porosity of the core sample is 25%. The fracturing fluids tested were 35 lb/Mgal guar (linear and crosslinked) and 35 lb/Mgal HPG (linear and crosslinked). The crosslinker used was borate. The base fluid pH for crosslinked fluids was maintained at 9.0. In order to evaluate the impact of fluid loss additives (FLA) on regain permeability, 25lb/Mgal silica flour was used as a FLA in some tests. The flow direction of test fluids, which is representative of flow directions near fracture face during and after fracturing, and the position of sectional pressure ports is shown in Fig. 6-1.

The experiments in the presence of mobile mineral or crude oil were conducted in the following sequence:

1. Initial permeability of the core sample was determined in the leak-off direction according to the procedure described in chapter 2. The initial, sectional and overall brine permeability of the core samples are summarized in Table 6-1.
2. The brine in the core sample was displaced with mineral or crude oil from the production direction (the procedure is described in details in Chapter 5). The initial, sectional and overall oil permeability of the core samples are summarized in Table 6-1.

3. **Leak-off of the fracturing fluid was initiated by pumping the fracturing fluid across the face of the core sample in the leak-off direction, at a shear rate of 55 sec^{-1} . A differential pressure of 500/1000 psi was maintained across the length of the core sample. The duration of leak-off test was 20 minutes. In the case of crosslinked fluids, the leak-off was initiated only after a good crosslinking was observed in the effluent fluid. The fluids and the FLA used for individual experiment are tabulated in Table 6-2.**
4. **The final step was to determine the alteration in permeability due to fracturing fluid leak-off. The core was shut-in for a period of at least 3 hours. At least 2 pore volumes of mineral or crude oil were then injected at a constant flow rate in the production direction. The variation in sectional and overall permeabilities was computed by continuously monitoring the sectional and overall differential pressures.**

For the purpose of establishing a good baseline to compare the effect of single and two-phase flow systems on return permeability after leak-off, two single-phase fracturing fluid leak-off experiments were also conducted. The fracturing fluids used were borate-crosslinked guar and HPG, without any FLA. Identical procedure as before was followed, except that step 2 was skipped and in step 4 brine was used instead of oil.

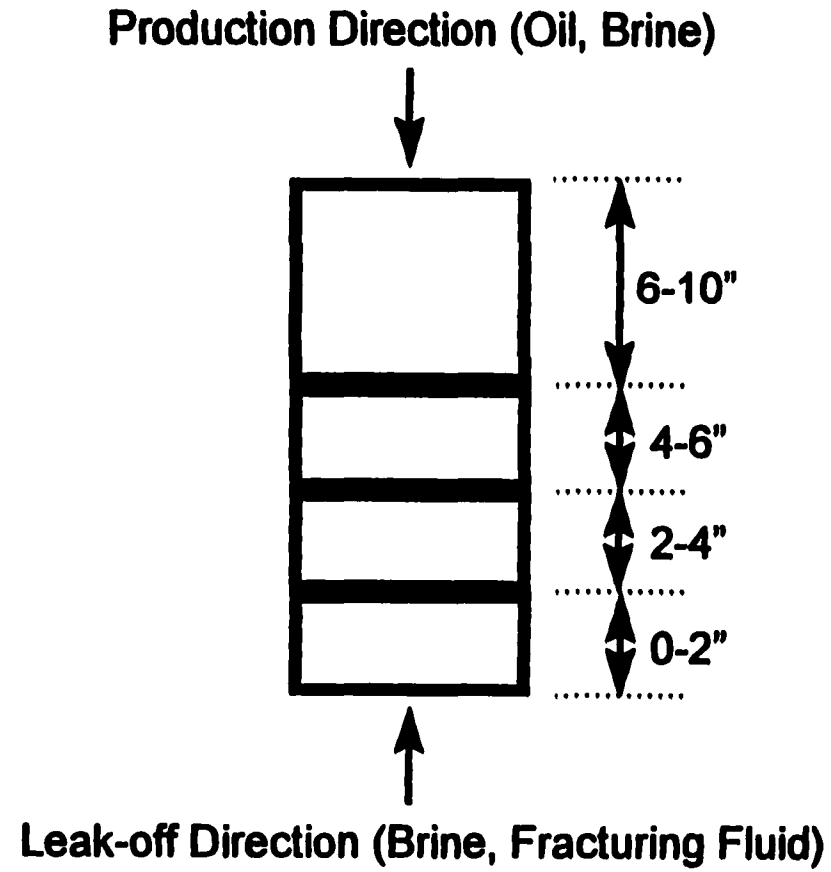


Fig. 6-1: Schematic of Flow Directions and Permeability Measurement Locations

Table 6.1: Sectional and overall brine and oil permeability (mD)

Test	Fluid Phase	0-2"	2-4"	4-6"	6-10"	0-10"
6-1	Brine (k)	44.2	96.3	144.1	19.6	35.5
	Final (k)	2.7	93.4	144.1	19.6	11.0
6-2	Brine(k)	106.3	72.3	167.4	169.1	121.8
	Mineral Oil (kk _{ro})	79.6	55.2	114.6	131.7	101.7
	Final (kk _{ro})	38.2	60.7	139.9	105.4	72.2
6-3	Brine (k)	25.0	74.7	5.9	12.8	13.2
	Final (k)	3.8	41.8	5.9	12.8	11.6
6-4	Brine(k)	28.3	66.9	99.7	94.5	61.3
	Mineral Oil (kk _{ro})	22.6	55.6	78.9	68.5	48.0
	Final (kk _{ro})	24.2	69.4	86.7	83.5	54.7
6-5	Brine(k)	44.3	35.4	60.7	53.5	47.8
	Mineral Oil (kk _{ro})	33.4	27.2	43.5	44.8	37.2
	Final (kk _{ro})	45.1	36.2	88.3	90.9	60.3
6-6	Brine(k)	99.2	117.7	159.2	188.9	141.1
	Mineral Oil (kk _{ro})	76.9	82.6	118.8	148.3	106.4
	Final (kk _{ro})	39.2	52.0	86.7	155.7	74.5
6-7	Brine(k)	12.9	12.7	16.3	23.0	16.4
	Mineral Oil (kk _{ro})	9.9	9.6	11.6	15.7	11.9
	Final (kk _{ro})	20.8	26.6	30.9	43.3	30.4
6-8	Brine(k)	24.4	27.5	146.8	90.5	47.1
	Mineral Oil (kk _{ro})	17.6	21.0	114.9	72.2	35.5
	Final (kk _{ro})	23.8	29.6	155.1	83.7	47.2
6-9	Brine(k)	22.5	29.0	32.2	37.7	30.7
	Crude Oil (kk _{ro})	4.9	7.0	12.6	4.3	5.7
	Final (kk _{ro})	2.8	3.4	5.2	1.6	2.0

Table 6.2: Fluids and FLA used and summary of total leak-off volume

Test	Fluid	FLA	S _w	Leak-off Volume (ml)
6-1	X-linked Guar	None	100%	38.1
6-2	X-linked Guar	None	S _{wc}	18.3
6-3	X-linked HPG	None	100%	31.0
6-4	X-linked HPG	None	S _{wc}	19.3
6-5	Linear HPG	None	S _{wc}	36.9
6-6	Linear Guar	None	S _{wc}	41.2
6-7	X-linked HPG	Silica flour	S _{wc}	9.8
6-8	X-linked HPG	Silica flour	S _{wc}	13.0
6-9	X-linked HPG	None	S _{wc}	15.5

6.3 Results and Discussion

Variation of permeability as a function of time/cumulative production for various sections are reported here for different fracturing fluids. In some tests, the flow rate was changed once the differential pressure across various sections of the core sample stabilized. Interestingly, an increase in flow rate was found to have a positive effect on regain permeability. This may be attributed to better gel removal at higher flow rates and/or reduction in drag. The flow rates during a given portion of a test are indicated on the plots.

6.3.1 Recovery of Return Permeability After Leak-off With Crosslinked Guar

Figures 6-2 and 6-3 (Test 6-1 & 6-2) allow the comparison of impairment in sectional and overall permeability, caused due to the leak-off of 35 lb/Mgal crosslinked guar and its subsequent recovery during flowback, in brine and oil saturated cores, respectively. For both tests, the leak-off time was 20 min. and the shut-in time was 3 hours. Although, the permeability was higher in the case of the oil core, the cumulative leak-off volume was less than half of that observed in the brine core (Table 6-1 & 6-2, Test 6-1 & 6-2).

In the case of the brine core, the permeability of the first two inch of the core was severely reduced (98%) followed by the next two inch (55%). However, no permeability reduction occurred in the last six inch of the core. During flowback, even after injecting three pore volumes of brine only six percent of the original permeability could be recovered for the first two inch and ninety seven percent was regained for the next two inch of the core sample. The damage can be attributed to the pore throat blocking by the polymer particles and the guar residue. These results are comparable

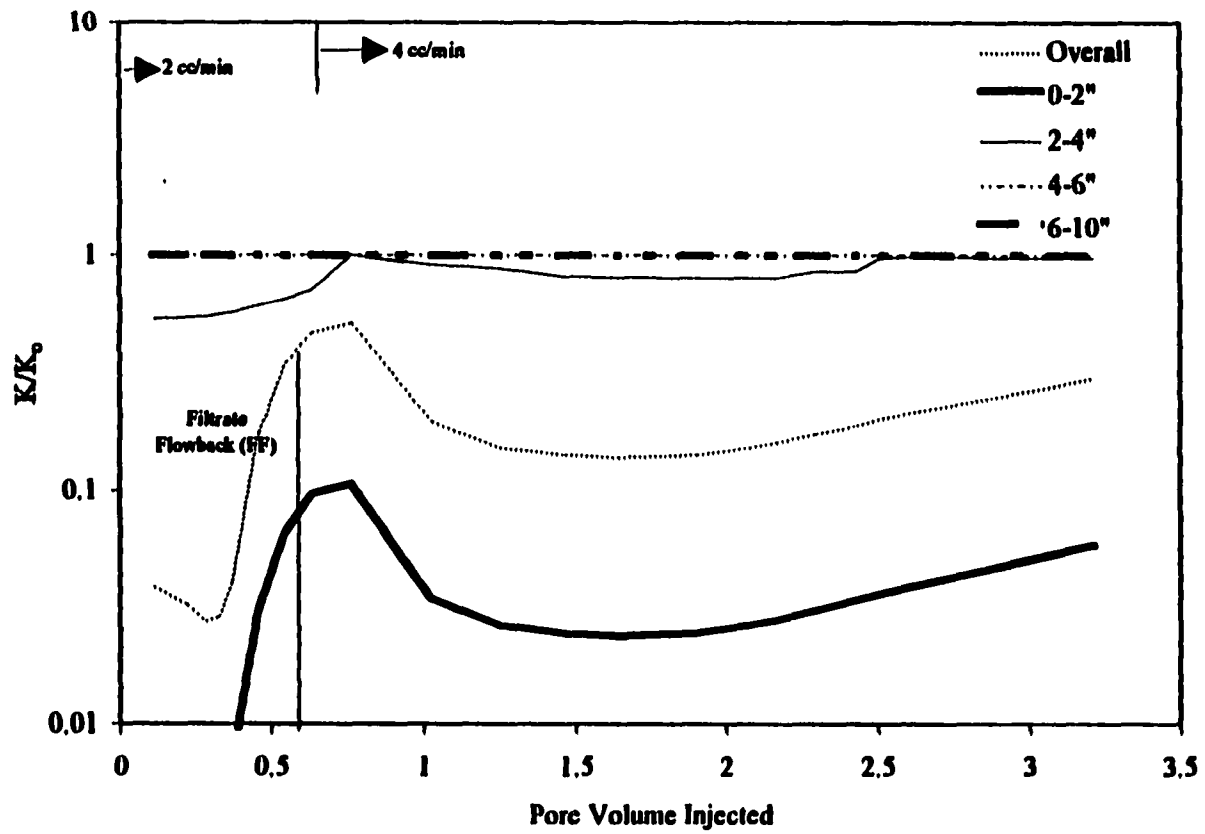


Fig. 6-2: Effect of 35 lb/Mgal Crosslinked Guar Leakoff on the Regain Permeability of Brine Core (Test 6-1)

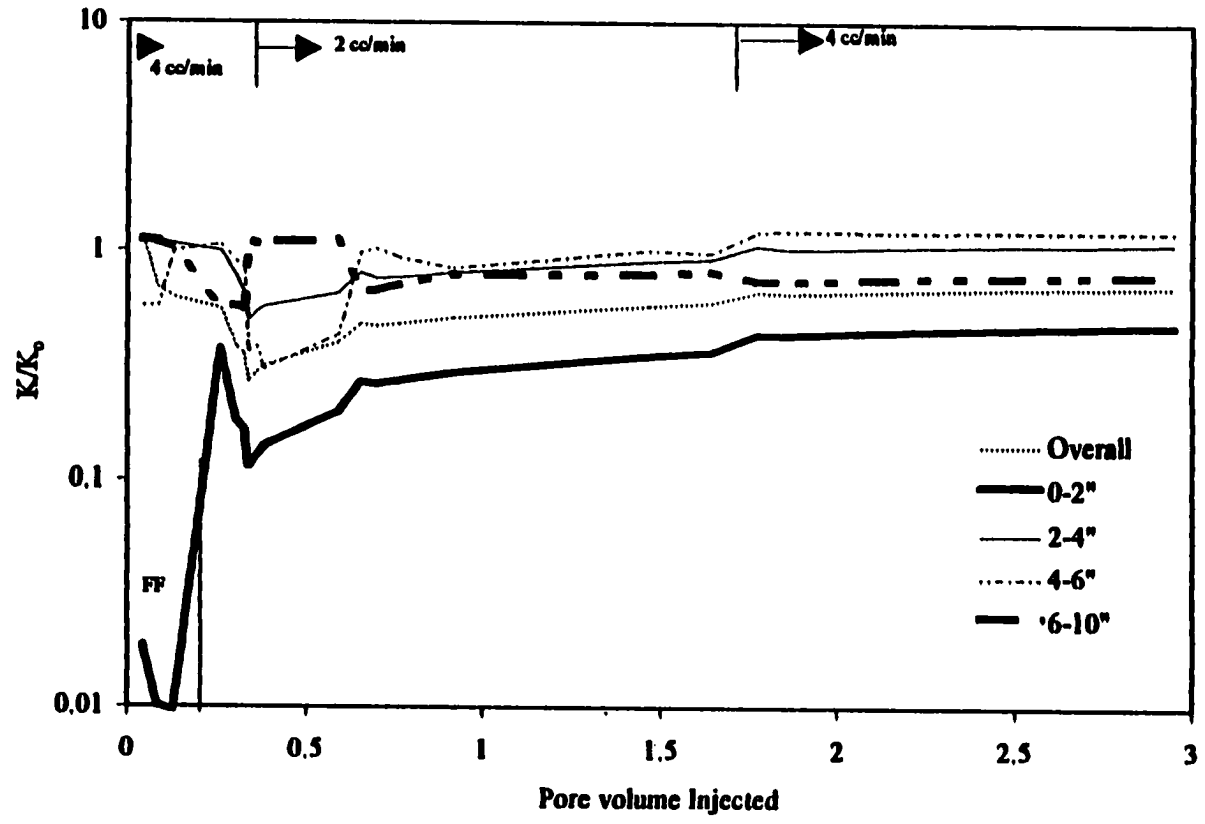


Fig. 6-3: Effect of 35 lb/Mgal Crosslinked Guar Leakoff on the Regain Permeability of Oil Core (Test 6-2)

with those reported by Lord *et al.*²⁰ and Navarrete *et al.*¹⁷ The regain permeability was also sensitive to flow rate. When the flow rate was increased, the return permeability of the first four inch of the core decreased and then gradually increased, indicating initial plugging and then clearing of the pore channels.

In the case of the oil core, it is evident from Fig. 6-3 (Test 6-2) that only the first two inch of the core experienced any significant permeability reduction during leak-off and it is not as severe as in the brine core. The cleanup was also better compared to brine core. Approximately 50% of the 0-2 inch original permeability and 80% of the deeper (6-10 inch) original permeability was recovered after injecting approximately three pore volumes of oil. This may be explained considering that the presence of oil may deny access to largest pore channel to the polymers, which in turn reduces the impact of pore plugging on the flow capacity. Further, the presence of oil on the pore-throat surface reduces the effectiveness of the polymer and its residue to adhere to the pore throats, thus decreasing the permeability reduction. In addition, a certain minimum invasion of polymer particles and its residue is required to effectively bridge the pore throats. Since the spurt loss was negligible in the case of oil core this minimum invasion was not achieved. Also, when the flow rate was doubled there was a slight increase in regain permeability. Two hypotheses are proposed to explain the phenomenon of increase in regain permeability with an increase in the flow rate. The first hypothesis is that better polymer gel removal is facilitated with an increase in the flow rate. The second hypothesis is that the polymer gel forms a thin film on the walls of pore channels and acts as a friction reducing agent. Therefore, when the flow rate is increased the drag exerted by the pore channels on the oil molecules is decreased. In

the past, Liang *et al.*³⁰ and Zaitoun *et al.*³¹ have also observed the above phenomenon in the case of other polymer gel systems. The results presented here suggests that the regain permeability may be sensitive to draw-down applied to a well, and a higher draw-down may allow a better clean-up of the fracture face.

6.3.2 Recovery of Return Permeability After Leak-off With Crosslinked HPG

The impact of 35 lb/Mgal crosslinked HPG leak-off on the regain permeability of brine and oil core is illustrated in Figs. 6-4 and 6-5 (Test 6-3 & 6-4), respectively. The permeability of the brine core was lower compared to that of the oil core (Table 6-1). The test conditions were identical.

Once again, the cumulative leak-off in the brine core was significantly higher compared to that in the oil core (Table 6-2). It is evident from Figs. 6-4 and 6-5 that the cleanup (overall and sectional) is significantly better in the case of oil core compared to that in the brine core. In the case of oil core, after injecting two pore volumes of oil, the sectional permeability for each section, and the overall permeability were restored to more than 100% of the original oil permeability. This phenomenon could be attributed to a possible change in wettability towards more water-wet behavior which increases the relative permeability of oil. The permeability loss caused after the leak-off of the crosslinked HPG in the oil core is significantly lower than that observed in the brine core. This provides additional evidence to the hypothesis that the presence of oil in the core prevents the polymer particles from effectively plugging the pore throats.

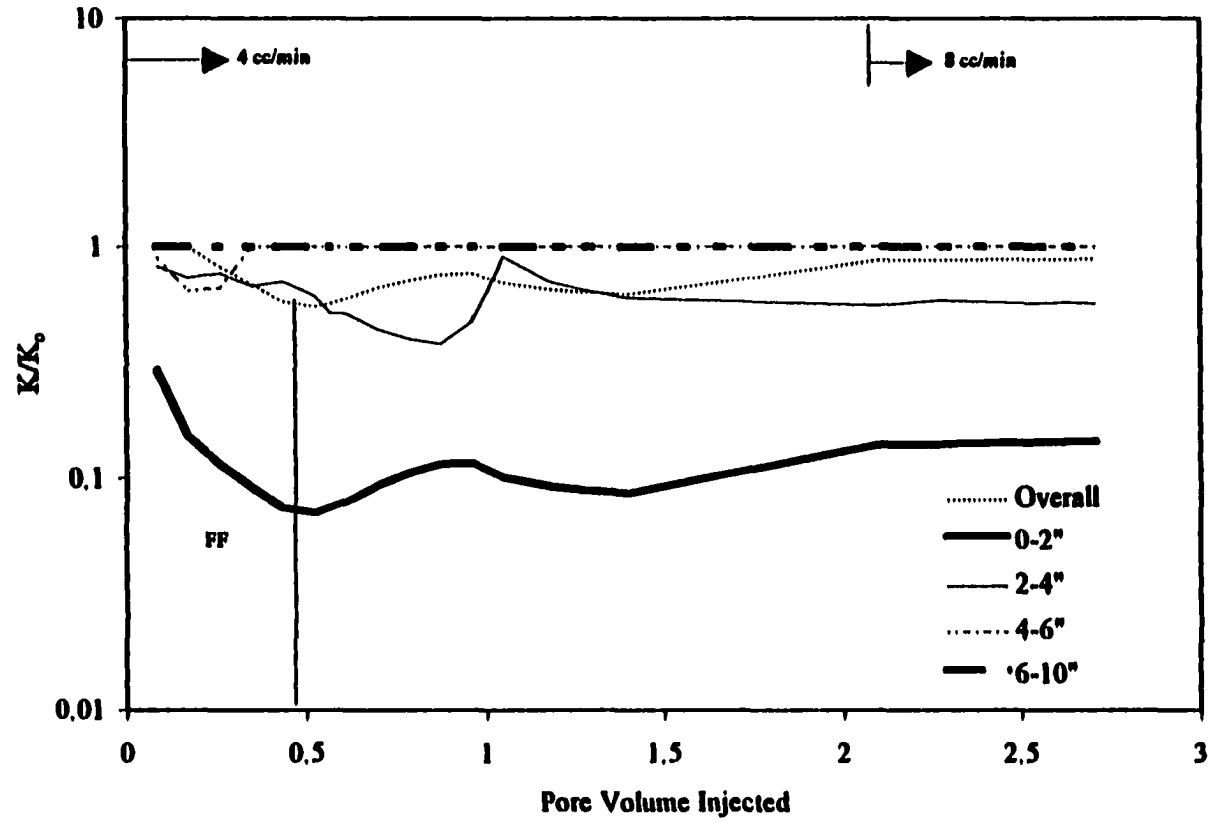


Fig. 6-4: Effect of 35 lb/Mgal Crosslinked HPG Leakoff on the Regain Permeability of Brine Core (Test 6-3)

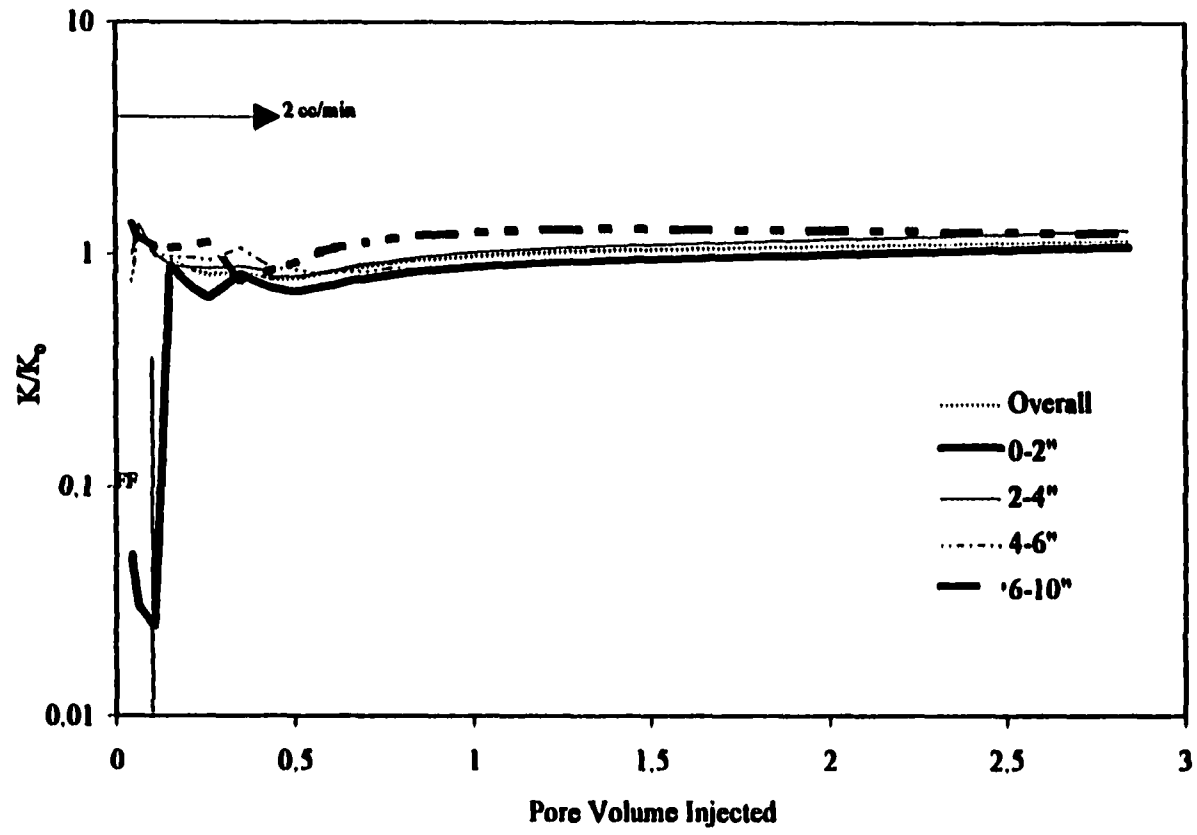


Fig. 6-5: Effect of 35lb/Mgal Crosslinked HPG Leak-off on Regain Permeability of Oil Core (Test 6-4)

HPG is a cleaner fluid (i.e. has practically no residue) compared to guar which explains the lower damage caused by crosslinked HPG as compared to crosslinked guar in both the brine and oil cores.

6.3.3 Return Permeability After Leak-off of Linear Gel in Oil Cores

In order to confirm the hypothesis that the polymer particles in the presence of oil do not effectively adhere to the pore throats, two leak-off tests were conducted with linear fluids (linear HPG and guar) in oil cores. Since the earlier tests have proved that the recovery of permeability in brine cores was less compared to that in the oil cores no further tests in brine cores were conducted. Both the tests were conducted without fluid loss additives, thus if there is any permeability reduction, it would be caused solely by the polymer particles. The polymer loading was 35 lb/Mgal for both linear HPG and guar. The leak-off and the shut-in times were 20 min. and three hours, respectively. In the case of HPG, the filtrate had penetrated approximately the first four inch (estimated based on the amount of leak-off), whereas for guar the filtrate had penetrated approximately the first five inch of the core. Based on the depth of penetration of the filtrate one would have expected the regain permeability to be low. However, that was not the case, especially for HPG.

Figure 6-6 (Test 6-5) shows the variation in sectional permeability caused due to the leak-off of linear HPG and its subsequent recovery during flowback with oil. It is evident from the figure that only 50% damage was caused to the first four inch of the core due to leak-off. Also, during the flowback, the sectional permeabilities were recovered more than 100% of the original permeabilities, similar to that observed in the case of crosslinked HPG. This provides additional strong evidence for the hypothesis

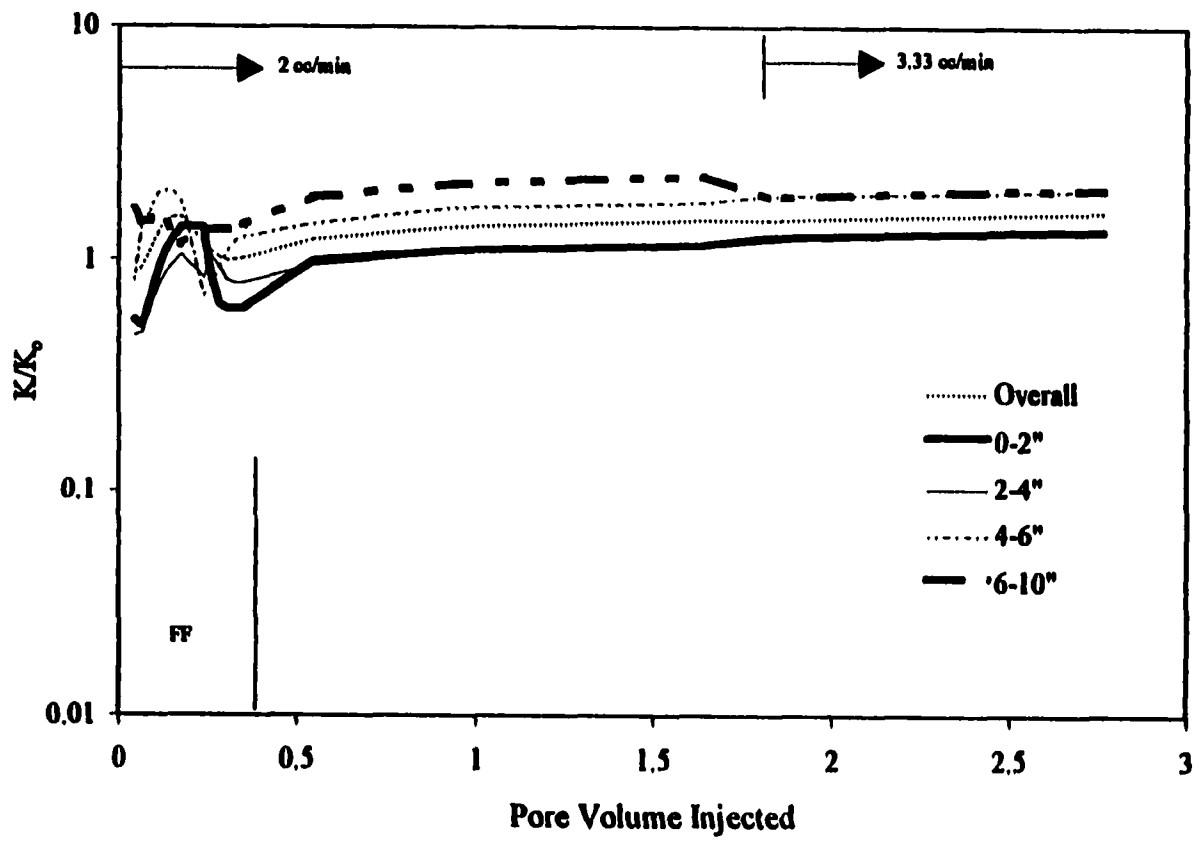


Fig. 6-6: Effect of 35 lb/Mgal Linear HPG Leakoff on the Regain Permeability of Oil Core (Test 6-5)

that the polymer particles do not effectively adhere to the pore throats in the presence of oil. Further, it appears that the HPG leak-off facilitated cleanup of damage that was caused by the initial injection of brine and a possible transition to strongly water-wet behavior.

Figure 6-7 (Test 6-6) illustrates the variation in sectional and overall permeability caused due to the leak-off of linear guar and its subsequent recovery during flowback with oil. In this case, the sectional damage caused to the first two inch of the core due to leak-off was severe compared to that caused by HPG leak-off. The presence of residue in guar attributes to the additional damage. However, during flowback the sectional permeability was gradually recovered. After injecting 2.5 pore volumes of oil, approximately 50%, 62%, 72%, and 100% for the 0-2 inch, 2-4 inch, 4-6 inch, and 6-10 inch sections of the original permeabilities were recovered, respectively.

6.3.4 Effect of Fluid Loss Additives and Shut-in Time

Two leak-off tests were conducted to investigate the effect of fluid loss additives and shut-in time on the regained permeabilities of oil cores. The fracturing fluid used was 35 lb/Mgal crosslinked HPG and the fluid loss additive used was 25 lb/Mgal silica flour. The shut-in time in the case of Test 6-7 (Fig. 6-8) was 12 hours, whereas in the case of Test 6-8 (Fig. 6-9) was 3 hours.

Figures 6-8 and 6-9 clearly demonstrate that the fluid loss additives do not cause additional permeability impairment compared to clean crosslinked fluids. Therefore, they have no effect on the regain permeability. In both tests, all the sectional permeabilities were recovered to more than 100% of their original values. In

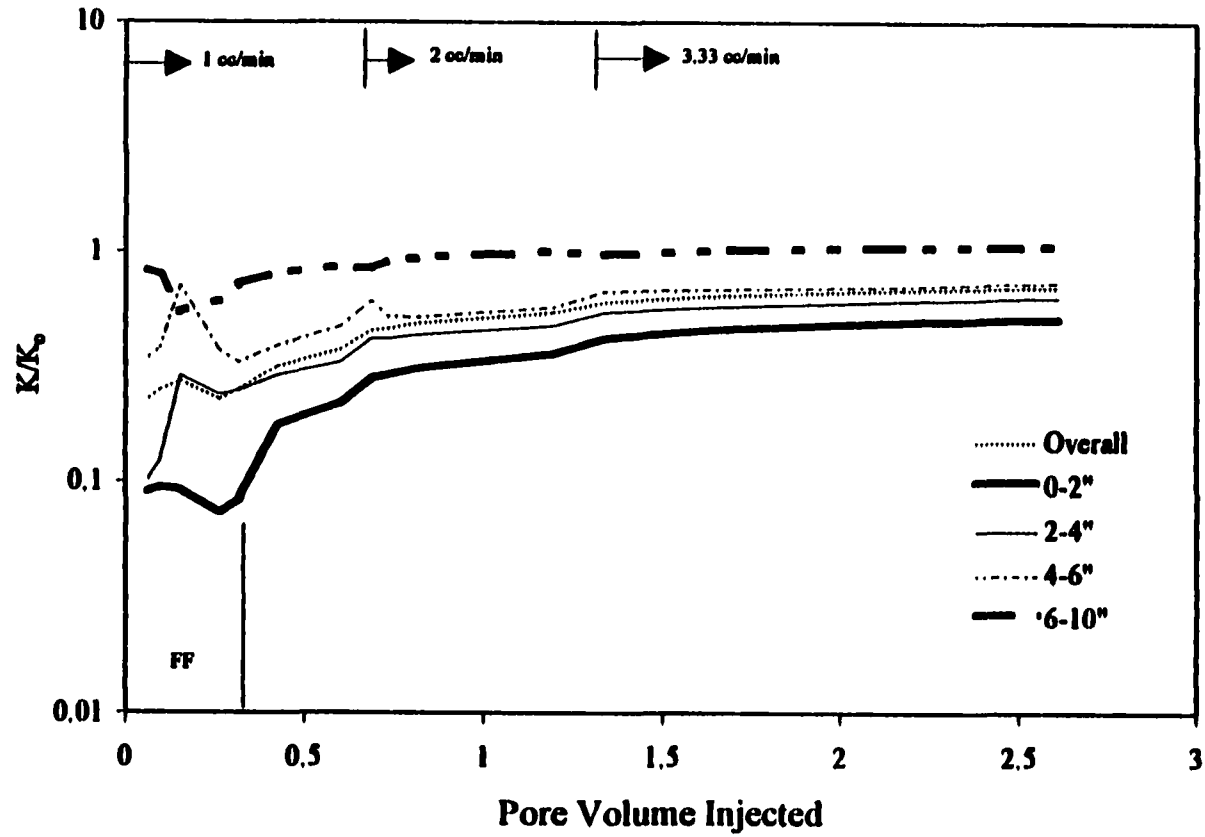


Fig. 6-7: Effect of 35 lb/Mgal Linear Guar Leakoff on the Regain Permeability of Oil Core (Test 6-6)

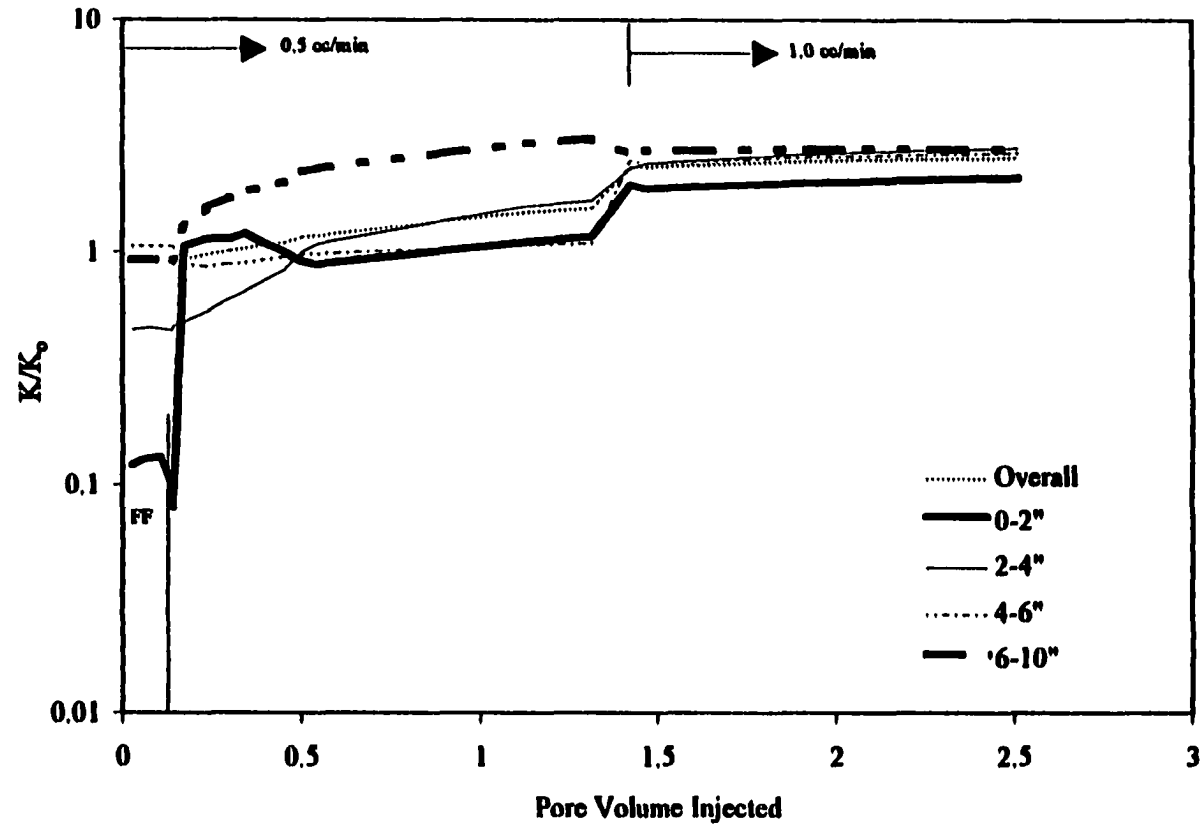


Fig. 6-8: Effect of 35 lb/Mgal Crosslinked HPG + 25 lb/Mgal FLA Leakoff on the Regain Permeability of 12 mD Oil Core (Test 6-7) Shut-in Time 12 hrs

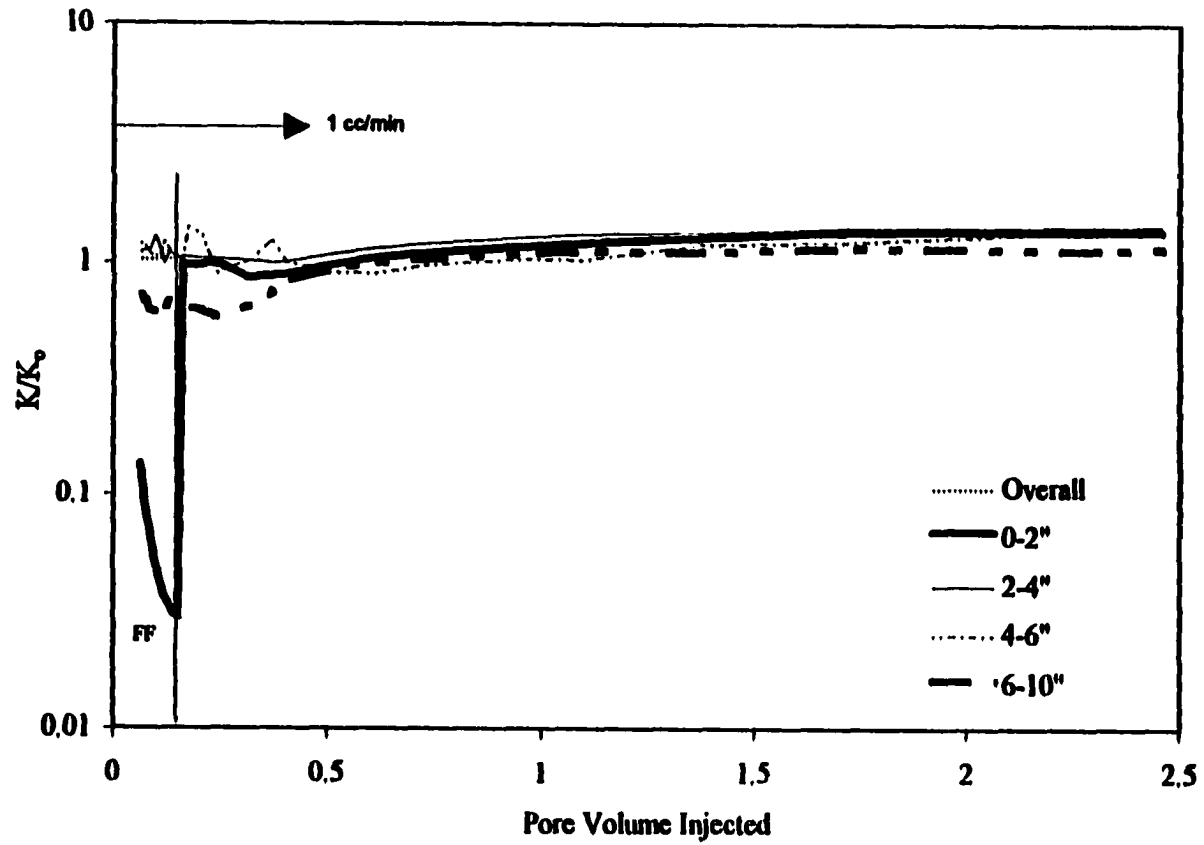


Fig. 6-9: Effect of 35 lb/Mgal Crosslinked HPG + 25 lb/Mgal FLA Leakoff on the Regain Permeability of 35 mD Oil Core (Test 6-8) Shut-in Time 3 hrs

the test with 12 hour shut-in, the regain permeability was 175-275% of the pre-leakoff permeability. The increase in flow rate also contributed to the increase in regain permeabilities. On the other hand, with identical fluid system and 3 hour shut-in, the regain permeability was nearly 100% of original permeability. The permeability recovery could be either due to removal of initial damage or it could be a result of alteration in wettability such that the relative permeability to oil is significantly increased. Comparison of tests with two different shut-in times suggests that 'removal of formation damage' effect cannot by itself completely explain the results for test with 12 hour shut-in.

A plausible explanation is that increased contact time with HPG filtrate might have allowed an opportunity for significant wettability alteration towards water-wet conditions. This could explain the significant increase in regain permeability (greater than 100%) in earlier tests. Similar behavior was observed for linear HPG as shown in Fig. 6-6. Permeability regain was lower for linear and crosslinked guar (approximately 100%). This suggests that it is the difference in the chemistry of guar and HPG which causes different behavior, leading further credence to the hypothesis that the interaction of HPG with the rock matrix causes the observed shift towards water-wet behavior.

6.3.5 Effect of Crude Oil on Regain Permeability

Figure 6-10 illustrates the variation of return permeability after the leak-off of 35 lb/Mgal crosslinked HPG in a core sample containing crude oil as the oil phase. The leak-off and shut-in time were 20 minutes and 3 hours, respectively. The pressure drop during the leak-off was maintained at 500 psi. The crude oil used in this experiment had some particulate components and it was not filtered prior to the test. The results

indicate that there was no damage caused to any part of the core due to the leak-off. This shows that under the given conditions crude oil does not allow any polymer particles to adhere to the pore throats. However, during the flowback (simulated oil production) there was a reduction in permeabilities for all sections. The reduction in permeability can be attributed to the deposition of the particulate components in the crude oil or to adverse interaction between crude oil and polymers. The last four inch section (6-10 inch), which was never contacted by the filtrate, was the most affected section which suggests that longer duration of exposure to crude oil causes greater damage. In fact, interaction with the filtrate appears to have inhibited the permeability reduction due to oil components.

In order to verify the hypothesis that the decrease in regain permeabilities was mainly caused due to the deposition of particulate components in oil, the crude oil was filtered using a 0.5 μm filter paper. The impact of filtered and non-filtered crude oil on the initial crude oil permeability is shown in Fig. 6-11. The figure clearly indicates that in the case of non-filtered crude oil (Test 6-9), the initial permeability to crude oil decreases dramatically with time whereas in the case of filtered crude oil (Test 6-11), there is not much variation in initial permeability to crude oil. This demonstrates that indeed the particulate components in the crude oil are the cause of permeability decline.

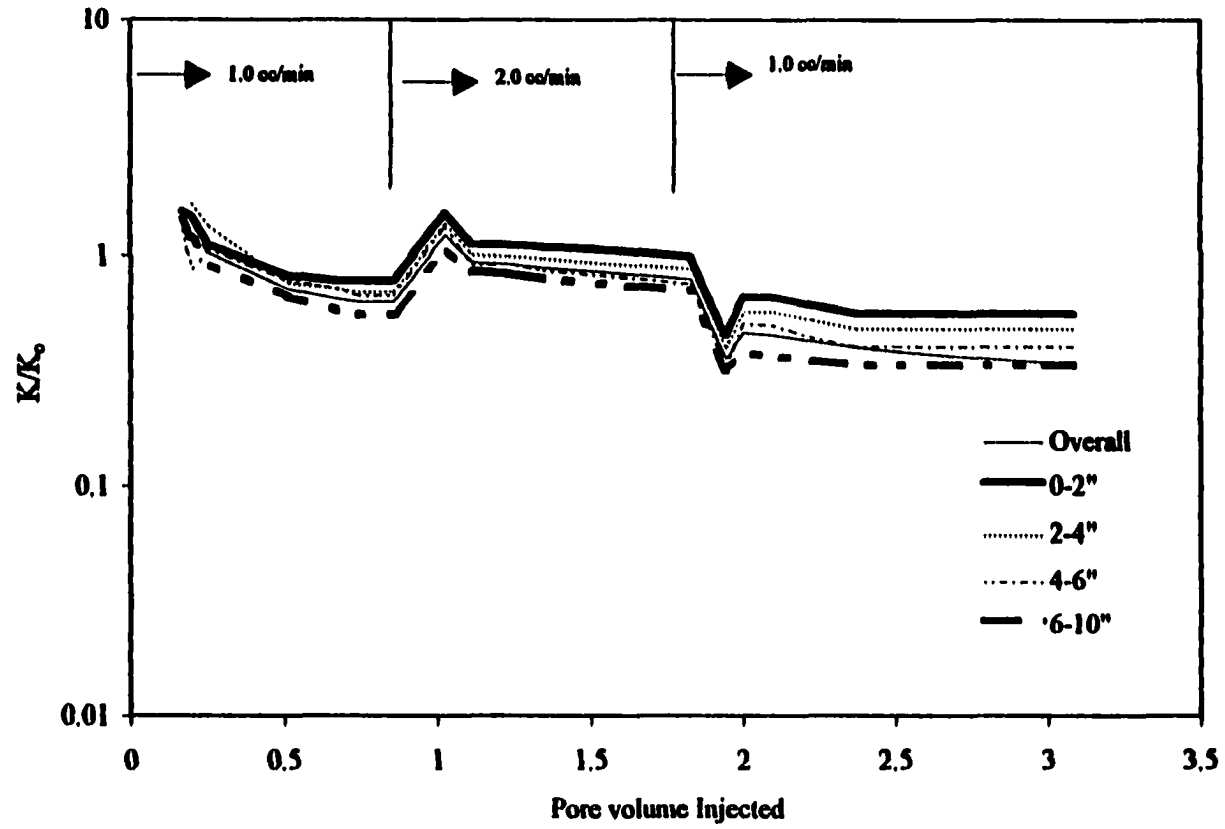


Fig. 6-10: Effect of crosslinked HPG Leakoff on the Regain Permeability of a Crude Oil Saturated Core (Test 6-9)

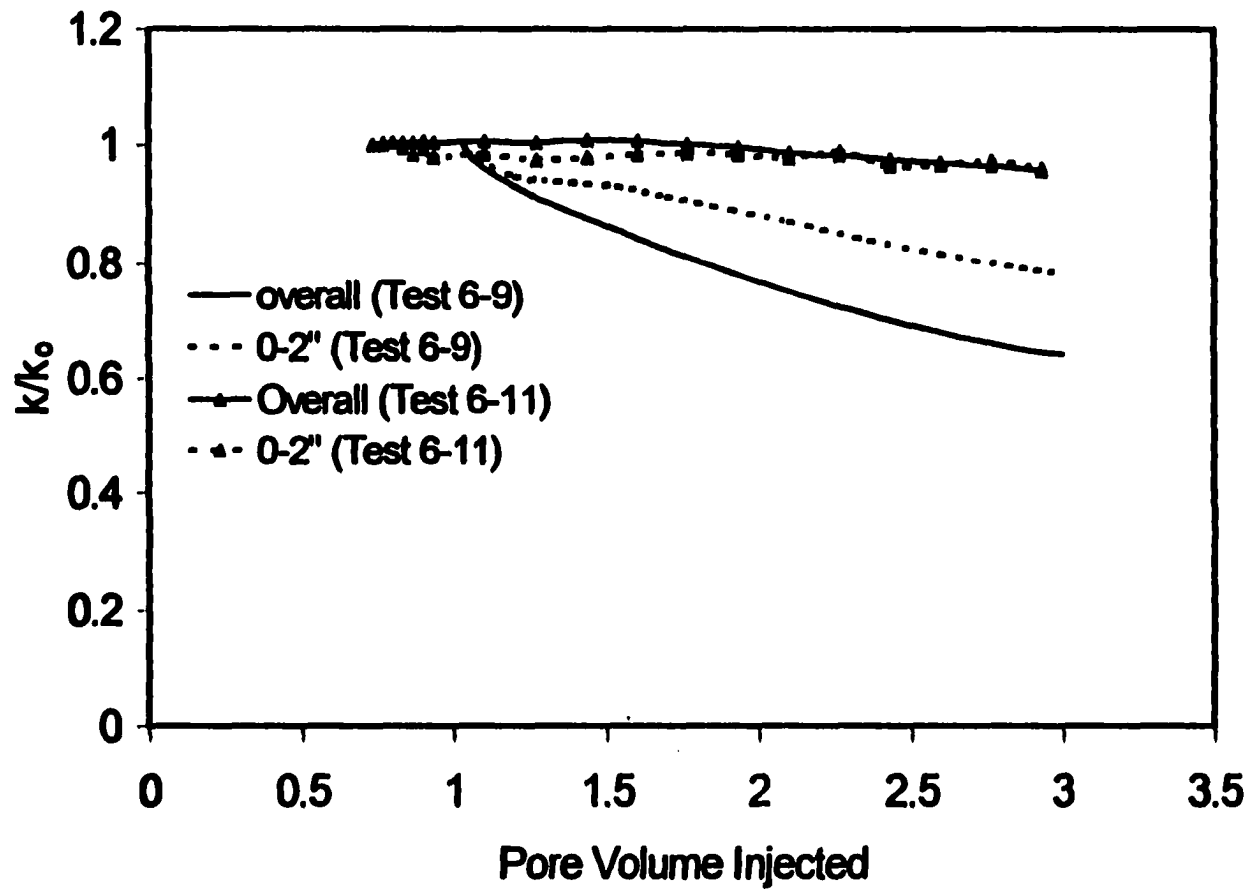


Fig. 6-11: Effect of Filtered and Non-filtered Crude Oil on Initial Crude Oil Permeability

Chapter 7

Development of a Dimensionless Correlation

7-1 Introduction

A thorough understanding of the filtration characteristics of fluids used for hydraulic fracturing is essential for realistic design and successful execution of hydraulic fracturing treatment. Therefore, an accurate prediction of leak-off plays an important role during the design of fracturing treatments. The most common technique of determining the leak-off rate of a given fracturing fluid is to conduct static or dynamic filtration experiments on core samples in the laboratory and plot the cumulative leak-off volume, V , as a function of time, t , or \sqrt{t} .

Several researchers have proposed analytical equations to predict leak-off volume based on dynamic and static leak-off data. Howard and Fast³² proposed a two-parameter static fluid loss equation that relates the cumulative leak-off volume, V , to \sqrt{t} as:

$$V = V_{sp} + 2C_w \sqrt{t} \quad (7-1)$$

where spurt loss, V_{sp} , is the amount of fluid lost prior to filter cake formation and wall building coefficient, C_w , is due to the resistance offered during the deposition of a filter

cake on the formation face. The V_{sp} and C_w are determined from the intercept and slope of the leak-off volume vs. \sqrt{t} plot, respectively, as shown in Fig. 1-1.

Roodhart⁴ proposed a three-parameter dynamic fluid loss equation that accounts for cake shearing effects in addition to spurt loss and cake deposition effects. The model is similar to Eq. 7-1 except that it consists of an additional term to represent a dynamic equilibrium region during which cake erosion is dynamically balanced by cake deposition.

Clark and Barkat³³ also proposed a three-parameter dynamic fluid loss equation which is given by:

$$V = V_{sp} (1 - e^{-c_b t}) + C_d t \quad (7-2)$$

where c_b indicates the rate of cake buildup and C_d is dynamic leak-off coefficient.

The major drawback of such models is that they do not represent the effect of shear rate on leak-off accurately. These models assume that the viscosity of the filtrate inside the porous media remains constant, whereas in reality the filtrate in the porous media behaves as a non-Newtonian pseudoplastic fluid, during the invasion process. As a result, initially, the apparent viscosity of the filtrate is low due to high shear rate and then increases as the shear rate decreases with time. The variation in apparent viscosity of the filtrate can have a significant impact on the leak-off rate.

The objective of this study is to develop a model based on dimensional analysis to predict dynamic leak-off of fracturing fluids. Charles and Xie³⁴ had developed a dimensionless model, however, the model does not take into account the variation of filtrate viscosity. The model developed in this study takes into account the variation of

filtrate viscosity with shear rate in the porous media. The major advantage of dimensional analysis over empirically derived equations is that considerably less experimentation is required to establish a relationship between the variables over a given range. The model developed in this study is validated with experimental data for leak-off in samples of varying size and a variety of fluids. The results predicted by the model are also compared with the traditional V vs. \sqrt{t} relationship.

7-2 Model Formulation

The instantaneous rate of dynamic leak-off is expected to depend on the fluid and rock properties as well as the flow parameters. Important fluid and rock properties are fluid viscosity, concentration of fluid loss additive, permeability, and porosity. The important flow parameters include the local pressure gradient and the shear rates in the core sample. Functionally, the leak-off volume may be expressed as:

$$V = f(\Delta P, \mu_a, \dot{\gamma}, k, L, A, t) \quad (7-3)$$

where V is the cumulative leak-off volume, ΔP is the pressure drop, μ_a is the apparent viscosity of the fluid, $\dot{\gamma}$ is the shear rate, k is the formation permeability, L is the length of the core sample, A is the cross-sectional area to leak-off, and t is the leak-off time.

Based on the method of dimensional analysis³⁵ the following relationship was obtained:

$$\left(\frac{V}{AL}\right) = \left(\frac{\Delta P t}{\mu_a}\right)^a \left(\frac{k}{L^2}\right)^b \left(\dot{\gamma} t\right)^c \quad (7-4)$$

where a, b, and c are parameters which must be determined from the experimental data.

The viscosity behavior of the filtrate in the porous media can be characterized by a power law model and the porous media shear rate can be determined from the following expression¹⁸:

$$\dot{\gamma} = \left(\frac{3n+1}{n} \right) \left(\frac{dv/dt}{\sqrt{8k\phi\lambda}} \right) \quad (7-5)$$

where $v = V/A$, n is the flow behavior index, ϕ is porosity, and λ is the rock characteristic factor.

The apparent viscosity of the filtrate is given by:

$$\mu_a = K \dot{\gamma}^{n-1} \quad (7-6)$$

where K is the fluid consistency index.

Substituting Eqs. (7-5) and (7-6) into Eq. (7-4) and rearranging, the following relationship is obtained:

$$\frac{dv}{dt} = \left[\frac{v}{c_1 t^{(s+c)}} \right]^{\frac{1}{(c-an+a)}} \quad (7-7)$$

where:

$$c_1 = L \left(\frac{\Delta P}{c_2} \right)^a \left(\frac{k}{L^2} \right)^b c_3^c \quad (7-8)$$

$$c_2 = K \left(\frac{3n+1}{n\sqrt{8k\phi\lambda}} \right)^{n-1} \quad (7-9)$$

$$c_3 = \left(\frac{3n+1}{n\sqrt{8k\phi\lambda}} \right) \quad (7-10)$$

Equation (7-7) is solved numerically using modified Euler's method. The parameters a, b, and c are refined using the built-in utility "SOLVER" in MS-EXCEL by seeking to minimize an objective function which is the sum-of-squared residuals defined as:

$$\text{obj} = \sum_{i=0}^1 (v_{\text{exp}_i} - v_{\text{cal}})^2 \quad (7-11)$$

where the subscripts "exp_i" and "cal_i" denote observed and calculated v at ith time, respectively.

It is advantageous to solve Eq. (7-7) numerically if the parameters in the model vary with time. However, for a case where the parameters do not vary with time, Eq. (7-7) can be integrated to obtain an analytical solution. The final form of the analytical solution is:

$$v = \left(\frac{1}{c_1} \right)^{\left(\frac{1}{c - an + a - 1} \right)} \left(\frac{c - an + a - 1}{-an} \right)^{\left(\frac{c - an + a}{c - an + a - 1} \right)} t^{\left(\frac{-an}{c - an + a - 1} \right)} \quad (7-12)$$

7.3 Results and Discussion

The model was validated using the data presented in Chapter 5 and by Lord *et al.*²⁰, based on leak-off studies in a large-scale, high-temperature, and high-pressure simulator (HPS). The experimental data reported in Chapter 5 and by Lord *et al.*²⁰ was obtained at ambient temperature.

Figures 7-1 through 7-4 compare the model predictions with the experimental data presented in chapter 5 and Figs. 7-5 and 7-6 compare the model predictions with the experimental data presented by Lord *et al.*²⁰

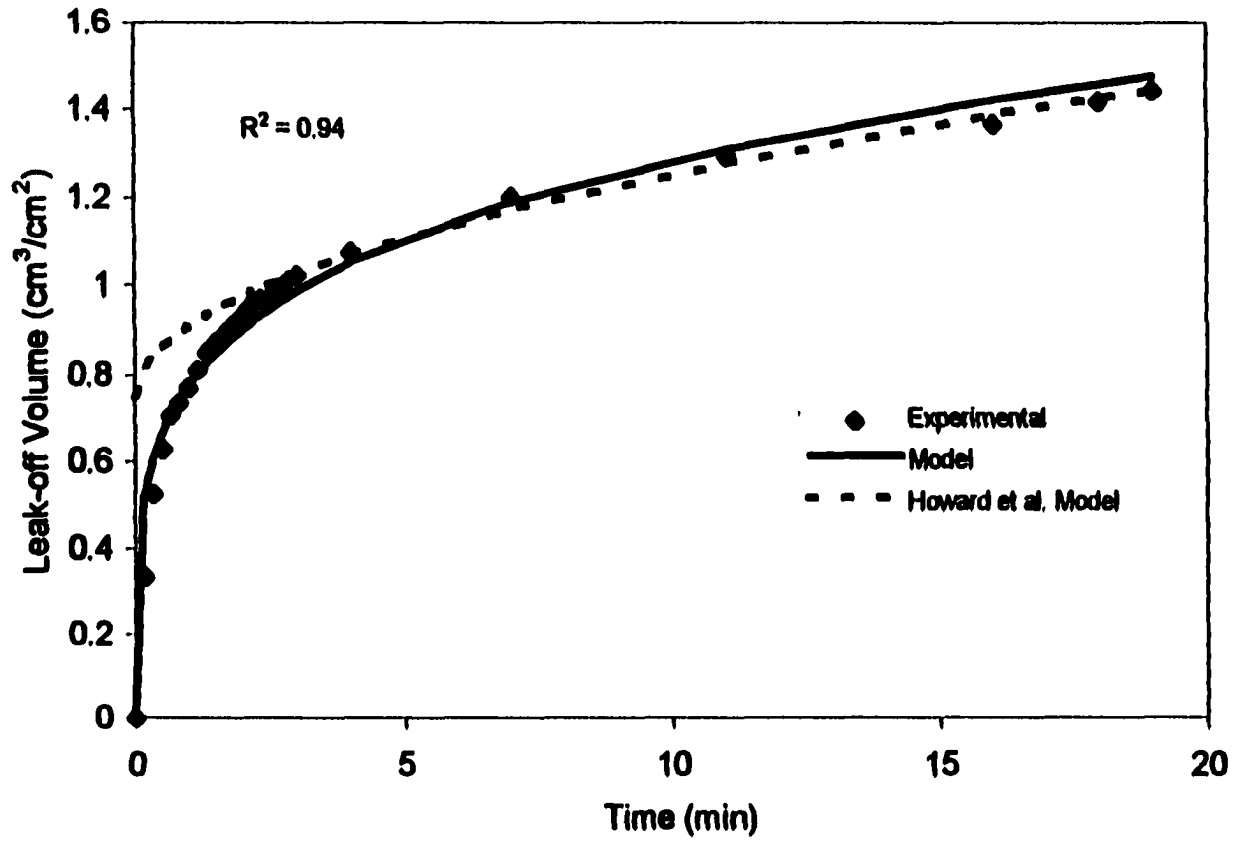


Fig. 7-1: Comparison of Model and Experimental Leakoff Results of Borate Crosslinked 35 lb/Mgal HPG (Test 6-3)

Figure 7-1 illustrates the comparison between the model prediction and experimental leak-off data of borate crosslinked 35 lb/Mgal HPG in 25 mD Berea sandstone core sample. The leak-off pressure drop and time were 500 psi and 20 minutes, respectively. As seen in this figure, a good match is obtained between the predictions and the experimental data. A correlation coefficient, R^2 , of 0.94 was obtained. The resulting optimized parameters for the experiments considered in this paper are listed in Table 7-1. In addition, based on the C_w and V_p data obtained from the experiment, a \sqrt{t} relationship is fitted through the experimental data. As seen from the figure, during initial time the \sqrt{t} fit over-predicts leak-off but at later times a good match with the experimental data is observed.

Table 7.1: Summary of optimized parameters

Figure	a	b	c
7-1	-0.0164	0.9463	1.1104
7-2	-0.1324	0.9107	0.9856
7-3, 7-4	-0.3111	1.0775	1.6329
7-5, 7-6	-0.2293	0.8233	1.0673

Figure 7-2 compares the model prediction and experimental leak-off data of borate crosslinked 35 lb/Mgal guar in 44 md Berea sandstone core sample. The test conditions are identical to those maintained for the crosslinked HPG leak-off test. For this case also, the quality of match obtained is excellent ($R^2 = 1$). However, the parameters obtained are different than those obtained for crosslinked HPG test (Table 7-1). This could be attributed to the difference in chemistry and rheology of the fluids which can lead to different interaction of the fluids with the core sample. In this case also, the \sqrt{t} fit over-predicts initial leak-off.

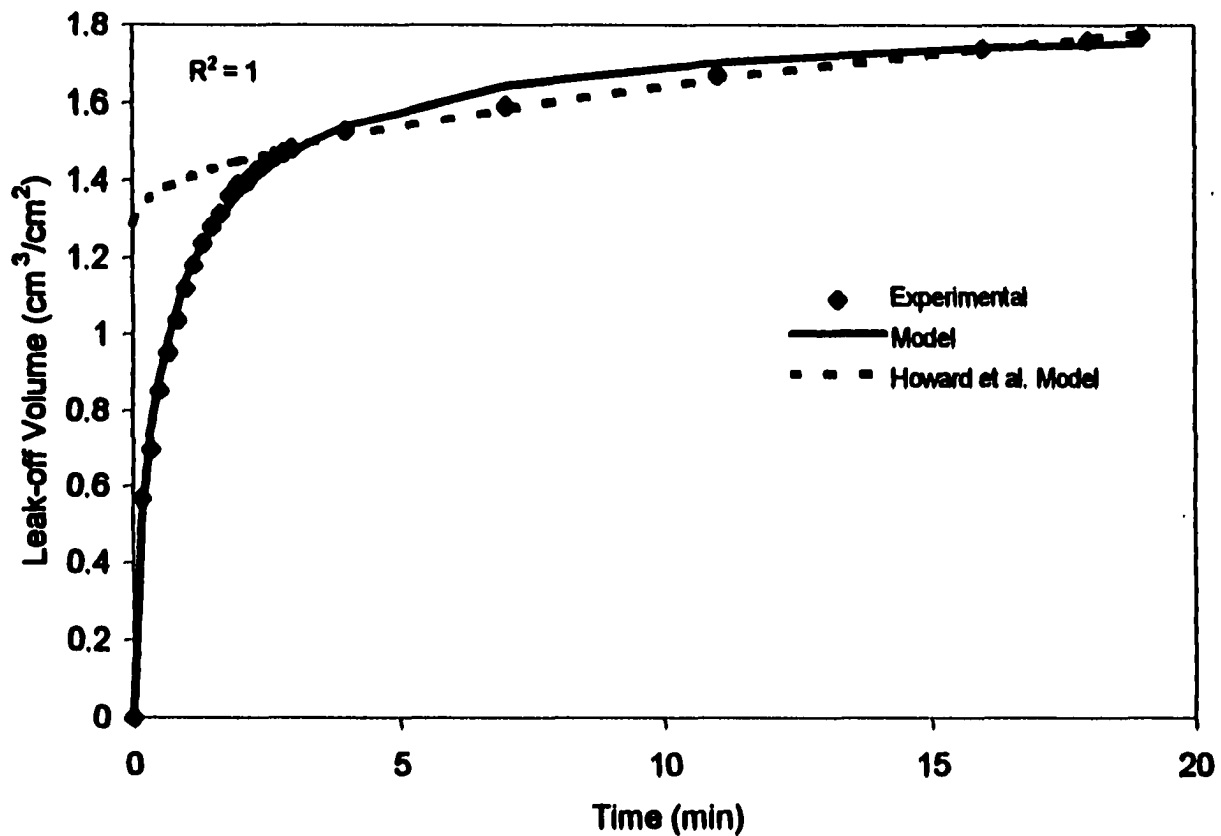


Fig. 7-2: Comparison of Model and Experimental Leak-off Results of Borate Crosslinked 35 lb/Mgal Guar (Test 6-1)

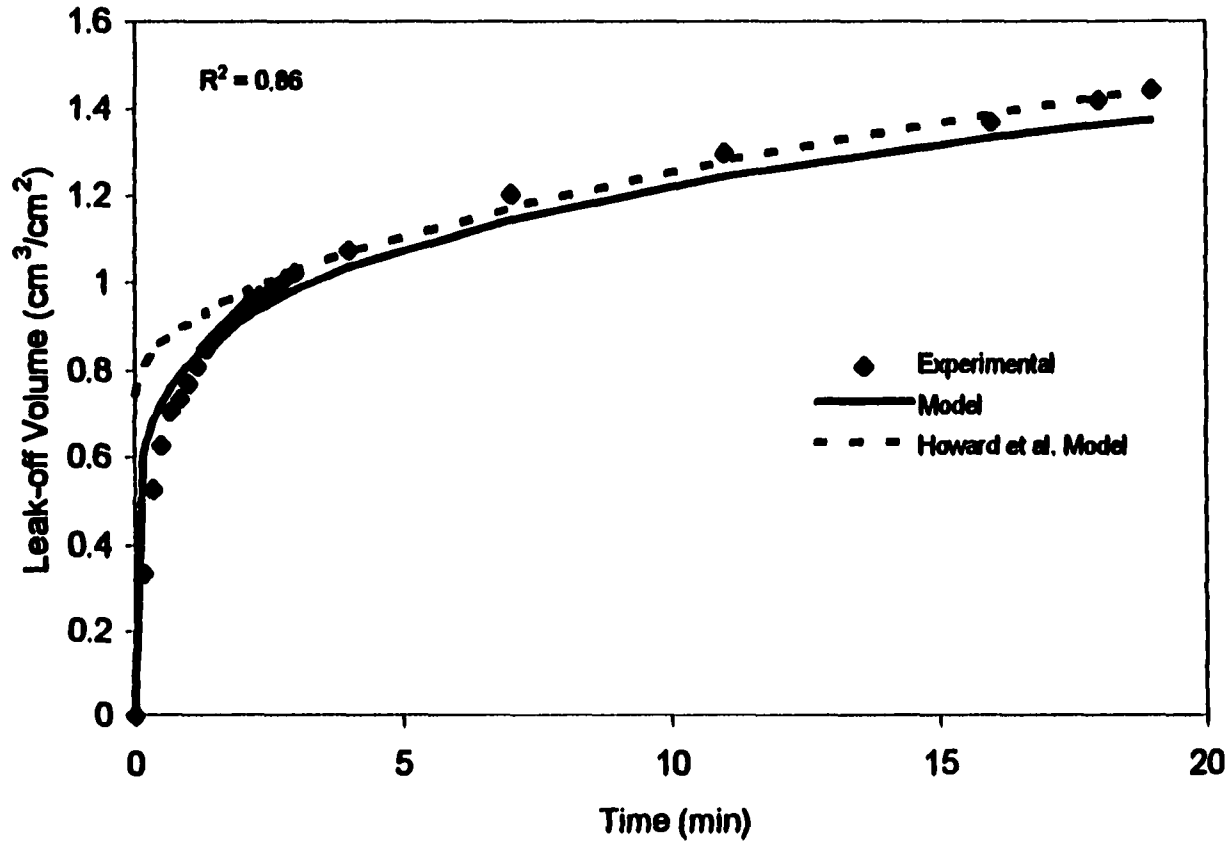


Fig. 7-3: Effect of Globalized Parameters on Model Predictions (Test 6-3)

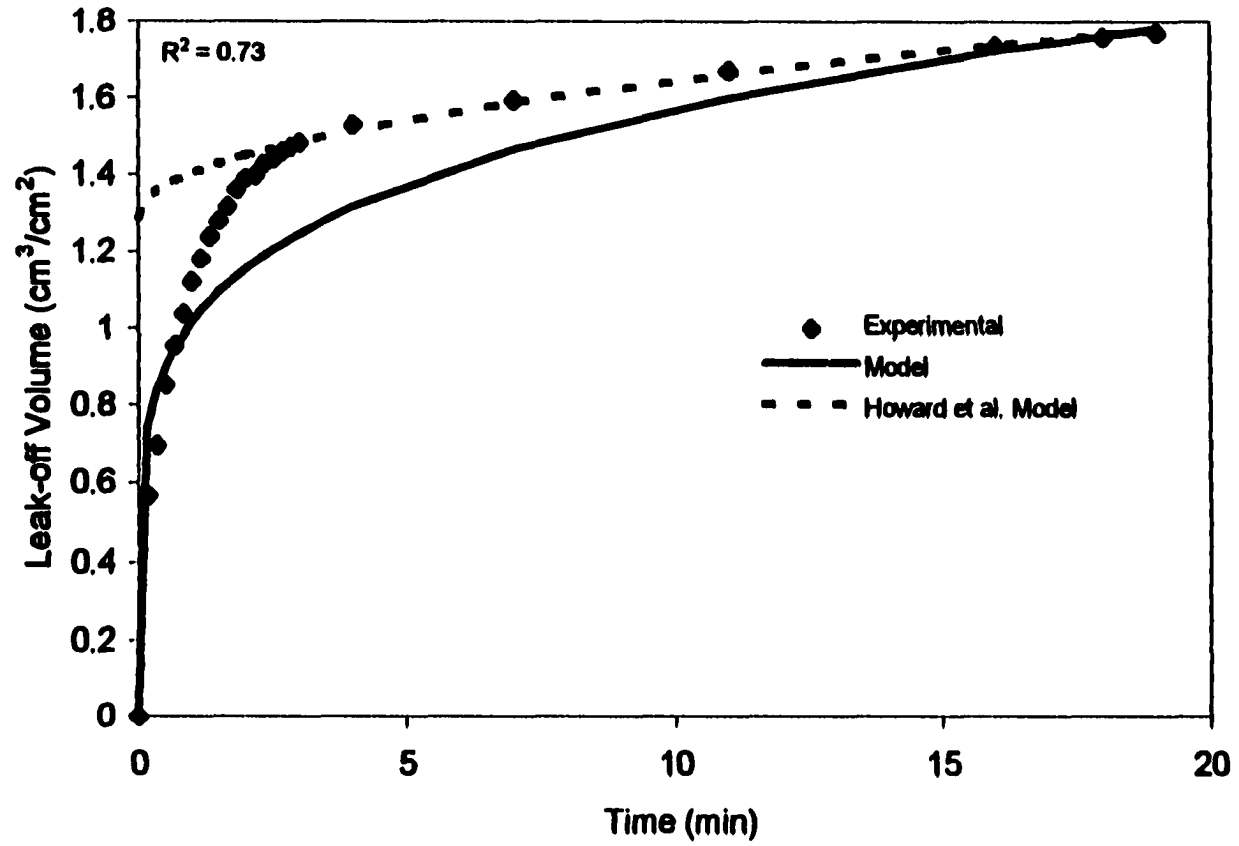


Fig. 7-4: Effect of Globalized Parameters on Model Predictions (Test 6-1)

The parameters in Figs. 7-1 and 7-2 were globalized by defining a new global objective function which was the summation of the objective function of individual experiments. Figures 7-3 and 7-4 show the impact of globalized parameters on the model prediction. For crosslinked HPG the model prediction is fairly good with a coefficient correlation of 0.86. However, for crosslinked guar the model underestimates leak-off during the time period from approximately 1 to 16 minutes ($R^2 = 0.73$). This indicates that the parameters are a function of the type of fluids used.

A comparison between the model prediction and experimental leak-off data of borate crosslinked 35 lb/Mgal HPG and 35 lb/Mgal crosslinked HPG + 25 lb/Mgal silica flour in the HPS is shown in Figs. 7-5 and 7-6, respectively. Synthetic core samples were used in both the experiments. The cross-sectional area to leak-off was 3873 cm². The pressure drop during leak-off was maintained at approximately 700 psi and the leak-off time was over 70 minutes. The permeability of the core samples in Figs. 7-5 and 7-6 are 6.9 and 7.7 md, respectively. Identical optimized parameters are obtained for both the cases (Table 7-1). In both the cases, the model prediction is very good with coefficient of correlation nearly equal to 1. In both the cases, Howard *et al.*³² model highly underestimates the leak-off at later times.

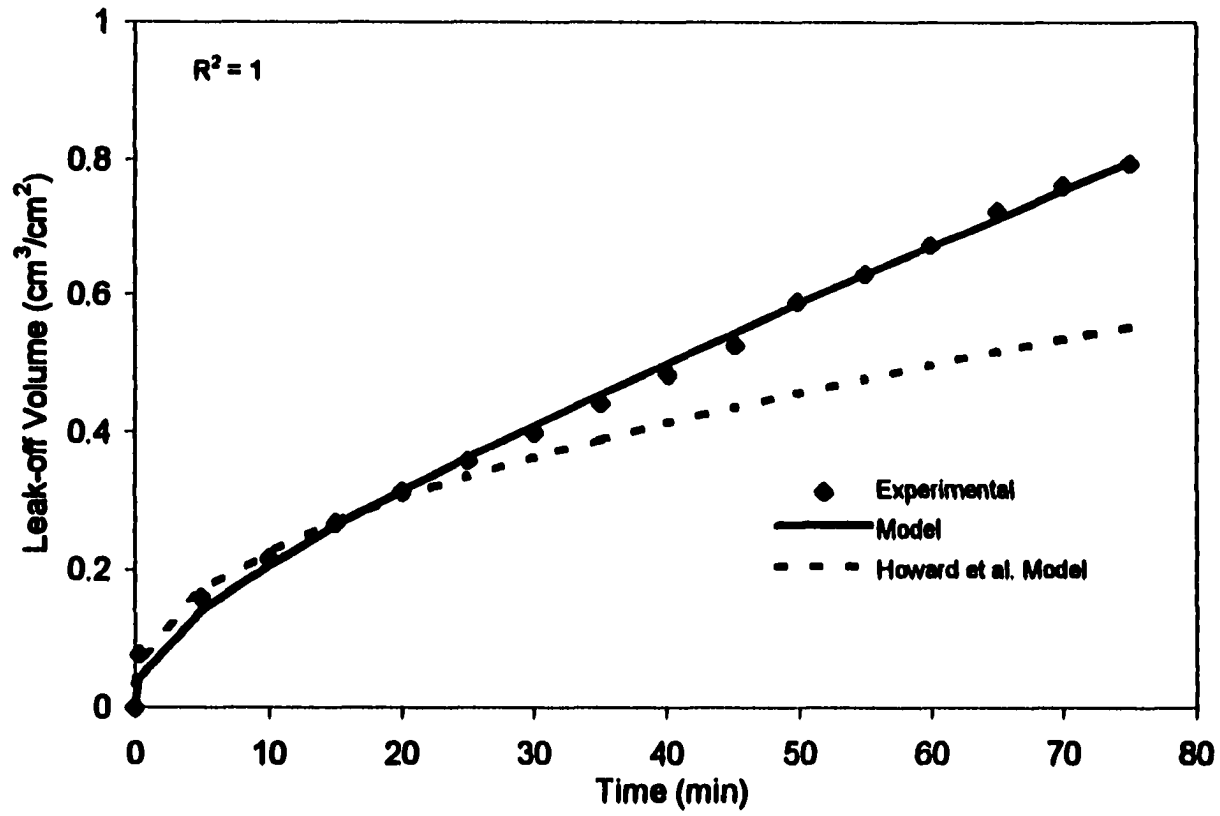


Fig. 7-5: Comparison of Model and Experimental Leakoff Results of Borate Crosslinked 35 lb/Mgal HPG in the HPS²⁰

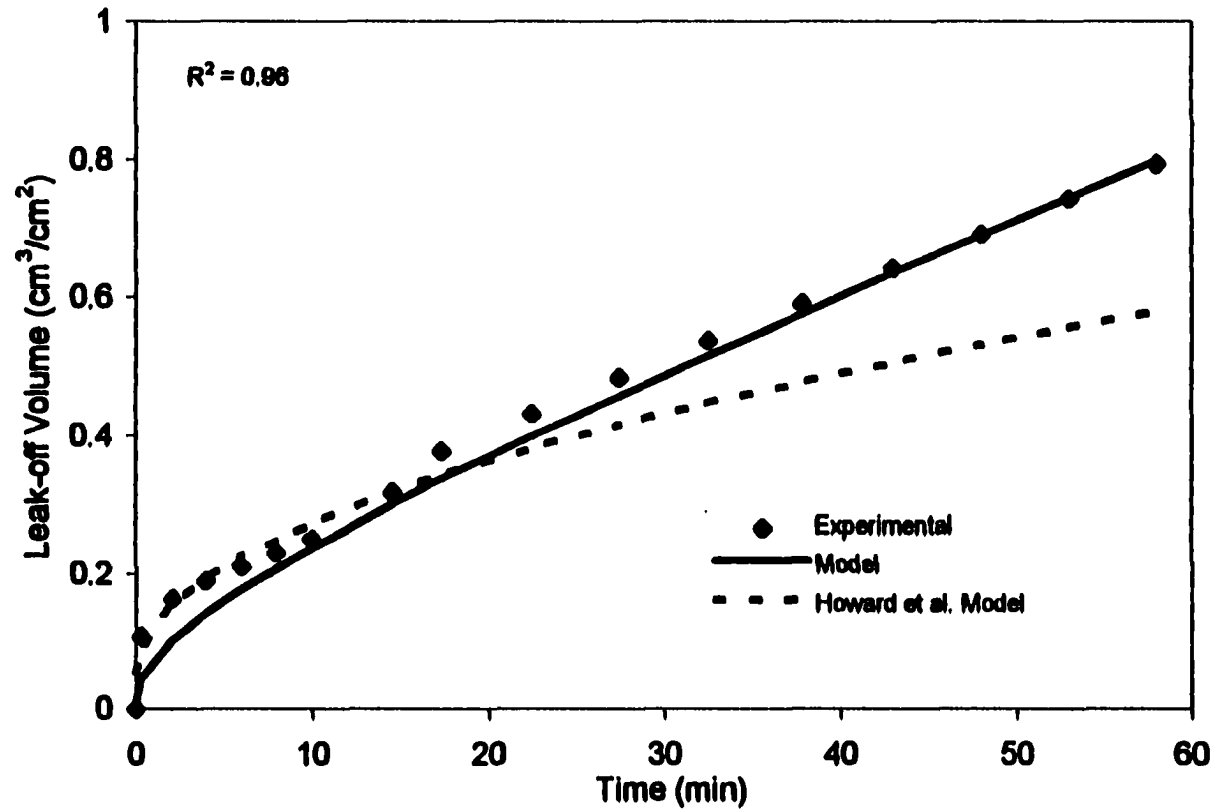


Fig. 7-6: Comparison of Model and Experimental Leakoff Results of Borate Crosslinked 35 lb/Mgal HPG + 25 lb/Mgal Silica Flour in the HPS²⁰

Chapter 8

Conclusions and Recommendations

8.1 Conclusions Drawn from Leak-off Studies

Based on modeling and experimental studies presented, the following conclusions are reached:

1. In the presence of mobile oil saturation, spurt loss of both linear and crosslinked fracturing fluids is significantly reduced compared to that obtained during single-phase leak-off.
2. In the presence of mobile gas saturation, spurt leak-off is driven by spontaneous imbibition followed by the relative permeability effects.
3. Reservoir properties govern spurt loss and time required for achieving a stable filter cake in the presence of mobile oil saturation.
4. The fluid leak-off in the presence of 100% brine saturation in tight reservoirs (permeability less than 0.1 mD) is significantly affected by reservoir properties.
5. The effectiveness of water-based fluid loss additives is significantly reduced in the presence of oil saturation. Fracturing fluids without FLAs' can be effectively used for fracturing reservoirs having a permeability less than 0.4 mD.

6. In the presence of mobile oil saturation, the wall building coefficient of a crosslinked fluid is a linear function of the fracture face permeability.
7. In the presence of mobile oil saturation, increase in leak-off pressure drop only has an effect on spurt loss.
8. Crosslinked fluids perform better compared to linear fluids in the presence of mobile oil saturation.
9. The model developed in this study can be used as an effective tool in predicting leak-off in the presence of two-phase flow.

8.2 Conclusions Drawn from Return Permeability Study

The following conclusions are drawn from this study:

1. The regain permeabilities in the case of oil saturated cores are significantly higher compared to that determined for 100% brine saturated cores for linear and crosslinked guar and HPG, respectively.
2. The cleanup of HPG (crosslinked and linear) is better compared to that of guar (crosslinked and linear) in oil saturated cores.
3. The fluid loss additive has no adverse effect on regain permeability.
4. In the case of HPG, the shut-in time has a positive impact on regain permeability.
5. HPG may have a tendency to alter the wettability of the formation towards more water-wet.

8.3 Conclusions Drawn from Dimensionless Model Study

The following conclusions are drawn from this study:

1. The proposed model is able to represent the experimental leak-off data more accurately than the conventional cumulative leak-off volume vs. \sqrt{t} plots.

2. **The model parameters exhibit sensitivity to rock and fluid properties.**
3. **A general set of model parameters achieves qualitative match with experimental data for a variety of systems.**
4. **The general parameters, when refined for the specific system achieve excellent match.**

8.4 Future Work

Following are the recommendations suggested for future work:

1. **Experiments should be conducted with core and fluid samples obtained from field locations.**
2. **Effect of fracture face area on leak-off in the presence of mobile hydrocarbon saturation needs to be investigated.**
3. **Further investigation needs to be carried out to determine the positive impact of production rate on regain permeability.**

NOMENCLATURE

A	cross-sectional area to leak-off, (L^2)
a, b	parameters defined by Eq. (7-4)
C_d	dynamic leak-off coefficient, (L^3/T)
C_{pf}	mass concentration of polymer in the filtrate, (M/L^3)
$C_{pf(out)}$	concentration of polymer in the filtrate penetrating inside the reservoir rock, (M/L^3)
$C_{pf(in)}$	concentration of polymer in the filtrate on the cake surface, (M/L^3)
C_w	wall building coefficient, ($L/T^{1/2}$)
c	parameter defined by Eq. (7-4)
$c_{1...3}$	constants
c_b	rate of cake buildup, (L^2/T)
D	dispersion coefficient, (L^2/T)
d	height of the fracture, (L)
g	acceleration due to gravity, (L/T^2)
h	height, (L)
h_c	filter cake thickness, (L)
K	fluid consistency index, (M/LT)
K_e	erosion rate constant, (T/L)
k	absolute permeability of reservoir rock, (L^2)
k_r	relative permeability
L	length of core sample, (L)
n	flow behavior index, (MT/L^2)
P	phase pressure, (M/LT^2)
P_c	capillary pressure, (M/LT^2)
P_{inj}	injection pressure, (M/LT^2)
q	flow rate, (L^3/T)
S	phase saturation
t	time, (T)
u	superficial velocity of phase, (L/T)
V	leak-off volume, (L^3)
V_{sp}	spurt loss volume, (L^3)
w_s	width of the slot, (L)
y	vertical distance, (L)
Greek	
γ	shear rate, (T^{-1})
λ	rock characteristic factor
μ	viscosity of the phase, (M/LT)
ρ	density of phase, (M/L^3)
ϕ	porosity

Subscripts

a	apparent
c	cake
bt	breakthrough time, (T)
f	filtrate
g	gas
o	oil
wr	residual water

LITERATURE CITED

1. **Gidley, J.L., Holditch, S.A., Nierode, D.E., and Veatch Jr., R.W.:** *Recent Advances in Hydraulic Fracturing*, SPE monograph series, Richardson, Texas (1989) V 12.
2. **McGowen, J.M. and Vitthal, S.:** "Fracturing-Fluid Leakoff Under Dynamic Conditions Part 1: Development of a Realistic Laboratory Testing Procedure," paper SPE 36492 presented at the 1996 SPE Annual Technical Conference and Exhibition, Denver, CO, Oct. 6-9, 805-20.
3. **Penny, G.S. and Conway, M.W.:** *Fluid Leakoff in Recent Advances in Hydraulic Fracturing*, SPE monograph series, Richardson, Texas (1989) V 12.
4. **Roodhart, L.P.:** "Fracturing Fluids: Fluid-Loss Measurements Under Dynamic Conditions," *SPEJ* (Oct. 1985) 629-36.
5. **Penny, G.S., Conway, M.W., and Lee, W.S.:** "Control and Modeling of Fluid Leak-off During Hydraulic Fracturing," *JPT* (June 1985) 1071-81.
6. **Ford, W.G.F. and Penny, G.S.:** "The Influence of Down Hole Conditions on the Leakoff Properties of Fracturing Fluids," *SPEPE* (Feb. 1988) 43-51.
7. **Gulbis, J.:** "Dynamic Fluid Loss of Fracturing Fluids," paper SPE 12154 presented at the 1983 SPE Annual Technical Conference and Exhibition, San Francisco, CA, Oct. 5-8.
8. **Harris, P.C. and Penny, G.S.:** "Influence of Bottomhole Temperature and Shear History on Fracturing-Fluid Efficiency," *SPEPE* (May 1989) 189-93.
9. **Hall, C.D. Jr. and Dollarhide, F.E.:** "Performance of Fracturing Fluid Loss Agents Under Dynamic Conditions," *JPT* (May 1968) 763-69.
10. **McGowen, J.M. and McDaniel, B.W.:** "The Effects of Fluid Preconditioning and Test Cell Design on the Measurement of Dynamic Fluid Loss Data," paper SPE 18212 presented at the 1988 SPE Annual Technical Conference and Exhibition, Houston, TX, Oct. 2-5.
11. **Penny, G.S.:** "Nondamaging Fluid Loss Additives for Use in Hydraulic Fracturing of Gas Wells," paper SPE 10659 presented at the 1982 Formation Damage Symposium, Lafayette, LA, March 24-25.
12. **Hall, C.D. Jr. and Dollarhide, F.E.:** "Effect of Fracturing Fluid Velocity on Fluid Loss Agent Performance," *JPT* (May 1964) 555-60, *Trans. AIME*, 231.

13. Zigrye, J.L., Whitfill, D.L., and Sievert, J.A.: "Fluid-Loss Control Differences of Crosslinked and Linear Fracturing Fluids," *JPT* (Feb. 1985) 315-20.
14. McGowen, J.M. and Vithal, S.: "Evaluation of Particulate and Hydrocarbon Fracturing Fluid-Loss Additives Under Dynamic Conditions," paper SPE 37488 presented at the 1997 Production Operations Symposium, Oklahoma City, OK, March 9-11.
15. Vitthal, S. and McGowen, J.M.: "Fracturing-Fluid Leakoff Under Dynamic Conditions Part 2: Effect of Shear Rate, Permeability, and Pressure," paper SPE 36493 presented at the 1996 SPE Annual Technical Conference and Exhibition, Denver, CO, Oct. 6-9, 821-35.
16. Navarrete, R.C., Cawiezel, K.E., and Constein, V.G.: "Dynamic Fluid Loss in Hydraulic Fracturing Under Realistic Shear Conditions in High Permeability Rocks," paper SPE 28529 presented at the 1994 SPE Annual Technical Conference and Exhibition, New Orleans, LA, Sept. 22-28.
17. Navarrete, R.C., and Mitchell, J.P.: "Fluid-Loss Control for High-Permeability Fracturing Under Realistic Shear Conditions," paper SPE 29504 presented at the 1995 Production Operations Symposium, Oklahoma City, OK, April 2-4.
18. McGowen, J.M., Vitthal, S., Parker, M.A., Rahimi, A., and Martch, W.E. Jr.: "Fluid Selection for Fracturing High-Permeability Formations," paper SPE 26559 presented at the 1983 SPE Annual Technical Conference and Exhibition, Houston, TX, Oct. 3-6.
19. Parlar, M., Nelson, E.B., Walton, I.C., Park, E. and Debonis, V.: "An Experimental Study of Fracturing Fluids and Formation Damage in High-Permeability Porous Media," paper SPE 30458 presented at the 1995 SPE Annual Technical Conference and Exhibition, Dallas, TX, Oct. 22-25.
20. Lord, D. L., Vinod, P. S., Shah, S. N., and Bishop, M. L.: "An Investigation of Fluid Leakoff Phenomena Employing a High Pressure Simulator," paper SPE 30496 presented at the 1995 SPE Annual Technical Conference and Exhibition, Dallas, TX, Oct. 22-25.
21. Civan F.: *Formation Damage Class Notes*, The University of Oklahoma, Norman, Oklahoma (summer 1995).
22. Liu, X. and Civan, F.: "Formation Damage and Skin Factor Due to Filter Cake Formation and Fines Migration in the Near-Wellbore Region," presented at the 1994 SPE Int. Symposium on Formation Damage Control, Lafayette, Feb. 7-10.
23. Cornell, F.L.: "Engineering Improvements for Red Fork Fracturing," presented at the 1989 SPE Joint Rocky Mountain Regional/Low Permeability Reservoirs Symposium and Exhibition, Denver, CO, March 6-8.

24. Agarwal, R.G., Carter, R.D., and Pollock, C.B.: "Evaluation and Performance Prediction of Low Permeability Gas Wells Stimulated by Massive Hydraulic Fracturing," *JPT* (March 1979) 362-72.
25. Johnson, E.F., *et al.*: "Calculation of Relative Permeability from Displacement Experiments," *Trans. AIME*, 216, 370, 1959.
26. Reimers, D.R., and Clausen, R.A.: "High Permeability Fracturing at Prudhoe Bay, Alsaska," paper SPE 22835 presented at the 1991 SPE Annual Technical Conference and Exhibition, Dallas, TX, Oct. 6-9.
27. Hannah, R.R., Park, E.I., Walsh, R.E., Porter, D.A., Black, J.W., and Waters, F.: "A Field Study of a Combination Fracturing/Gravel Packing Completion Technique on the Amberjack, Miss Canyon 109 Field," paper SPE 26562 presented at the 1993 SPE Annual Technical Conference and Exhibition, Houston, TX.
28. Mullen, M.E., Stewart, B.R., and Norman, W.D.: "Justification for Fracturing Medium to High Permeability Formations in Sand Control Environments," paper SPE 95-70 presented at the 46th Annual Technical Meeting of the Petroleum Society of CIM, Banff, Alberta, Canada, May 14-17, 1995.
29. Stewart, B.R., Mullen, M.E., Howard, W.J., and Norman, W.D.: "Use of a Solid-Free Viscous Carrying Fluid in Fracturing Applications: An Economic and Productivity Comparison in Shallow Completions," paper SPE 30114 presented at the European Formation Damage Control Conference, The Hague, The Netherlands, May 15-16, 1995.
30. Liang, J.T., Sun, H., and Seright, R.S.: "Why Do Gels Reduce Water Permeability More Than Oil Permeability?," *SPEPE* (Nov. 1995) 282-86.
31. Zaitoun, A. and Kohler, N.: "Thin Polyacrylamide Gels for Water Control in High-Permeability Production Wells," paper SPE 22785 presented at the 1991 SPE Annual Technical Conference and Exhibition, Dallas, TX, Oct. 6-9.
32. Howard, G.C. and Fast, C.R.: "Optimum Fluid Characteristics for Fracture Extension," *Drill. Prod.* (1957), pp. 261-270.
33. Clark, P.E. and Barkat, O.: "Analysis of Fluid-Loss Data," *SPEPE* (August 1990), 306-310.
34. Charles, D.D. and Xie, X.: "New Concepts in Dynamic Fluid-loss Modeling of Fracturing Fluids," *Journal of Petroleum Science and Engineering* 17 (1997), 29-40.
35. Shames, I.H.: *Mechanics of Fluids*, McGraw-Hill, Inc., New York (1992).

APPENDIX A

Calculation of Cake Permeability

The filter cake formed during leak-off (Fig. 3-1) is in series with the invaded zone. The overall permeability across the first section of the core sample and the filter cake can be determined based on the measured pressure profiles and leak-off velocity. The overall permeability is a harmonic average of the permeability in the first section and cake permeability:

$$k_{av} = \frac{(L_1 + h_c)}{\frac{L_1}{k_1} + \frac{h_c}{k_c}} \quad (A-1)$$

where L_1 is the length of the first section of the core sample, h_c is the thickness of the filter cake, k_1 is permeability of the first section of the core sample which is assumed to remain constant as the leak-off progresses, and k_c is the cake permeability.

Based on the leak-off velocity and pressure drop at a given time, k_{av} is determined using Darcy's law. A constant cake thickness is assumed and k_c is calculated by substituting k_{av} in Eq. A-1.